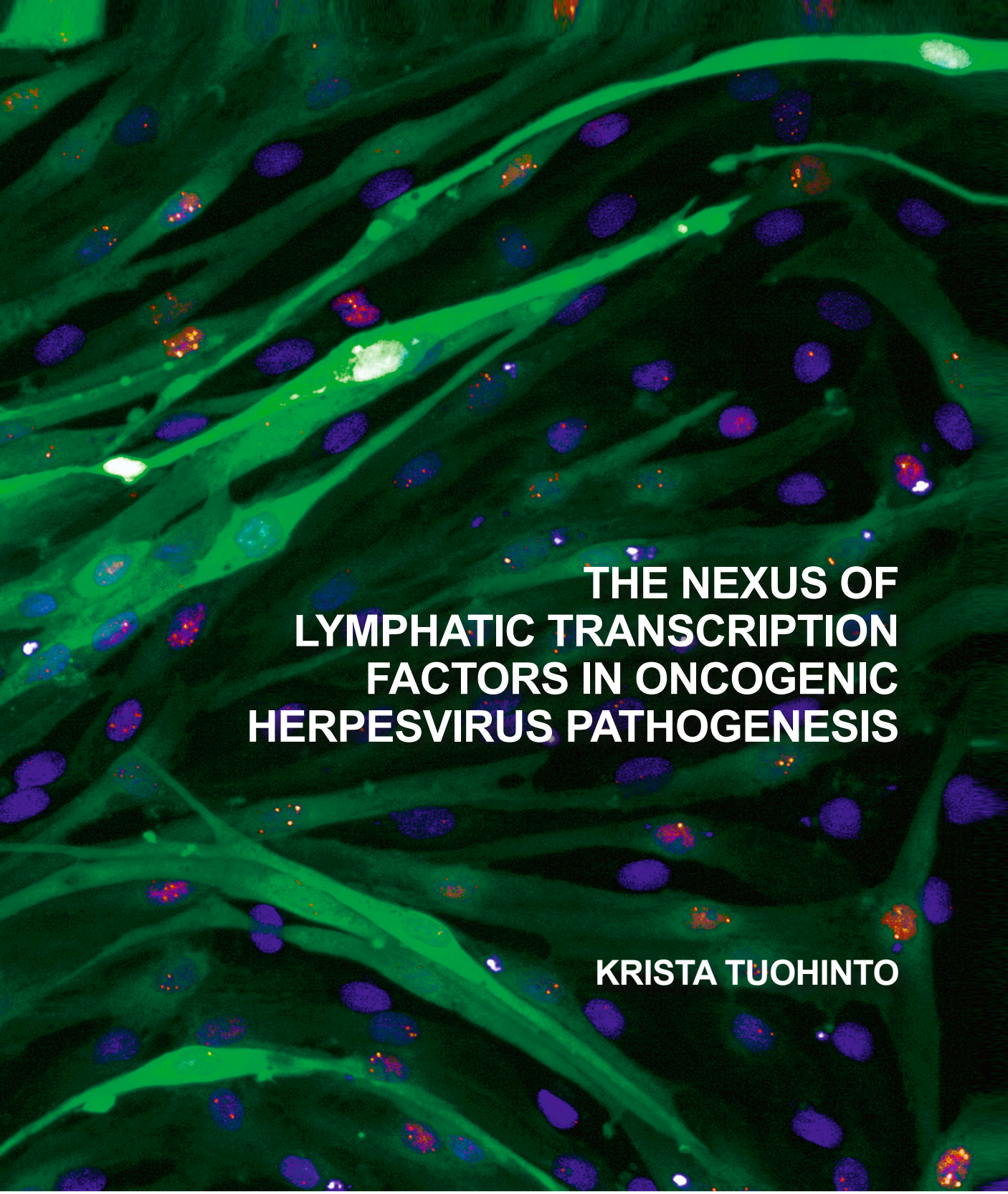

THE NEXUS OF LYMPHATIC TRANSCRIPTION FACTORS IN ONCOGENIC HERPESVIRUS PATHOGENESIS

KRISTA TUOHINTO

University of Helsinki
Dissertationes Universitatis Helsingiensis 50/2026

THE NEXUS OF LYMPHATIC TRANSCRIPTION FACTORS IN ONCOGENIC HERPESVIRUS PATHOGENESIS

Krista Tuohinto

Translational Cancer Medicine Program
Research Programs Unit
Faculty of Medicine
University of Helsinki

Doctoral Programme in Biomedicine
University of Helsinki Doctoral School
University of Helsinki

DOCTORAL DISSERTATION

To be presented for public discussion with the permission of
the Faculty of Medicine of the University of Helsinki,
in Lecture Hall 2, Biomedicum 1 Helsinki,
on the 30th of January, 2026 at 1pm o'clock.

The Faculty of Medicine uses the Ouriginal system (plagirism recognition) to examine all doctoral dissertations.

Publisher: University of Helsinki
Series: Dissertationes Universitatis Helsingiensis 50/2026

ISBN 978-952-84-1882-5 (print)
ISBN 978-952-84-1881-8 (online)
ISSN 2954-2898 (print)
ISSN 2954-2952 (online)
PunaMusta, Joensuu 2026

University of Helsinki
Faculty of Medicine, Research Progams Unit (RPU)
Translational Cancer Medicine Program (CAN-PRO)
Doctoral Programme in Biomedicine (DPBM)

Supervisor & Custos
Professor Päivi M Ojala
Translational Cancer Medicine Program
Research Programs Unit &
Department of Pathology, Medicum
Faculty of Medicine
University of Helsinki
Helsinki, Finland

Thesis Committee
PhD, Docent Biswajyoti Sahu
Applied Tumor Genomics Research
Research Program
Faculty of Medicine
University of Helsinki
Helsinki, Finland

PhD, Docent Sinem Karaman
Individualized Drug Therapy
Program
Faculty of Medicine
University of Helsinki
Helsinki, Finland

Reviewers
Professor Miikka Vikkula
Human Molecular Genetics
de Duve Institute
UCLouvain
Brussels, Belgium

Professor Lea Sistonen
Faculty of Science and Engineering
Åbo Akademi University
Turku, Finland

Faculty representative
PhD, Docent Kari Vaahtomeri
Translational Cancer Medicine
Program
Research Program Unit
Faculty of Medicine
University of Helsinki
Helsinki, Finland

Opponent
Professor Erle S. Robertson
Perelman School of Medicine
University of Pennsylvania
Philadelphia, USA

“To strive, to seek, to find, and not to yield.”
From Ulysses by Lord Alfred Tennyson

To my sister, for guiding the way
towards all things unknown.

Contents

PUBLICATIONS

Original publications

I. Gramolelli S, Elbasani E, **Tuohinto K***, Nurminen V*, Guenther T, Kallinen R, Kaijalainen SP, Diaz R, Haglund C, Grundhoff A, Ziegelbauer JM, Bower M, Francois M, and Ojala PM. *Oncogenic herpesvirus engages endothelial transcription factors SOX18 and PROX1 to increase viral genome copies and virus production.* Cancer Research 80, 3116-3129 (2020). doi.org/10.1158/0008-5472.CAN-19-3103

II. **Tuohinto K***, DiMaio T*, Kiss EA, Laakkonen P, Saharinen P, Karnezis T, Lagunoff M, and Ojala PM. *KSHV infection of endothelial precursor cells with lymphatic characteristics as a novel model for translational Kaposi's sarcoma studies.* PLoS Pathogens 19, e1010753 (2023). doi.org/10.1371/journal.ppat.1010753

III. **Tuohinto K***, Graus MS*, Staab P, Tiusanen V, Liangru F, Pradhan S, Wong YY, Weissmann S, Lou J, Hinde E, Wong J, Lee Q, Terskikh A, Alvarez-Kuglen M, Karnezis T, Günther T, Grundhoff A, Sahu B, Francoís M, and Ojala PM. *Oncogenic virus hijacks SOX18 pioneer function to enhance viral persistence.* bioRxiv (2025). doi.org/10.1101/2025.06.28.662102 (original manuscript under review at Nature Communications).

*Equal contribution.

The publications will be referred to in the text by their Roman numerals.

Additional unpublished material is also presented.

Related publications

Tuohinto K, Ojala PM.
Kaposin Sarkooma – Enigmaattinen virusperäinen syöpä.
Short review, BestPractice Nordic, Onkologia & Hematologia: FI/NR.5/2020
https://issuu.com/ckn-bpno/docs/bpno-fi-onkohema-nr5-2020?fr=sYWM0ODIzNjcxMDg

Tuohinto K, Ojala PM.
Virukset ja syöpä – mitä uutta?
Lääkärilehti: Scientific editorial, 9/2019.
https://www.laakarilehti.fi/ajassa/paakirjoitukset-tiede/virukset-ja-syopa-ndash-mita-uutta/

Pekkonen P, Alve S, Balistreri G, Gramolelli S, Tatti-Bugaeva O, Paatero I, Niiranen O, **Tuohinto K**, Perala N, Taiwo A, Zinovkina N, Repo P, Icay K, Ivaska J, Saharinen P, Hautaniemi S, Lehti K and Ojala PM. *Lymphatic endothelium stimulates melanoma metastasis and invasion via MMP14-dependent Notch3 and beta1-integrin activation.* Elife, 7 (2018). https://doi.org/10.7554/eLife.32490

Gramolelli S, Cheng J, Martinez-Corral I, Vaha-Koskela M, Elbasani E, Kaivanto E, Rantanen V, **Tuohinto K**, Hautaniemi S, Bower M, Haglund C, Alitalo K, Makinen T, Petrova TV, Lehti K and Ojala PM. *PROX1 is a transcriptional regulator of MMP14.* Sci Rep, 8(1), 9531 (2018). doi.org/10.1038/s41598-018-27739-w

Balistreri G, Viiliainen J, Turunen M, Diaz R, Lyly L, Pekkonen P, Rantala J, **Ojala K***, Sarek G, Teesalu M, Denisova O, Peltonen K, Julkunen I, Varjosalo M, Kainov D, Kallioniemi O, Laiho M, Taipale J, Hautaniemi S and Ojala PM. *Oncogenic Herpesvirus Utilizes Stress-Induced Cell Cycle Checkpoints for Efficient Lytic Replication.* PLoS Pathog 12(2): e1005424 (2016). doi.org/10.1371/journal.ppat.1005424

**Please note the family name change from Ojala to Tuohinto during March 2018.*

ABBREVIATIONS

3D	three dimensional
ACBI1	BRG1/BRM ATPase PROTAC
ActD	actinomycin D
AIDS	acquired immunodeficiency syndrome
AMC	AIDS malignancy consortium
ARID1A	AT-rich interactive domain-containing protein 1
ATAC	assay for transposase-accessible chromatin
ATPase	adenosine 5'triphosphatase
BAC	bacterial artificial chromosome
BAF	BRG1/BRM-associated factor
BEC	blood endothelial cell
BET	Bromodomain and extra-terminal domain
BrdU	bromodeoxyuridine
BRG1	brahma-related gene 1
BSA	bovine serum albumin
BSL2	bio-safety level 2
BrdU	5′-bromo-2′-deoxyuridine
BRM	brahma
cART	combination antiretroviral therapy
cBAF	canonical BAF
CD	cluster of differentiation
ChIP	chromatin immunoprecipitation
CRC	chromatin remodeling complex
CTG	CellTiter-Glo
Co-IP	co-immunoprecipitation
CoREST	REST corepressor 1
COUPTF2	COUP-transcription factor 2
DMEM	Dulbecco's modified Eagle's medium
DMSO	dimethyl sulfoxide
DNA	deoxyribonucleic acid
Dox	doxycycline
dsDNA	double stranded DNA
EBV	Epstein-Barr virus
EC	endothelial cell
ECFC	endothelial colony forming cell
ECFCBL	BEC-like (arterial) ECFCs
ECFCLY	LEC-like (lymphatic) ECFCs

EDTA	ethylenediaminetetraacetic acid
EdU	5-ethynyl-2'-deoxyuridine
EF-1	human elongation factor 1
EndMT	endothelial-to-mesenchymal transition
ETS	erythroblast transformation specific
FACS	fluorescence-activated cell sorting
FBS	fetal bovine serum
FDA	U.S Food and Drug Administration
FFPE	Formalin-fixed, paraffin-embedded
FHT-1015	BRG1/BRM ATPase allosteric inhibitor
GFP	green fluorescent protein
GPCR	G protein-coupled receptor
H&E	hematoxylin & eosion stain
HBV	hepatitis B virus
HCV	hepatitis C virus
HDACs	histone deacetylases
HEK293	human embryonic kidney 293 (cell line)
HemECs	hemangioma endothelial cells
HHV	human herpesvirus
HIV	human immunodeficiency virus
HLTRS	hypotrichosis-lymphedema-telangiectasia-renal syndrome
HMG	high mobility group
HP1α	heterochromatin protein 1 alpha
HPV	human papillomavirus
HRP	horseradish peroxidase
HSPG	heparan sulfate proteoglycans
HTVL-1	human T-cell Lymphotropic virus
HUVEC	human umbilical vein endothelial cells
IDR	intrinsically disordered region
IF	immunofluorescence
IgG	immunoglobulin G
IH	infantile hemangioma
IHC	immunohistochemistry
IPR	intellectual property rights
K-bZIP	KSHV-basic domain-leucine zipper
kDa	kilodalton
KICS	KSHV inflammatory cytokine syndrome
KLEC	KSHV-infected LEC
KS	Kaposi's sarcoma
KSHV	Kaposi sarcoma herpesvirus
KS-IRIS	immune reconstitution inflammatory syndrome
LANA/ ORF73	latency-associated nuclear antigen

LBS	LANA binding site
LEC	lymphatic endothelial cell
LGBTQ	lesbian, gay, bisexual, transgender, or queer/questioning
LNB	LANA nuclear bodies (speckles)
LSD1	lysine-specific histone demethylase 1A
LYVE-1	lymphatic vessel endothelial hyaluronan receptor-1
mAb	monoclonal antibody
MCD	multicentric Castleman's disease
MCM	minichromosomal maintenance
MCPyV	Merkel cell polyomavirus
MIEL	microscopic imaging of epigenetic landscape
MSM	men having sex with men
mIHC	multiplex IHC
MTA	mRNA transcription accumulation factor ORF57
mRNA	messenger RNA
MUT	mutant
MVP	mevalonate pathway
NaB	sodium butyrate
NF-κB	nuclear factor κ-light-chain-enhancer of activated B cells
NLS	nuclear localization signal
NOD	non-obese diabetic
NR2F2	nuclear receptor subfamily 2 group F member 2
NSG	NOD scid gamma / immunodeficient mouse strain
ns	non-significant
ORC	origin recognition complex
ORF	open-reading frame
PAA	phosphonoacetic acid
pAb	polyclonal antibody
PAGE	polyacrylamide gel electrophoresis
PAN	polyadenylated nuclear
PBAF	polybromo-associated BAF
PBMC	peripheral blood mononuclear cells
PBS	phosphate-buffered saline
PCA	principal component analysis
PCR	polymerase chain reaction
PEL	primary effusion lymphoma
PFA	paraformaldehyde
PFI-3	BRG1/BRM bromodomain inhibitor
PLA	proximity ligation assay
pRB	retinoblastoma protein
Pre-RC	pre-replication complex proteins
PROTAC	proteolysis-targeting degraders

PROX1	prospero homeobox 1
PTM	post-translational modifications
RBC	red blood cell
RelA	reticuloendotheliosis viral oncogene homolog A
RFP	red fluorescent protein
RNA	ribonucleic acid
RSV	rous sarcoma virus
RT	room temperature
RTA	replication and transcription activator ORF50
RT-qPCR	real time quantitative polymerase chain reaction
SC	spindle cell
SCID	severe combined immunodeficiency
SD	standard deviation
SDS	sodium dodecyl sulphate
seq	sequencing
SIN	self-inactivating vectors
siRNA	small interfering RNA
Sm4	small molecule inhibitor 4
SMT	single molecule tracking
SOX18	SRY-box transcription factor 18
STED	stimulated emission depletion
SWI/SNF	SWItch/Sucrose non-fermentable complex
siRNA	short interfering RNA
SV40	simian virus 40
SVM	support vector machine
TAD	topologically associating domains
TBS-T	tris-buffered saline-tween
TF	transcription factor
TR	terminal repeat
TSA	trichostatin A
U2OS	human osteosarcoma cell line
VEGF	vascular endothelial growth factor
VEGFR	VEGF receptor
vFLIP	viral FLICE-inhibitory protein ORF71
vGPCR	viral G protein-coupled receptor ORF74
VSV-G	vesicular stomatitis virus coat G glycoprotein
WB	Western blotting
WHO	World Health Organization
wt	wild-type

ABSTRACT

Kaposi sarcoma (KS) is an endothelial tumor caused by persistent infection of Kaposi sarcoma herpesvirus (KSHV). AIDS-related KS remains prevalent in sub-Saharan Africa, where HIV, a major cofactor, amplifies the disease burden. KS lesions are characterized by aberrant vasculature and KSHV-infected spindle cells (SC), which are the pathological hallmarks of the disease. Current KS therapies are inadequate and non-curative, reflecting limited validated targets and an incomplete mechanistic understanding of viral persistence.

KSHV persists as nuclear dsDNA episomes tethered to host chromosomes by LANA, the principal latency-associated protein. Latency is the dominant mode of infection. LANA orchestrates latent DNA replication of the viral episome from the KSHV origins of replication, ensuring episome duplication and faithful segregation during mitosis. Like all herpesviruses, KSHV can reactivate into a lytic replication phase. Viral RTA protein, the gene product of ORF50, initiates the lytic cycle leading to release of new virions to maintain infected cell population. Oncogenic viruses like KSHV can hijack host cellular factors to support the viral lifecycle and drive genome remodeling that both contribute to tumorigenesis. However, how these mechanisms are orchestrated in a cell-specific manner remains poorly defined.

KSHV is endotheliotropic, and preferentially establishes infection in lymphatic endothelial cells (LECs), which undergo profound changes in morphology, genomic organization, and identity, acquiring features of SCs. Infected LECs (KLECs) harbor high number of viral episome copies and uniquely undergo spontaneous lytic reactivation, in contrast to any other cell type. The aim of this thesis was to investigate the viral and host factors that render LECs particularly permissive to KSHV infection. This thesis combined genome-wide chromatin and transcriptome profiling, proximity proteomics, high-resolution imaging including epigenetic landscape mapping, functional two- and three-dimensional in vitro infection models and assays to dissect the early molecular mechanisms that drive KSHV persistence in lymphatic endothelial environment, as well as a translational in vivo model to assess therapeutic utility of blocking a LEC-specific factor.

The first study identified LEC developmental transcription factors (TFs) as critical regulators of KSHV pathobiology. During embryogenesis, SOX18 and COUPTF2 drive LEC differentiation by inducing PROX1, the master regulator of LEC identity. SOX18 and PROX1 were found to be co-expressed with LANA in KS patient samples, and to regulate the viral infection cycle through

distinct mechanisms, whereas COUPTF2 did not show significant involvement. SOX18 binds near the latent viral DNA replication origin and increases the intracellular viral episome copies. Genetic or pharmacologic inhibition of SOX18 reduced KSHV episomes and halted infection progression, revealing SOX18 as a potential therapeutic target for KS. In contrast, transcriptionally active PROX1 interacted with ORF50/RTA and bound its promoter to enhance spontaneous lytic reactivation in KLECs. Contrary to SOX18, currently PROX1 is not pharmacologically tractable.

The second study characterized circulating lymphatic SOX18- and PROX1-positive endothelial-like progenitor cells as a KSHV reservoir with high viral load, spontaneous lytic activity, and oncogenic properties. These LEC-precurors could be utilized as a physiologically relevant model to evaluate the pre-clinical potential of targeting SOX18 in KSHV pathobiology. SOX18 inhibition reduced the SC phenotype and intracellular viral episomes in vivo, highlighting its potential as a therapeutic target for KS.

The third study showed that mechanistically SOX18 functions as a pioneer factor, hijacked by KSHV to enhance host chromatin accessibility in KLECs. Upon infection, LANA recruits SOX18 to engage the SWI/SNF chromatin remodeling complex through its ATPase BRG1. This promotes an accessible chromatin environment for efficient viral episome maintenance and duplication. Disruption of SOX18-BRG1 axis, either genetically or pharmacologically, reduced episome copies and attenuated the KSHV infection and SC hallmarks in KLECs.

Collectively, this thesis reveals how a human herpesvirus engages lymphatic lineage-specific transcriptional regulators SOX18 and PROX1 to balance two imperatives – latent persistence and intermittent reactivation – thereby sustaining the infected spindle-cell population, the pathological hallmark of KS. KSHV infection is actively maintained condition reliant on a dynamic interplay of host-viral axis, modulating cellular microenvironment for its own persistence. The findings reposition SOX18 as a pioneering factor in chromatin remodeling, with therapeutic implications for targeting SOX18 and chromatin regulators in viral infections, virus-induced cancers, and SOX18-linked endothelial disorders.

TIIVISTELMÄ

Kaposin sarkooma (KS) on endoteeliperäinen kasvain, jonka aiheuttaa Kaposin sarkooma herpesviruksen (KSHV) krooninen infektio. AIDS:iin liittyvä KS on yhä yksi yleisimmistä syövistä Saharan eteläpuolisessa Afrikassa HIV-epidemian alueilla. KS-leesioille on ominaista poikkeava veri- ja imusuonten kasvu ja KSHV-infektoidut sukkulasolut (SC), jotka ovat taudin histopatologisia tunnusmerkkejä. Nykyiset KS-hoidot ovat riittämättömiä, sillä validoituja täsmälääkekohteita ei ole tunnistettu, ja viruksen persistenssin mekanismeja ymmärretään vielä puutteellisesti.

KSHV aiheuttaa elinikäisen infektion ja sen genomi persistoi isäntäsolun tumassa kaksijuosteisena DNA episomeina. Viruksen proteiini LANA kiinnittää episomit isäntäsolussa tuman kromosomeihin ja orkestroi virusepisomin latenttia replikaatiota. Näin virus varmistaa episomin kopioimisen ja kopioiden tasaisen siirtymisen sisarsoluihin solun jakautumisen yhteydessä ja siten pitkäaikaisen infektion takaamisen. Kuten kaikki herpesvirukset, myös KSHV voi reaktivoitua lyytiseen vaiheeseen. Viruksen RTA-proteiini, ORF50-geenin tuote, käynnistää lyytisen syklin, mikä johtaa uusien viruspartikkelien tuottoon ja vapauttamiseen. Onkogeeniset virukset kuten KSHV voivat kaapata isäntäsolun tekijöitä tukeakseen kroonista infektiota ja muokatakseen isäntäsolun kromatiinin rakennetta, edistäen KS:n kehittymistä.

KSHV on endoteelitroopinen ja infektoi herkästi lymfaattisia endoteelisoluja (LEC), joiden morfologia, genominen organisaatio ja soluidentiteetti muuntuvat SC-kaltaiseksi. Infektoidut solut (KLEC) kantavat runsaasti virusepisomeja ja pystyvät ainutlaatuisesti spontaaniin lyyttisen replikaation aloittamiseen ja uusien virusten tuottoon, toisin kuin mikään muu solutyyppi. Tämän väitöskirjan tavoitteena oli tutkia niitä viruksen ja isäntäsolun tekijöitä, jotka aiheuttavat LEC:eissä tämän erityisen KSHV-infektiotyypin.Väitöskirja yhdistää koko genomin kattavan kromatiinin ja transkriptomin profiloinnin, interaktio-proteomiikan, korkean resoluution kuvantamisen sisältäen kromatiinin epigeneettisen maiseman kartoituksen, translationaalisen hiirimallin, sekä toiminnalliset kaksi- ja kolmiulotteiset infektiokokeet niiden varhaisten molekyylimekanismien selvittämiselle, jotka ajavat KSHV:n persistenssiä LEC:eissä.

Ensimmäisessä tutkimuksessa tunnistettiin LEC-spesifiset, kehitysbiologiset transkription säätelytekijät keskeisiksi KSHV:n patobiologialle. Kehityksen aikana SOX18 ja COUPTF2 ohjaavat LEC-erilaistumista indusoimalla PROX1:n ilmentymistä. SOX18 ja PROX1 osoitettiin ekspressoituvan LANA:n kanssa KS-potilasnäytteissä ja säätelevän virusinfektion kiertoa erillisillä mekanismeilla, kun taas

COUPTF2 ei vaikuttanut merkittävästi infektioon. SOX18 sitoutuu viruksen latentin DNA replikaation aloituskohdan läheisyyteen ja lisää virusepisomien määrää infektoiduissa soluissa. SOX18:n geneettinen ja farmakologinen inhibitio vähensi episomien määrää ja esti infektion etenemisen, tuoden esiin SOX18:n potentiaalin terapeuttisena kohteena KS:ssa. Sen sijaan transkriptionaalisesti aktiivinen PROX1 interaktoi ORF50/RTA:n kanssa ja sitoutui sen promoottoriin tehostaen spontaania lyyttistä reaktivaatiota KLEC-soluissa. Toisin kuin SOX18, PROX1 ei kuitenkaan ole vielä toistaiseksi farmakologisesti kohdennettavissa.

Toinen tutkimus selvitti verenkierrossa esiintyvien lymfaattisten, SOX18 ja PROX1-positiivisten, endoteelin esiastesolujen roolia KSHV:n infektiossa. Myös näille LEC-esiasteen soluille on ominaista korkea latenttien episomien määrä, spontaani lyyttinen aktiivisuus ja onkogeeniset ominaisuudet. Näitä soluja voitiin hyödyntää fysiologisesti merkittävänä mallina SOX18 aktiivisuuden estämisen prekliinisen potentiaalin arvioimiseksi KSHV:n patobiologiassa. SOX18:n esto vähensi hiireen istutettujen, infektoitujen LEC-esiastesolujen SC-fenotyyppiä ja solunsisäisiä virusepisomeja, korostaen sen potentiaalia terapeuttisena kohteena KS:ssa.

Kolmas tutkimus osoitti, että mekanistisesti SOX18 toimii pioneeritekijänä, jonka KSHV kaappaa lisätäkseen isäntäsolun kromatiinin avautumista KLEC-soluissa. LANA rekrytoi SOX18:n kanssa isäntäsolun kromatiinia muokkaavan SWI/SNF kompleksin BRG1 proteiinin KSHV-infektoiduissa soluissa, edistäen avointa kromatiiniympäristöä virusepisomien säilymisen varmistamiseksi. SOX18-BRG1-akselin geneettinen ja farmakologinen estäminen vähensi solunsisästen episomien määrää ja heikensi KSHV-infektion SC-tunnuspiirteitä KLEC-soluissa.

Tässä väitöskirjatössä osoitettiin, miten ihmisen onkogeeninen herpesvirus valjastaa lymfaattisen endoteelin spesifiset transkription säätelijät SOX18:n ja PROX1:n tehostamaan infektion eri vaiheita – latenttia pysyvyyttä ja ajoittaista reaktivaatiota – ja siten ylläpitämään elinikäistä kroonista infektiota. KSHV-infektio on aktiivisesti ylläpidetty tila, joka on riippuvainen isäntäsolun ja viruksen dynaamisesta vuorovaikutuksesta, muokaten solun mikroympäristöä oman pysyvyytensä turvaamiseksi. Löydös, jonka mukaan SOX18 voi toimia pioneeritekijänä kromatiinin muokkauksessa, avaa terapeuttisia mahdollisuuksia estää niin transkription keskeistä säätelytekijää sekä kromatiinisäätelijöitä virusinfektioiden hoidossa, virusten aiheuttamissa syövissä sekä muissa SOX18:aan liittyvissä endoteeliperäisissä sairauksissa.

1 INTRODUCTION

Cancer is not generally considered contagious; however, oncogenic viruses account for 13-20% of human cancers worldwide and 45% in parts of sub-Saharan Africa (de Martel et al., 2020; Krump & You, 2018; Lunn et al., 2017). This, however, is an underestimate since developing countries are particularly hard hit by viral cancers yet tend to have inadequate cancer registries. Acquired immunodeficiency is the major risk factor for virus-induced cancers. Immunodeficiency occurs in diverse settings, including solid-organ transplantation, immunosuppressive therapies such as chemotherapy or biologics for autoimmune disease, advanced age, and among the 40 million people living with human immunodeficiency virus (HIV) worldwide.

One such cancer is Kaposi sarcoma (KS), caused by human herpesvirus 8 (HHV-8), also known as Kaposi sarcoma herpesvirus (KSHV) (Chang et al., 1994). On the basis of extensive epidemiologic and mechanistic evidence, the World Health Organization (WHO) classifies KSHV as a human carcinogen responsible for KS and other inflammatory and lymphoproliferative disorders. There is a clear limitation of current KS therapies, of which none are curative and outcomes are particularly poor in low-income countries with the greatest disease burden (Cesarman et al., 2019). Deeper insights into the virus-host interactions are needed to identify rational and accessible therapeutic targets for KSHV-associated diseases.

KS presents as multifocal lesions composed of aberrant vasculature and proliferating KSHV-infected spindle cells (SC), which are considered the histopathological hallmark of KS and of endothelial cell origin. Lymphatic endothelial cells (LECs) are strikingly susceptible to KSHV compared with other cell types (Aguilar et al., 2012; Carroll et al., 2004; Hong et al., 2004; Wang et al., 2004). Infection of LECs induces profound reprogramming of cell morphology and identity, resulting in the characteristics of KS spindle cells with high KSHV burden (Cheng et al., 2011; Gasperini et al., 2012; Ojala & Schulz, 2014).

This thesis investigates viral and host determinants that render LECs particularly permissive to KSHV and explores their therapeutic implications. The results presented show that the developmental lymphatic factors SOX18 and PROX1 enhance KSHV infection through distinct mechanisms. Notably, this study repositions SOX18 as a pioneer factor in chromatin remodeling, with broad implications for therapies targeting both transcription factor and chromatin regulators to treat viral infections, virus-induced malignancies, and SOX18-related vascular disorders.

2 REVIEW OF THE LITERATURE

2.1 Oncogenic viruses

Studies of oncogenic viruses have shaped the foundations of modern cancer biology. The identification of oncogenes within virus genomes capable of inducing tumors prompted the realization that similar genes exist in the host genome. Early research on viruses like Rous sarcoma virus (RSV) and simian virus 40 (SV40) led to the discovery of proto-oncogenes and tumor suppressors that are normal cellular genes which can drive cancer when mutated or dysregulated. The identification of v-src, the RSV form of the human src gene, provided the first direct link between a cellular gene and tumor formation (Rous, 1911; Stehelin et al., 1976). Similarly, studies of SV40 large T antigen revealed that viral proteins could inactivate key tumor suppressors such as p53 and retinoblastoma protein (pRB) (Ludlow et al., 1989), defining them as critical guardians of genome stability. These discoveries established the fundamental concept that cancer can result from a disruption in the delicate balance between oncogene activation and tumor suppressor inactivation.

Human oncogenic viruses span diverse families, including DNA viruses, RNA viruses, and retroviruses. Currently recognized oncogenic human viruses are human papillomaviruses (HPV), hepatitis B virus (HBV), hepatitis C virus (HCV), Epstein Barr virus (EBV), human T-cell lymphotropic virus type 1 (HTLV-1), Merkel cell polyomavirus (MCPyV), and Kaposi sarcoma herpesvirus (KSHV), also known as human herpesvirus 8 (HHV-8). Despite their differences, they share a unifying capacity to rewire host processes in ways that can promote malignant transformation (Schiller & Lowy, 2021).

Oncogenic viruses persist by evading immune detection and subverting growth control. Viral oncoproteins directly disable tumor-suppressor pathways, such as HPV's proteins E6 and E7 targeting host p53 and pRB, respectively, driving uncontrolled proliferation and genomic instability (McLaughlin-Drubin & Munger, 2009). Chronic HBV and HCV infections create mutagenic environments through sustained inflammation and oxidative stress, increasing hepatocellular carcinoma risk (Ringelhan et al., 2017). EBV and KSHV establish lifelong infections, typically in B cells or endothelial cells. Their viral proteins enhance cell survival and proliferation, while facilitating immune evasion, enabling the gradual accumulation of oncogenic changes (Ganem, 2010). Beyond direct protein interactions, a key hallmark of viral oncogenesis involves the reprogramming of host gene expression

through epigenetic modifications of chromatin structure. Viral factors co-opt host chromatin-modifiers, remodel three-dimensional (3D) genome architecture, and reshape epigenetic landscapes to maintain persistence, drive transformation, and resist immune clearance (Ka-Yue Chow et al., 2022; Kgatle et al., 2025; Neugebauer et al., 2023).

Viral systems have not only provided the first molecular tools to define core principles of tumorigenesis but also served as experimental models for studying cell transformation and epigenetic reprogramming. Although oncogenic viruses account for only a subset of human cancers, their study has offered broader understanding of cancer biology in general. Research in viral oncology not only ascertains infectious causes of cancer but also continues to define how we understand and effectively treat cancer.

2.2 Kaposi sarcoma herpesvirus

Kaposi sarcoma herpesvirus (KSHV) is the eighth discovered human herpesvirus (HHV-8) and the etiological agent of Kaposi sarcoma (KS). KSHV is consistently detected in biopsies from all clinical forms of KS, and, conversely, KS does not arise in the absence of KSHV infection (Chang et al., 1994; Dupin et al., 1999; Whitby et al., 1995). Beyond KS, KSHV is implicated in two lymphoproliferative disorders: primary effusion lymphoma (PEL) (Cesarman et al., 1995) and multicentric Castleman disease (MCD), in approximately 50% of cases (Soulier et al., 1995). Furthermore, a rare and often fatal condition known as KSHV inflammatory cytokine syndrome (KICS) has been described (Uldrick et al., 2010).

A defining feature of the *Herpesviridae* family, including KSHV, is a large double-stranded DNA (dsDNA) genome, and a structurally complex virion comprising an icosahedral capsid, a tegument layer, and a lipid envelope (Chang et al., 1994; Wu et al., 2000). The 165 kb KSHV genome forms a covalently closed circular episome in the host nucleus and contains 140.5 kb of protein-coding sequence flanked by 801-bp GC-rich terminal repeats (TR). This includes over 90 open reading frames (ORFs), that control both latent and lytic phases of viral replication (Losay & Damania, 2025).

KSHV transmission routes vary, but KSHV predominantly resides in the oral cavity epithelium, where it can replicate and shed high levels of infectious particles into saliva (Pauk et al., 2000; Vieira et al., 1997). Consequently, saliva is considered the principal vehicle for primary infection of the oropharyngeal mucosa. KSHV DNA is also detected in semen and in rectal and cervicovaginal secretions, supporting sexual transmission. Less commonly, transmission occurs via blood transfusion or vertically during childbirth and additionally KSHV can be found in peripheral blood

mononuclear cells (PBMCs) (Della Bella et al., 2008). KSHV seroprevalence in the general population is less than 10% in Northern Europe, Asia, and the United States. In contrast, it ranges between 10-30% in the Mediterranean region and exceeds 50% in sub-Saharan Africa (Cesarman et al., 2019). Men who have sex with men (MSM) show the highest seroprevalence globally (Martin et al., 1998). Despite elevated seroprevalence in some populations, KS incidence remains low in the general population, indicating that additional cofactors are required for the disease development.

2.2.1 KSHV infection cycle

A hallmark of herpesviruses is their ability to establish lifelong persistent infection, characterized by a biphasic life cycle consisting of quiescent latency and active lytic replication (Miller et al., 1997; Renne et al., 1996). Both phases are essential for long-term persistence in the host, and gene products from each expression program contribute to the pathogenesis of KSHV-associated diseases (Grundhoff & Ganem, 2004).

KSHV entry is mediated by coordinated interactions between viral envelope glycoproteins and host-cell surface receptors (van der Meulen et al., 2021). Heparan sulfate proteoglycans (HSPGs), which are broadly expressed on host cells, function as key attachment factors that facilitate target-cell recognition (Losay & Damania, 2025). Productive entry then proceeds via specific receptors on epithelial and endothelial cells (ECs) and fibroblasts, including integrins and ephrin receptor tyrosine kinases, most notably EphA2 and EphA4 (Hahn et al., 2012). Recent work shows that during entry, KSHV virions can directly bind CD109, which is expressed in senescent ECs and enhances viral uptake and infection, suggesting an age-regulated determinant of KSHV susceptibility (Lee et al., 2024).

Following endocytic entry, the viral envelope fuses with the endosomal membrane, releasing the capsid into the cytoplasm. The viral capsid then moves and binds to the nuclear pore and the linear viral genome is released into the nucleus where it circularizes to form an episome (Losay & Damania, 2025). This way the viral genome is not eradicated but establishes viral latency to persist lifelong in the host cells, sporadically reactivating to lytic cycle to spread (**Figure 1**).

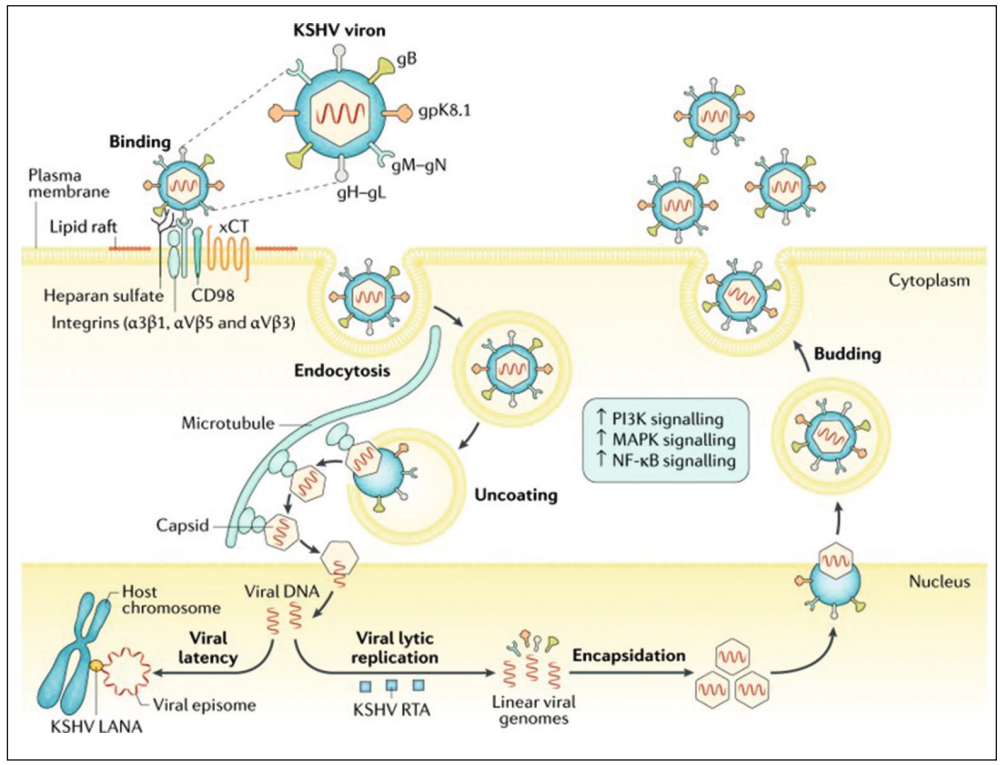

Figure 1. KSHV infection cycle in the host cell. Published with permission from Springer Nature (Cesarman et al., 2019).

2.2.2 Latency establishment and latent replication

During latency, which is the default, quiescent phase of infection, the circularized KSHV dsDNA genome persists as an extrachromosomal minichromosome (episome) tethered to host chromatin. The latency locus includes ORF71 (encoding viral FLICE inhibitory protein vFLIP), ORF72 (encoding viral cyclin vCYC), ORF73 (encoding latency-associated nuclear antigen LANA), K12 encoding signaling proteins kaposins, and 12 distinct microRNAs (Cesarman et al., 2019). Latent genes are expressed in KSHV-infected tumour SCs and contribute to KS tumorigenesis.

Among latent factors, LANA is the major protein expressed across KSHV-associated malignancies. Through interactions with viral and cellular proteins, LANA promotes episome replication, maintenance, and faithful segregation, and supports host-cell survival and proliferation (Hu et al., 2002). LANA is a multifunctional DNA binding protein, made of 1162 amino acids and 220-230 kDa in size (Verma et al., 2007). LANA is required for tethering the viral DNA episomes to host chromatin via docking through its N-terminal domain onto host core histones H2A and H2B, while binding conserved terminal repeat (TR) sequences on the KSHV genome through its

C-terminal domain (Barbera et al., 2006; Garber et al., 2001). This bidirectional tethering enables KSHV to exploit host replication machinery to duplicate and segregate episomal DNA during mitosis in latently infected cells (Ballestas & Kaye, 2001; Hu et al., 2002; Purushothaman et al., 2016; Uppal et al., 2014).

LANA recruits host replication machinery to mediate viral latent DNA replication. Eukaryotic DNA replication is a highly regulated and accurate process that ensures the faithful duplication of the entire genome before a cell divides in mitosis. It occurs during the S phase of the cell cycle and involves multiple steps from origin licensing, helicase activation, primer synthesis, strand elongation, to eventual termination, coordinated by a complex array of enzymes and regulatory proteins (Hu & Stillman, 2023). Replication of KSHV latent DNA can be initiated at different sites of origin, ori-P with LANA, and ori-A independently of LANA (Verma et al., 2007; Verma et al., 2011). In ori-P replication, replication occurs at the one of two LANA binding sites (LBS) within TR region. This subsequently leads to the recruitment and assembly of host pre-replication proteins (pre-RC), such as origin recognition complexes (ORCs) and minichromosomal maintenance (MCM) helicase, to the viral TR and initiates latent replication (Verma et al., 2007). In summary, KSHV latent replication is a stealth strategy where the viral genome is replicated alongside the host's once at every cell division, exploiting the human cellular replication machinery to pursue viral DNA maintenance.

In latently infected cells, LANA and viral episomes concentrate in characteristic nuclear speckles termed LANA nuclear bodies (LNB; (Ballestas & Kaye, 2001; Kedes et al., 1997). LANA forms dimers that bind adjacent LBSs and then oligomerize into higher-order assemblies. This LANA oligomerization contribute to latent episome replication and maintenance that are stabilized by interactions with LBS at viral genome, chromatin-associated proteins such as BET (Bromodomain and Extra-Terminal domain) family, and other host partners (Hellert et al., 2013), (**Figure 2**). Collectively, LANA oligomers orchestrate episome tethering, replication, and host-chromatin engagement to sustain latency.

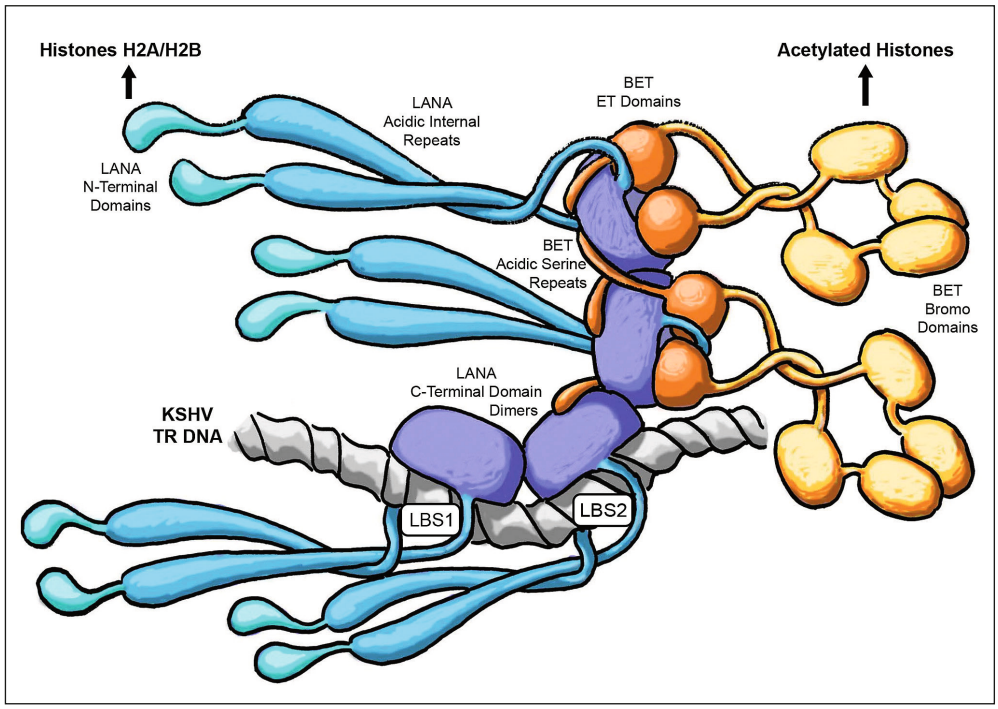

Figure 2. Hypothetical model of KSHV LANA oligomers. *Dark blue:* LANA C-terminal DNA binding domain dimers. *Cyan:* LANA acidic internal repeat regions and N-terminal domains. *Grey:* KSHV DNA with TR latent DNA replication origin. *Orange:* BET proteins as example of chromatin-associated proteins interacting with LANA in oligomers. Published with permission from PLOS (Hellert et al., 2013).

2.2.3 Lytic replication cascade

Latency can be disrupted upon appropriate stimuli or by spontaneous reactivation, reflecting the recurrent infectious cycle of herpesviruses. While lytic genes are epigenetically repressed during latency, periodic entry into the lytic program is required to produce and release infectious virions. Spontaneous reactivation occurs in a subset of latently infected cells and can be triggered by several mechanisms. In addition to immunosuppression, other viral co-infections and unbalanced inflammatory cytokines (Mercader et al. 2000; Vieira et al. 2001), hypoxia (Davis et al. 2001), host kinases and signaling molecules (Cheng et al., 2009; Dillon et al., 2013; Varjosalo et al., 2008; Yu et al., 2007), oxidative stress (Ye et al. 2011), and pharmacological agents have been shown to reactivate KSHV. *In vitro*, chemical inducers are routinely used to achieve efficient reactivation; for example, sodium butyrate (NaB), a histone deacetylase (HDAC) inhibitor, relieves chromatin-based repression and boosts KSHV lytic gene expression (Miller et al., 1997).

The replication and transcription activator (RTA), encoded by ORF50, is the first lytic gene expressed during reactivation and is both necessary and sufficient to initiate the lytic cycle (Sun et al., 1998). RTA binds to a multitude of sites on the viral genome, including promoters of lytic genes in addition to its promoter, as well as both origins of lytic replication (OriLyt) (Chen et al., 2009), and drives the full lytic cascade (Guito & Lukac, 2012). Lytic genes, such as ORF45, ORF57, and K8α also known as K-basic domain-leucine zipper (K-bZIP), cooperate with RTA to continually amplify lytic progression (Losay & Damania, 2025). ORF45 is expressed early and remains abundant through late stages; it is a highly phosphorylated, largely cytoplasmic tegument protein present in mature virions (Zhu et al., 2005; Zhu et al., 1999). ORF57 (MTA), a conserved nuclear protein, promotes lytic replication by recruiting cellular mRNA-processing machinery to enhance viral mRNA nuclear export and translation, thereby increasing lytic protein production and virion yield (Bello et al., 1999; Boyne et al., 2010; Lukac et al., 2001). K-bZIP has been shown to promote transactivation of RTA and other lytic promoters and recruit HDACs to the RTA promoter to act as a modulator of lytic reactivation (Martinez & Tang, 2012; Wang et al., 2011). Among late genes, K8.1 encodes an envelope glycoprotein incorporated into the virion during budding from the plasma membrane and is essential for efficient production of new particles (Birkmann et al., 2001). The release of multiple encapsidated virions induces a cytopathic effect and is ultimately lethal to the host cell, enabling dissemination within the infected individual and transmission to new hosts.

2.2.4 Contribution of infection phases to tumorigenesis

Most cells within KS lesions harbor latent KSHV infection, with only a minority undergoing spontaneous lytic reactivation (Cesarman et al., 2019), resulting in an asynchronous infection state. Latency drives oncogenesis by promoting proliferation and cellular reprogramming while suppressing apoptosis. By contrast, intermittent lytic replication is essential to maintain and expand the pool of infected cells via production of new virions. Lytic phase is a major source of inflammatory mediators, such as viral chemokines, triggering host signaling cascades leading to recruitment of inflammatory cells and secretion of cytokines and pro-angiogenic growth factors. Together, the latent and lytic programs cooperatively shape the tumor microenvironment and infected-cell phenotype, contributing to KS pathogenesis (Grundhoff & Ganem, 2004).

2.3 Kaposi sarcoma

Kaposi sarcoma (KS) is considered to originate from KSHV-infected endothelial cells (ECs) and consists of malformed vasculature and proliferation of KSHV-positive spindle-shaped cells (spindle cells; SC) as a pathological hallmark (Gramolelli & Ojala, 2017).

KS was first described in 1872 by the Hungarian dermatologist Moritz Kaposi as “idiopathic multiple pigmented sarcoma of the skin” based on erythematous patch lesions (Sternbach & Varon, 1995). Although Kaposi classified the neoplasm as a sarcoma, reflecting its mesenchymal features, subsequent work has highlighted KS’s unique biology (Ganem, 2010). KS lesions are histologically complex and contain diverse cell types, including ECs, mesenchymal cells, B and T lymphocytes, plasma cells, and monocytes (Cesarman et al., 2019). Prominent inflammation and abundant, irregular, endothelial-lined vascular spaces underlie the characteristic reddish discoloration. Unlike many solid tumors, KS lesions are multifocal and arise independently in the dermis rather than via metastasis, and advanced lesions show evidence of polyclonal proliferation (Duprez et al., 2007). Although cutaneous involvement is most common, KS can affect mucous membranes, lymph nodes, and visceral organs and can be fatal (Cesarman et al., 2019). Clinically, as KS lesions evolve, abnormal, leaky neovasculature expands through the dermis, accompanied by erythrocyte extravasation causing red-colored patches, that progress to plaques and as SCs aggregate in vascular spaces prone to leakage. The resulting hemorrhage and local edema produce the characteristic dark red to violaceous nodules, which may remain localized or disseminate widely (Cesarman et al., 2019).

Figure 3. Widespread KS lesions on the skin of upper extremities on aged patient diagnosed with disseminated advanced disease. Published with permission from MDPI (Park & Lee, 2024).

Four epidemiologic forms of KS are recognized: classic, endemic, iatrogenic, and acquired immunodeficiency syndrome (AIDS)-related, also known as epidemic KS (Damania & Dittmer, 2023). Classic KS corresponds to Kaposi original description as a rare, indolent disease with lesions typically on the lower extremities of older men of Mediterranean or Eastern European descent. Endemic KS occurs in regions with high KSHV seroprevalence, notably sub-Saharan Africa and in parts of Xinjiang, China, particularly among Kazakh and Uyghur populations. Iatrogenic KS arises in solid-organ transplant recipients, sometimes following donor-derived transmission of KSHV (Damania & Dittmer, 2023). The most aggressive form is AIDS-related KS, which remains among the most prevalent cancers in sub-Saharan Africa and a major malignancy in people living with HIV (Cesarman et al., 2019).

2.3.1 Immunosupression is a major risk factor for KS

In immunocompetent individuals, sporadic episodes of KSHV reactivation are typically contained by an intact immune system. Most infected cells maintain latency with minimal antigen expression, limiting immune recognition and clearance, and the infection is under control. As the virus is dependent on the host to survive and reproduce, it is not the intend of viruses to exhaust their residence. The host-virus equilibrium generally disfavors widespread lytic infection. Disruption of this balance by immunosuppression or other stressors drives enhanced reactivation and lytic replication (Aneja & Yuan, 2017). Consequently, more KS promoting lytic oncogenes are encoded, and cytokines and chemokines secreted, in addition to enhanced production of new viral particles to infect nearby cells. In case of immunodeficient individuals, the CD4+ T-cell count and the host immune response is not sufficient to suppress the infection, and KSHV thrives uncontrollably (Cesarman et al., 2019). Accordingly, iatrogenic KS was recognized in solid-organ transplant recipients receiving immunosuppressive therapy, who showed markedly increased KS incidence (Lebbe et al., 2008).

Untreated HIV infection targets CD4+ T cells (helper T cells), causing progressive immunosuppression and, ultimately, AIDS, the major risk state for KS. AIDS patients develop aggressive forms of KS as disfiguring lesions widespread on the skin of the body and face. The high morbidity and mortality of these KS cases results from the occurrence of the lesions in visceral organs, such as lungs and gastrointestinal tract, leading to serious and fatal complications causing respiratory failure, hemorrhage, diarrhea or obstruction (Cesarman et al., 2019). KS drew intense attention in Western countries in the early 1980s as one of the sentinel malignancies of the emerging AIDS epidemic, with a dramatic surge in cases and substantial health burden (Friedman-Kien, 1981). The association of KS and HIV infection was immense, and co-occurrence suggested HIV as a proximate cause. However, not all KS patients had HIV infection thus the notion of HIV as a main cause of KS was excluded (Beral, 1991). Classical and endemic forms of KS had no link to HIV infection, as no HIV was detected in the tumor biopsies. In addition, HIV-positive individuals had a varying risk of developing KS depending on the source of infection. KS occurrence was highest among MSM, suggesting a link to sexual transmission (Martin et al., 1998). Consequently, researchers prospected a yet unidentified sexually transmitted human pathogen as a causative agent of KS (Beral, 1991). In 1994, DNA fragments from an unknown pathogen in KS tumors were identified as a new human herpesvirus; Kaposi sarcoma herpesvirus (KSHV/HHV-8) (Chang et al., 1994).

As of 2024, an estimated 40.8 million people were living with HIV worldwide, with over one million new infections (UNAIDS: Global AIDS Update 2025). Eastern and Southern Africa carry the largest burden, with several countries sustaining

adult prevalence of HIV above 15%. Asia and the Pacific account for roughly a quarter of global new infections, while Latin America and Eastern Europe and Central Asia have seen net increases, especially the Russian Federation. Russia's epidemic is expanding, with over one million people living with HIV and oncology sources also report increased HIV-associated KS presentations (Lebedev et al., 2025; Ogarkova et al., 2023). Globally, HIV prevalence is far higher than in the general population among MSM, people who inject drugs, sex workers, transgender people, and people in prisons (Mody et al., 2024). Women and girls accounted for 45% of new infections in 2024 worldwide, and 63% in sub-Saharan Africa, reflecting entrenched gender, social, and economic vulnerabilities (UNAIDS: Global AIDS Update 2025). As KS incidence mirrors untreated HIV, the efforts to control HIV epidemic is of importance also in controlling surges in KS cases.

2.3.2 Treatment of KS

Management of KS is individualized according to lesion type and extent, and typically requires a multidisciplinary approach beyond dermatology for accurate assessment and longitudinal monitoring. The primary goals of KS treatment are to slow disease progression, reduce tumor burden and associated edema, prevent organ involvement, and minimize psychological distress (Schneider & Dittmer, 2017). Although several therapeutic options are currently available – including liposomal doxorubicin, radiation therapy, surgery, traditional chemotherapeutics, and novel agents such as immune chechkpoint blockage therapy, angiogenesis inhibitors, tyrosine kinase inhibitors, and matrix metalloproteinase inhibitors (Losay & Damania, 2025) – none of these are curative and overall prognosis remains poor (70% 5-year survival). WHO's clinical guidelines note that no direct antiviral prevention of KSHV infection exists in routine practice.

For HIV-associated KS, combination antiretroviral therapy (cART), targeting HIV, is the most effective first-line intervention. Before the development of cART in 1996, around 50% of people living with HIV and detectable KSHV developed KS (Whitby et al., 1995). With widespread cART access in high-income settings, KS incidence declined and outcomes improved substantially (Ambinder & Cesarman, 2007; Boshoff & Weiss, 2002; Eltom et al., 2002). However, while cART can reduce tumor size and control disease progression, it does not eradicate the underlying KSHV infection or fully prevent recurrence. ART coverage continues to expand and 77% of all people living with HIV are on treatment in 2024, but this still falls short of universal control (UNAIDS). The access to cART remains uneven and in some regions policies that stigmatize LGBTQ people, restrict harm reduction, and constrain civil society limit prevention and care.

AIDS-related KS is still widespread in sub-Saharan Africa due to persisting HIV epidemic and unavailability of antiretroviral therapy (Chokunonga et al., 2000; Wabinga et al., 1993). KS remains a significant health burden and persistent clinical challenge particularly in low-resource settings as even standard therapies can be difficult to deliver owing to cost and logistical constraints (Damania & Dittmer, 2023). KS can be life-threatening, especially among patients with advanced or cART-resistant disease (Cesarman et al., 2019), and patients may undergo repeated cycles of expensive, toxic chemotherapy with significant long-term risks. WHO-aligned studies estimate that over 70% of incidence and nearly 87% of deaths from KS occur in sub-Saharan Africa (Ibrahim Khalil et al., 2022). Reflecting these disparities, a prospective cohort of cART-naïve, HIV-positive patients with KS demonstrated a 2.5-fold higher risk of KS-IRIS and a 3-fold higher overall mortality in sub-Saharan Africa versus a United Kingdom cohort (Letang et al., 2013). These findings underscore the urgent need for more effective, yet affordable and accessible, treatment strategies.

Given that KS is driven by KSHV-infection, the virus itself presents an attractive therapeutic target. However, as with other herpesviruses, complete eradication of KSHV remains unachievable. Most current treatments are nonspecific, carry substantial toxicity, and fail to eliminate latent reservoirs, limiting durability. LANA, essential for episome maintenance and latency, is a compelling target, yet no approved therapies directly inhibit it. Also, no vaccine is currently available, although several strategies are in preclinical development, mainly targeting key viral glycoproteins such as K8.1 (Losay & Damania, 2025). The progress is hampered by incomplete definition of protective immunity, the challenges of latent infection, and relatively low KS incidence in most regions with resources for further investigation.

To overcome these limitations, a deeper understanding of KSHV pathogenesis and the molecular mechanisms governing viral persistence is needed. In particular, targeting the viral or host factors essential for maintaining latency may hold the key to disrupting persistent infection and, ultimately, achieving viral clearance. Investing in the development of targeted antivirals or host-directed therapies represents a promising direction for more precise and less toxic therapeutic strategies for KS. These approaches have the potential to improve outcomes in patient populations where conventional therapies are inadequate or inaccessible.

2.3.3 Endothelial origin of KS spindle cells

KSHV infects a broad range of cell types, including endothelial cells (ECs), B cells, epithelial cells, dendritic cells, monocytes, and fibroblasts (Cesarman et al., 2019). Despite this tropism, KS is defined by the proliferation of SCs derived from ECs, which

in physiological conditions line blood and lymphatic vessels. These EC-derived SCs constitute the histopathological hallmark of KS and are major drivers of the tumor's aberrant vasculature.

In advanced KS lesions, SCs express several markers characteristic of endothelial, but also some markers of mesenchymal, fibroblast, smooth muscle, and other lineages, highlighting the heterogeneous nature of the SC population (Gessain & Duprez, 2005). In ECs, KSHV infection triggers cytoskeletal remodeling that yields the spindle-shaped morphology and induces profound changes in cellular metabolism, proliferation, and gene expression. SCs display heightened angiogenic and migratory capacity, reinforcing their tumorigenic phenotype (Cheng et al., 2011; Ojala & Schulz, 2014; Wang & Damania, 2008). These features underscore the central role of KSHV-induced endothelial reprogramming in KS pathogenesis. KSHV can also induce endothelial-to-mesenchymal transition (EndMT) by activating Notch signaling through the viral proteins vFLIP and vGPCR (Cheng et al., 2011; Gasperini et al., 2012). The latent gene product vFLIP has also been shown to drive primary ECs toward a spindle-cell morphology (Alkharsah et al., 2011) by acting as a sustained activator of the NF-κB pathway (Liu et al., 2002). NF-κB activity correlates with increased cell survival and proliferation and inhibition of apoptosis in KSHV-infected cells (Grossmann & Ganem, 2008).

Among endothelial subtypes, lymphatic endothelial cells (LECs) show a distinctive susceptibility to KSHV (Choi et al., 2020; DiMaio et al., 2020; Golas et al., 2019). Compared with blood endothelial cells (BECs), LECs more readily support viral entry, genome maintenance, and spontaneous reactivation, culminating in the release of infectious virions. The capacity to spontaneously reactivate is unique to LECs, and gives rise to asynchronous infection program. Also this points out to LEC origin as most SCs in KS lesions harbor latent KSHV, however a minority of cells are undergoing spontaneous lytic reactivation to serve as a reservoir for *de novo* infection and viral spread (Gramolelli & Schulz, 2015). This KSHV-induced reprogramming of LECs during latency, together with the inflammatory microenvironment due to sustained lytic reactivation, drives tumorigenic traits such as invasiveness and angiogenesis towards SC phenotype (Gramolelli & Ojala, 2017) (**Figure 4**).

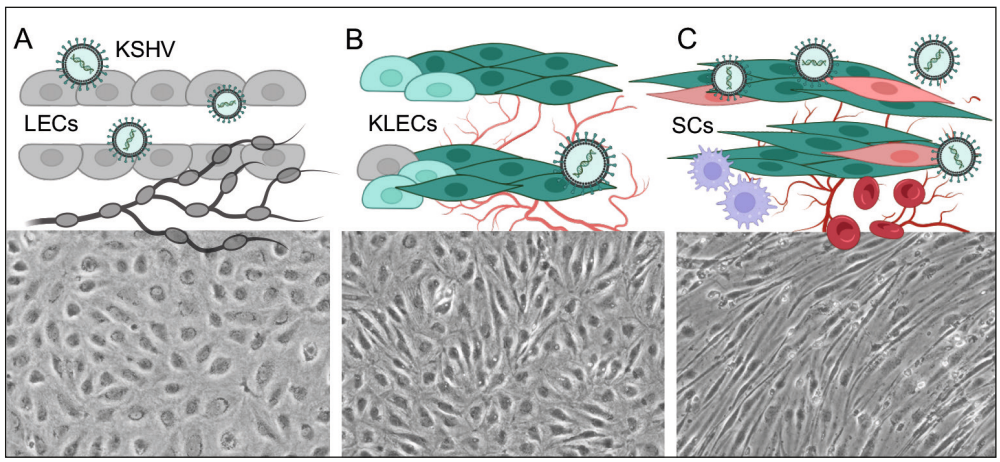

Figure 4. Schematic model of a KS lesion development (upper panels) and corresponding steps in spindle cell (SC) formation from lymphatic endothelial cells (LECs) in vitro (below panels) upon KSHV-infection. **A.** KSHV virions infect LECs. **B.** Early KS lesion where latently infected KLECs start to resemble spindle cells (green). **C.** Late KS lesion with latent SCs (green) as dominant cell type, and a fraction in lytic phase (red) to maintain infected cell population. Pro-angiogenic and inflammatory cytokines attract immune cells (purple) to the infected site. Angiogenesis takes place and causes the extravasation and accumulation of red blood cells (RBC: red). Upper panels are created with BioRender, lower panel images are taken by the author.

Notably, KSHV can reprogram BECs toward a lymphatic phenotype, and the transcriptional profile of KS lesions more closely resembles LECs than BECs (Hong et al., 2004). Together with evidence from a recent mouse model in which the complete KSHV genome induced KS-like vascular tumors expressing lymphatic markers (Sin et al., 2024), these observations suggest that LECs are not only permissive but likely central to KS tumorigenesis. Nevertheless, lymphatic-specific host factors that support oncogenic KSHV infection remain incompletely defined.

Beyond mature ECs, circulating endothelial precursors may also contribute to KS. Endothelial colony-forming cells (ECFCs) are a subset of CD34-positive progenitors capable of homing to sites of active angiogenesis (Asahara et al., 1997; Le Ricousse-Roussanne et al., 2004). Their precise role in neovascularization and KS development, however, remains debated. Evidence from transplantation medicine is suggestive: in a post-transplant KS case, lesions developed in distal extremities and the tumor SCs were genetically matched to the donor rather than the recipient (Barozzi et al., 2003), implying that circulating KSHV-infected progenitors from the donor may have seeded the lesions. In support of this idea, KSHV-positive ECFCs have been isolated from patients with classic KS (Della Bella et al., 2008). It has therefore been proposed that KSHV-infected ECFCs circulate systemically and contribute to lesion formation (Cancian et al., 2013;

Della Bella et al., 2008; Yoo et al., 2011). Additional work is needed to define their conclusive role in KSHV pathobiology.

2.4 Lymphatic endothelial cells

The specification of LECs from venous endothelial precursors is a critical developmental event, tightly regulated by transcriptional programs. Unlike BECs, which form the lining of blood vessels and blood vascular system, LECs are specialized endothelial cells that form the thin-walled, highly permeable vessels of the lymphatic system (Alitalo et al., 2005).

2.4.1 Development of lymphatic vasculature

The circulatory system consists of endothelial cells forming blood and lymphatic vessels interconnected to form a complex and functional network able to deliver oxygen, nutrients and hormones throughout the body and to regulate fluid homeostasis and metabolic waste products. The lymphatic vasculature additionally mediates dietary fat absorption and immune cell trafficking as part of immune surveillance (Alitalo et al., 2005; Witte et al., 2001). The formation of new blood and lymphatic vessels – angiogenesis and lymphangiogenesis, respectively – occurs primarily during embryogenesis. Nevertheless, vascular plasticity persists into adulthood to support tissue repair and remodeling, but may also contribute to the pathological processes, such as in KS (Adams & Alitalo, 2007).

During embryogenesis, mesoderm-derived endothelial precursors assemble into a primary vascular plexus that remodels via angiogenesis into a hierarchical vascular tree. BECs subsequently acquire tissue-specific specializations of the vascular endothelium (Alitalo et al., 2005). After cardiovascular development is underway, a subset of venous ECs commits to the lymphatic lineage and sprouts from the embryonic cardinal veins to generate lymph sacs and the early lymphatic plexus, ultimately forming the lymphatic system (Wigle & Oliver, 1999; Yang & Oliver, 2014). Differentiated LECs are distinguished from BECs by characteristic gene-expression programs. Blood and lymphatic vessel morphogenic events in both the normal development and in pathological remodeling are mediated by vascular endothelial growth factors (VEGFs) and their receptors (VEGFRs). VEGFR-1 and -2 expressions are specific for BECs whereas VEGFR-3 (FLT-4) is predominantly expressed in LECs (Ferrara et al., 2003; Makinen et al., 2001). Among VEGFs, VEGF-A is the dominant angiogenic cue that drives endothelial proliferation, sprouting, and permeability mainly via VEGFR-2 on BECs (Ferrara et al., 2003; Leung et al., 1989). By contrast, VEGF-B signals chiefly through VEGFR-1 with context-dependent effects (Olofsson et al., 1996), whereas proteolytically activated

VEGF-C engages VEGFR-3 (and to lesser extent VEGFR-2) to promote lymphatic sprouting and growth (Alitalo et al., 2005; Tammela & Alitalo, 2010).

Markers such as podoplanin, LYVE-1, CD31/PECAM-1, VE-cadherin, and CD34 are widely used to identify and characterize lymphatic endothelium. Podoplanin is a transmembrane glycoprotein expressed on LECs that maintains lymphatic vessel integrity, promotes cell migration, and facilitates separation of lymphatic and blood vasculature (Breiteneder-Geleff et al., 1999). LYVE-1 (lymphatic vessel endothelial hyaluronan receptor-1) is enriched in initial lymphatic capillaries, where it mediates hyaluronan uptake and contributes to immune cell trafficking, though its expression is not strictly lymphatic-specific (Banerji et al., 1999). CD31/PECAM-1 is expressed on both BECs and LECs, where it maintains endothelial junctions and mediates leukocyte transmigration; accordingly, it serves as a general endothelial marker rather than a lymphatic-specific protein (Newman, 1997). VE-cadherin (cadherin-5/CDH5) is an endothelial-specific adherens-junction protein localized to cell-cell contacts; it is widely used as a marker of endothelial identity and is essential for vascular integrity and development (Carmeliet et al., 1999; Navarro et al., 1998). CD34 is best known on hematopoietic progenitors, but it is also linked to endothelial precursors and constitutively expressed by endothelium, especially capillaries and small vessels (Pusztaszeri et al., 2006). Together, these markers delineate endothelial identity and function in physiological settings, yet are dynamically regulated in pathology, making them informative biomarkers of vascular state.

Several studies show that SCs in KS lesions express pan-endothelial markers CD31/PECAM-1 and CD34 (Gasperini et al., 2012), together with LEC-resticted podoplanin, LYVE-1, and VEGFR-3 (Hong et al., 2004; Wang et al., 2004), consistent with lymphatic endothelial lineage of SCs. Moreover, SCs express upstream developmental transcription factors (TF) that function as the master regulators of LEC identity and fate.

2.4.2 Key transcription factors in LEC specification

The coordinated activity of the developmental TFs SOX18 and COUPTF2 (also known as NR2F2) forms a core module governing the earliest steps of LEC specification. By directly inducing the prospero-related homeobox transcription factor PROX1, these three factors initiate a stable lymphatic gene expression program that underpins the development and expansion of the lymphatic vasculature (Aranguren et al., 2013; Duong et al., 2012; Francois et al., 2008; Srinivasan et al., 2010; Wigle & Oliver, 1999). Although COUPTF2 alone is insufficient to initiate *PROX1* transcription, its cooperation with SOX18 is essential for establishing and maintaining LEC identity. COUPTF2 also shapes a broader transcriptional environment favoring lymphatic over

blood endothelial fate by repressing arterial programs and supporting lymphatic gene expression. SOX18 is critical during early developmental stages but dispensable for maintenance of mature LECs, whereas PROX1 remains required (Francois et al., 2008; Srinivasan et al., 2010). Once specified, PROX1-positive cells upregulate VEGFR-3 and sprout from the embryonic cardinal vein in response to VEGF-C signaling, initiating the primitive lymphatic plexus. PROX1 is essential for acquisition of LEC identity and drives initial lineage commitment during embryogenesis. Beyond lymphatic development, PROX1 regulates organogenesis in the lens (Wigle et al., 1999), liver (Sosa-Pineda et al., 2000), pancreas (Burke & Oliver, 2002), brain (Lavado & Oliver, 2007), inner ear (Kirjavainen et al., 2008), and heart (Risebro et al., 2009). Dysregulated PROX1 expression and function are implicated in multiple human cancers, with context-dependent tumor-suppressive or oncogenic roles (Elsir et al., 2012).

KSHV infection of differentiated BECs reprograms them toward a lymphatic-like state by inducing LEC-specific genes, including PROX1, while downregulating blood-vascular programs, resulting in a partial LEC phenotype (Hong et al., 2004). In KS, PROX1 expression increases from early lesions to advanced nodules, with the majority (over 90%) of neoplastic spindle cells positive for PROX1, supporting its involvement in KS pathogenesis (Benevenuto de Andrade et al., 2014). The roles of the upstream factors SOX18 and COUPTF2 in KSHV infection and in KS lesions remained incompletely defined.

2.4.3 Transcription factor SOX18

The SOX18 gene encodes a TF of the SOX (SRY-related HMG-box) family. In humans, SOX proteins comprise 20 paralogs grouped into eight classes (A-H) (Bowles et al., 2000). SOX factors are an essential transcriptional regulators for physiological development and in pathological conditions. They share a high-mobility group (HMG) box DNA-binding domain that confers high-affinity sequence recognition (Sinclair et al., 1990). The SOX HMG-box protein can bind linear DNA to the sequence motif (A/T A/T CAA A/T G) at a high affinity (Hosking et al., 1995), enabling diverse roles in embryogenesis, developmental disorders, and carcinogenesis (Lovell-Badge, 2010).

SOX18, together with SOX7 and SOX17, belongs to the conserved SOXF subfamily, which is characterized by a transactivation domain adjacent to the C-terminus of the HMG box and requirement of protein-protein interactions for full transcriptional activity (Francois et al., 2008). Beyond SOX18, other SOXF members participate in VEGF- driven angiogenesis and lymphangiogenesis (Francois et al., 2008). Through these processes, SOXF factors contribute to wound healing and, when dysregulated or mutated, to neoangiogenesis and cancer metastasis (Downes & Koopman,

2001; Schock & LaBonne, 2020). SOXF activity is also implicated in cardiac muscle formation, hematopoiesis, and hair-follicle development (He et al., 2023; Liu et al., 2007; Nobuhisa et al., 2024). All SOXF proteins can heterodimerize with one another and with other TFs on DNA. Uniquely, SOX18 can also homodimerize via a distinct binding architecture: it engages DNA cooperatively at an IR5 consensus composed of two inverted SOX18 motifs separated by five nucleotides (Moustaqil et al., 2018). SOX18 dimerization at IR5 sites modulates an endothelial-specific transcriptional program and influences endothelial-cell fate by regulating target genes harboring this motif in their promoters.

SOX18, together with SOX7 and SOX17, belongs to the conserved SOXF subfamily, which is characterized by a transactivation domain adjacent to the C-terminus of the HMG box and requirement of protein-protein interactions for full transcriptional activity (Francois et al., 2008). Beyond SOX18, other SOXF members participate in VEGF-driven angiogenesis and lymphangiogenesis (Francois et al., 2008). Through these processes, SOXF factors contribute to wound healing and, when dysregulated or mutated, to neoangiogenesis and cancer metastasis (Downes & Koopman, 2001; Schock & LaBonne, 2020). SOXF activity is also implicated in cardiac muscle formation, hematopoiesis, and hair-follicle development (He et al., 2023; Liu et al., 2007; Nobuhisa et al., 2024). All SOXF proteins can heterodimerize with one another and with other TFs on DNA. Uniquely, SOX18 can also homodimerize via a distinct binding architecture: it engages DNA cooperatively at an IR5 consensus composed of two inverted SOX18 motifs separated by five nucleotides (Moustaqil et al., 2018). SOX18 dimerization at IR5 sites modulates an endothelial-specific transcriptional program and influences endothelial-cell fate by regulating target genes harboring this motif in their promoters.

2.4.4 SOX18 in vascular anomalies

Due to the important role of SOX18 during embryogenesis, changes in expression or mutations in the gene can result in developmental disorders. Mutations in SOX18 are linked to hereditary lymphedema, specifically hypotrichosis-lymphedema-telangiectasia (HLTS) and a renal-defect variant (HLTRS) (Irrthum et al., 2003). This is a rare condition, characterized by sparse hair, alopecia totalis, lymphedema, and telangiectatic lesions, and in some cases also renal malfunction. Both dominant and recessive alleles are described, including a dominant-negative nonsense variant, p.Cys240Ter (C240X), which truncates the C-terminal transactivation domain and has been reported in HLTRS families (Dailey et al., 2022; Irrthum et al., 2003).

Recently, SOX18 has been shown to have an etiological role in vascular neoplasms and tumor vascularization. Development of infantile hemangioma (IH) tumors, made up of proliferating hemangioma endothelial cells (HemECs), has been

associated to SOX18 (Holm et al., 2025; Holm et al., 2024; Overman et al., 2019). IH is the most common benign vascular tumor of infancy, affecting about 4-5% of infants. For most children it poses no serious risk, however, about 10-15% of IHs cause serious problems, such as cutaneous expansion, ulceration, and necrosis, particularly in facial features. This may cause disfigurement, and functional impairment including vision loss and airway obstruction, and also consumptive hypothyroidism and high-output cardiac failure is reported. It has been shown that SOX18 is upregulated in proliferating IH tissue and activates key downstream genes, which promotes a lymphatic-like or immature endothelial phenotype which is the hallmark of hemangioma cells (Holm et al., 2024).

2.4.5 Pharmacological targeting of SOX18

Because of its emerging role in pathological conditions, SOX18 has been pursued as a molecular drug target. Despite the general difficulty of inhibiting TFs with small molecules, a compound, Sm4, was identified to inhibit SOX18 protein activity. Sm4 is an analog of a natural product found from the brown alga *Caulocystis cephalornithos*, native in Australian and Tasmanian coastal regions (Fontaine et al., 2017). The compound was discovered via high-throughput screening of marine extracts (Marine Chemical Diversity Library) collected from a selection of Australian and Antarctic marine organisms. Structurally, Sm4 is a salicylic acid (ortho-hydroxybenzoic) derivative with a scaffold core similar to the natural product and additional hydrophobic naphthalene group connected via an ethyl spacer. Mechanistically, Sm4 exerts its effects by selectively disrupting SOX18 dimerization, thereby suppressing its transcriptional activity and output *in vitro.* Binding of Sm4 likely alters SOX18 protein conformation, affecting both DNA binding and interaction surfaces with protein partners disrupting their recruitment (Fontaine et al., 2017). In a pre-clinical *in vivo* mouse model of breast cancer, Sm4 treatment significantly improved survival by reducing tumor vascular density and metastatic spread (Overman et al., 2017). These findings led to the biotech spin-off Gertrude Biomedical Pty Ltd (Australia), now developing new generation of SOX18-targeted molecules.

More recently, SOX18 inhibition was also achieved by two FDA-approved beta (β) blockers, propranolol and atenolol. Propranolol acts as a non-selective antagonist of β_1- and β_2-adrenergic G protein-coupled receptors (GPCR), and atenolol is β_1-selective. Both are raremic 1:1 mixtures of S(-) and R(+) enantiomers, meaning mirror-image molecules. The S(-) enantiomers are potent β blockers, while the R(+) enantiomers are largely devoid of this activity. However, R(+) enantiomers have been recently shown to specifically interfere with SOX18 activity (Holm et al., 2025; Overman et al., 2019; Seebauer et al., 2022). Chemical structures and proposed mechanisms of SOX18 inhibitors Sm4 and propranolol are presented in **Figure 5**.

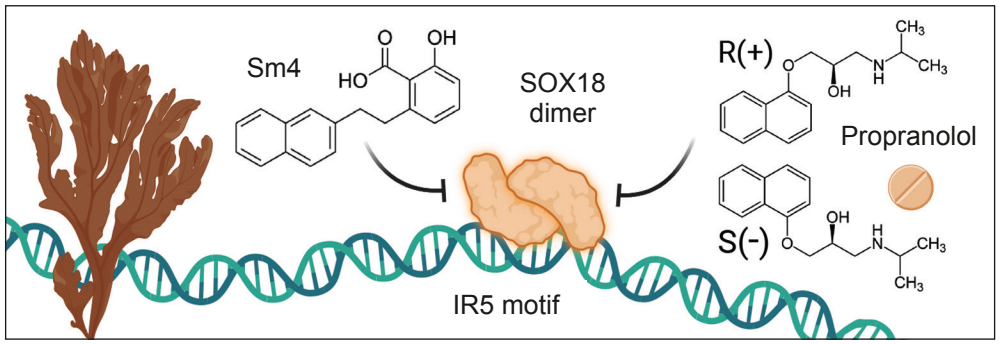

Figure 5. Pharmacological SOX18 targeting; small molecule inhibitor Sm4 and R(+) enantiomer of FDA-approved propranolol both disrupt SOX18 dimer formation and DNA-binding. Image created with Biorender.

These findings have led to the repurposing of propranolol in patients with HLTRS, providing evidence for the pharmacogenetic interaction between SOX18 and propranolol in a vascular disease. Oral propranolol is also the only FDA-approved drug and the standard systemic therapy for IH. Proposed mechanisms in IH include rapid vasoconstriction, anti-angiogenic effects (reduced VEGF), and induction of HemEC apoptosis. Notably, SOX18-targeted inhibition using Sm4 or the R(+) enantiomer of propranolol phenocopies key therapeutic effects independent of the β-blockade (Overman et al., 2019; Seebauer et al., 2022). This suggests that SOX18 inhibition may be a key mechanism in the therapeutic effect of propranolol in IH, and represent possibilities for targeting SOX18-related mechanisms, with fewer side effects compared to the systemic β-adrenergic blockade. The reported β-blockade side-effects include hypotension, bradycardia, peripheral vasospasm, bronchospasm, hypoglycemia and seizures, sleep disturbance, and potentially adverse neurocognitive outcomes in infants (Bar et al., 2022; Leaute-Labreze et al., 2016). As isolated pure R(+) propranolol is not available for clinical therapeutic use as of yet, other options are considered to target SOX18 downstream mechanisms in HemECs. Recently, mevalonate pathway (MVP) was discovered as a target of R(+) propranolol, representing therapeutic opportunity to use statins, that were recently shown to efficiently suppress IH vessel formation via SOX18-MVP axis (Holm et al., 2025).

Propranolol was a revolutionary discovery in the 1960s by Sir James Black, who sought to reduce the heart's oxygen demand in patients with angina (Stapleton, 1997). By developing the first successful β blocker, he earned the Nobel Prize in 1988 for a drug that transformed cardiovascular medicine. Today, propranolol is still widely used to treat a variety of conditions, including high blood pressure, irregular heartbeats, and angina. Its uses have expanded beyond heart-related issues, and it is commonly prescribed for the prevention of migraines, the management of essential tremors, and to reduce the physical symptoms of anxiety due to its β blocker activity (Archer et al., 2025; Zesiewicz et al., 2011). Included in the

WHO's list of essential medicines, propranolol is generally inexpensive and globally accessible. This low cost, combined with its simple oral administration and stable storage requirements, makes it a highly accessible and practical treatment option in various healthcare settings. Propranolol's use for vascular anomalies is a prime example of drug repurposing and further exploration of propranolol for other pathological conditions is ongoing.

2.5 Pioneer transcription factors

Transcription factors (TFs) are essential proteins that orchestrate the initiation and regulation of gene expression by binding specific DNA sequences at promoters and enhancers. Acting as molecular switches, they integrate signals from the cellular environment to modulate transcription through protein-protein interactions and epigenetic modifications. Beyond transcriptional control, TFs regulate chromatin organization and condensation, which are critical processes for cellular homeostasis, differentiation, and cell-fate decisions (Shaban et al., 2024). Functionally, TFs are often grouped into three categories: pioneer factors, which establish chromatin accessibility; settler factors, which maintain chromatin conformation; and migrant factors, which primarily adjust transcription rates (Sherwood et al., 2014).

Pioneer TFs can bind target motifs within condensed chromatin, even when nucleosomes partially occlude those sites. Their binding can destabilize local nucleosome structure or recruit chromatin-remodeling complexes, thereby opening previously inaccessible DNA regions (Bulyk et al., 2023; Neugebauer et al., 2023). This creates a permissive chromatin environment that enables additional factors to engage and, ultimately, reprograms gene expression (Zaret & Carroll, 2011). Several pioneer factors have been studied extensively for roles in development and disease. Members of the FoxA family are archetypal pioneers that govern cell identity in endoderm-derived organs such as the liver, pancreas, and lungs (Zaret & Carroll, 2011). Another pioneer, PU.1, shapes hematopoietic lineage commitment and immune cell identity (Heinz et al., 2010), while within the SOX family, SOX2 maintains pluripotency and neural lineage specification (Avilion et al., 2003).

Although direct evidence that viruses systematically hijack pioneer factors remains limited, many viruses exploit host transcriptional machinery in ways reminiscent of pioneer activity (Kgatle et al., 2025; Neugebauer et al., 2023). For example, oncogenic hepatitis B virus (HBV) can co-opt FoxA family pioneers to reprogram liver cells (Chen et al., 2024). During latent infection, EBV exploits PU.1 to activate latency-associated genes essential for B-cell immortalization (Laux et al., 1994; Zhao et al., 2011). The capacity of pioneer TFs to reshape chromatin makes them compelling targets for future studies on viral manipulation of host gene regulation.

2.6 Chromatin architecture

Genomic DNA is normally tightly condensed in a structure known as chromatin. Chromatin is composed of nucleosomes, which is a stretch of DNA approximately 147 base pairs long, wrapped around an octamer composed of two copies of the four core histone proteins: H2A, H2B, H3, and H4 (Clapier & Cairns, 2009). This structure serves for the efficient storage and regulation of DNA, and presents a barrier to DNA-associated processes. Chromatin and nucleosome pattern regulate gene expression by controlling how accessible DNA is to replication and transcription machinery. The location and modification state of nucleosomes is dynamic, and regulates access to the DNA and partitions the genome into distinct chromatin states, primarily classified as euchromatin or heterochromatin (Clapier & Cairns, 2009), depicted in **Figure 6**.

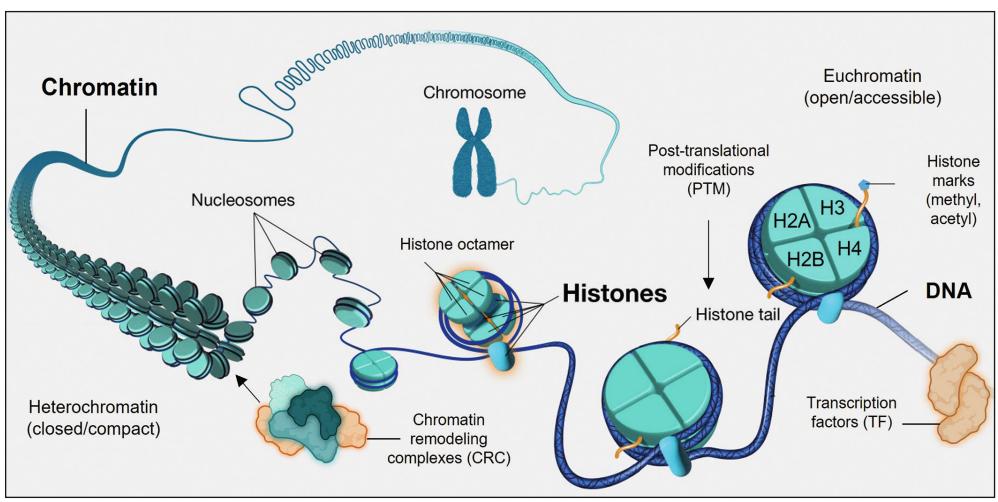

Figure 6. Chromatin architecture and modification events. Modified with the permission from the publisher NIH educational recources.

Euchromatin is a loosely packed form of chromatin associated with actively transcribed genes. Its open configuration allows TFs and RNA polymerase to access DNA. Euchromatin is typically enriched in histone acetylation (e.g. H3K9ac) and activating methylation marks (e.g. H3K4me3). It tends to occupy the interior of the nucleus and appears lightly stained under electron microscopy due to its low density (Allis & Jenuwein, 2016). Heterochromatin is a tightly packed form of chromatin linked to transcriptional repression. It is enriched in repressive histone modifications (e.g. H3K9me3 and H3K27me3) and is often located at the nuclear periphery or surrounding nucleoli. Microscopically, heterochromatin appears as dark, electron-dense regions. A hallmark marker of heterochromatin formation and integrity is heterochromatin protein 1α (HP1α), which binds H3K9me3 and contributes

to chromatin compaction (Schoelz & Riddle, 2022). HP1α can spontaneously phase-separate in solution, forming liquid-like droplets that preferentially sequester heterochromatin components such as nucleosomes and DNA, thereby promoting gene silencing (Bartkova et al., 2011; Larson et al., 2017; Strom et al., 2017).

2.6.1 Chromatin remodeling

Chromatin remodeling is the dynamic reorganization of chromatin architecture to regulate access to underlying DNA. Because DNA is wrapped around histone octamers to form nucleosomes, its accessibility to TFs, replication machinery, and repair enzymes is inherently limited. Chromatin remodeling mechanisms modify this structure classically either via opening to activate or via compaction to repress, thereby controlling gene expression and genome stability (Clapier & Cairns, 2009). Dysregulation of remodeling complexes is implicated in cancer, developmental disorders, and viral infection strategies, including the recruitment of chromatin remodelers by viral proteins to reprogram host chromatin (Allis & Jenuwein, 2016).

Regulation of nuclear events, such as gene expression, DNA replication, repair, or recombination, are conducted with both ATP-dependent multiprotein complexes, known as chromatin remodelers, and ATP-independent chromatin remodeling mechanisms, such as histone post-translational modifications (PTM). The N-terminal tail of histones protrudes from the nucleosomes and as such, is subject to various PTMs, including acetylation, methylation, phosphorylation and ubiquitination. These regulatory mechanisms have been shown to work in conjugation with chromatin remodeling complexes for a more efficient spatial and temporal regulation of gene expression and DNA replication (Singh et al., 2023). Specific protein complexes, such as chromodomain helicase DNA-binding (CHD), SWItch/Sucrose Non-Fermentable (SWI/SNF), imitation switch (ISWI), and INO80, dynamically reorganize chromatin. These complexes can interact with the nucleosomes and use the energy from ATP hydrolysis to alter their structure, allowing for traditional TFs to access the DNA and initiate transcription (Clapier & Cairns, 2009).

2.6.2 SWI/SNF (BAF) complex

One of the ATP-dependent chromatin remodelers in mammals is SWI/SNF complex also known as BRG1/BRM-associated factor (BAF) complex, that plays a vital role in regulating genomic architecture. SWI/SNF complexes are multimeric and highly conserved across eukaryotes; they modulate transcription by increasing DNA accessibility, often after recruitment to regulatory DNA by pioneer TFs and other cofactors. These remodelers slide or evict nucleosomes to facilitate accessibility and thereby regulate nuclear processes (Kruger et al., 1995; Wang et al., 1996). This allows for the BAF complex to disrupt the nucleosome,

expose regulatory regions in the DNA, and most often activate gene expression (Muchardt & Yaniv, 1999).

Remodeling activity of SWI/SNF depends on ATP hydrolysis by the core ATPase subunits BRG1 or BRM (also known as SMARCA4/2), which drive nucleosome mobilization and eviction (Cohen et al., 2010). BRG1 has additionally been implicated in maintaining genome stability by promoting efficient replication-fork progression during DNA replication. The ATPase motor engages core histones H2A, H2B, H3, and H4, and nucleosome movement proceeds through transient disruption of histone-DNA contacts to reposition DNA around the octamer (Singh et al., 2023).

BAF complexes segregate into three major assemblies; canonical BAF (cBAF), PBAF, and non-canonical BAF (ncBAF). The AT-rich interactive domain-containing protein (ARID) subunits are the major determinants of complex assembly. ARID1A or ARID1B are found in assembly of cBAF, ARID2 in PBAF and ncBAF is ARID-independent (Mashtalir et al., 2018). ARIDs are the structural DNA-binding proteins responsible for stabilizing the complex and serving as the molecular hub. ARIDs also direct the ATPase activity with high affinity to bind chromatin and shown to interact with different TFs (Cohen et al., 2010; Wanior et al., 2021). Both ATPase and ARID subunits are critical for the proper functioning of the complex, however different complex formations are common in different physiological and pathological conditions, including up to 29 subunits and multiple paralogs, generating extensive diversity in composition (Mashtalir et al., 2018). Most commonly depicted assembly of cBAF is shown in **Figure 7**.

Over the past several years, connections between cancer and the SWI/SNF (BAF) complex has been uncovered, showing striking mutational frequencies in the genes encoding their subunits across a range of human diseases, from cancer to neurologic disorders. Large-scale cancer genome studies indicate that mutations in BAF-encoding genes occur in roughly 20% of human tumors, with recurrent driver alterations in ARID1A/B, ARID2, and BRG1/BRM, among others; ARID1A is among the most frequently mutated (Kadoch et al., 2013).

Recent work has yielded BAF-targeting small molecules, including proteolysis-targeting chimera (PROTAC) degraders, allosteric ATPase inhibitors, and bromodomain antagonists. The compounds ACBI1, FHT-1015, and PFI-3 work to either inhibit or degrade the BRG1 protein. The mechanisms of the compounds can be seen in **Figure 7**. ACBI1 is a PROTAC composed of a target-binding ligand linked to an E3-ligase recruiter and it directs the ubiquitin-proteasome system to BRG1/BRM for selective degradation (Farnaby et al., 2019). FHT-1015 is an allosteric inhibitor that binds outside the catalytic site, induces a conformational

shift in BRG1/BRM, and suppresses ATPase activity (Battistello et al., 2023). PFI-3 is a bromodomain inhibitor of BRG1/BRM that blocks recognition of acetyl-lysine marks, however the bromodomain blockade does not dislodge cBAF from chromatin or inhibit BRG1/BRM ATPase activity (Singh et al., 2023; Wanior et al., 2021).

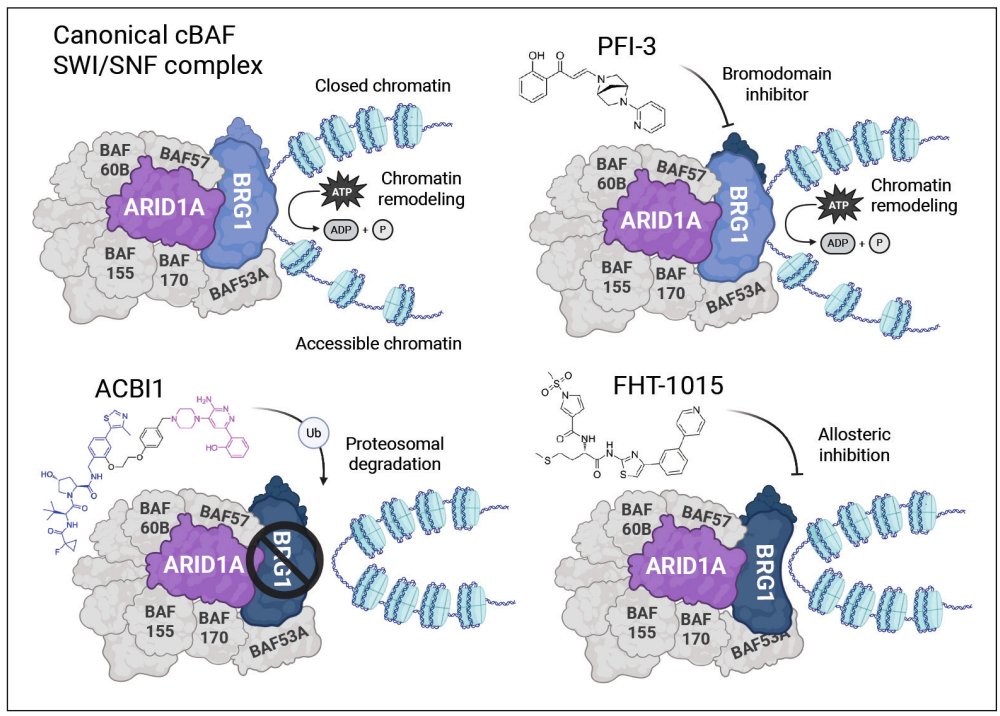

Figure 7. Model of the ATP-dependent chromatin remodeling activity of the SWI/SNF, also called cBAF complex and upon ACBI1, FHT-1015, and PFI3 inhibitor treatments. Created with BioRender.

2.6.3 Chromatin landscape in herpesvirus infection

For many herpesviruses, including the common herpes simplex virus (HSV) in addition to oncogenic EBV and KSHV, the host cell rapidly associates histones with the viral genome in the nucleus (Torne & Robertson, 2024). This chromatinization acts as a first line of defense, allowing the cell to impose transcriptionally repressive marks through heterochromatin protein complexes (Pei et al., 2020; Uppal et al., 2015). These modifications help to restrict productive lytic replication unless counteracted by viral proteins induced by various stimuli or immunosuppression. During latency, herpesvirus genomes as episomes are generally packaged into nucleosomes enriched in repressive histone marks such as H3K9me3 and H3K27me3, along with HP1α recruitment, to silence lytic genes (Toth et al., 2013). Upon reactivation, viral factors recruit chromatin remodelers and histone acetyltransferases (HATs) to remove repressive marks, increase histone acetylation

(e.g. H3K9ac, H3K27ac), and promote transcriptional activation of lytic genes (Lieberman, 2013). On the contrary, deacetylation by histone deacetylases (HDACs) often is associated with silencing of viral lytic gene expression.

Herpesviruses also often manipulate the host cell's chromatin landscape by modulating or hijacking host chromatin remodelers to create a nuclear environment favorable for their replication, persistence, and immune evasion (Pei et al., 2020). During latency, both KSHV and EBV actively reconfigure the host chromatin to promote its own survival, maintain latency, and consequently drive oncogenesis. EBV achieves this by hijacking host proteins and modifying the host's three-dimensional (3D) genome architecture (Tian et al., 2025; Wang et al., 2023). The EBV episome interacts with the nuclear lamina, a protein network that lines the inner nuclear membrane and helps to organize cellular chromatin (Caruso et al., 2022). EBV's latent nuclear antigens (EBNAs) interact with host transcription factors, such as YY1 to reconfigure 3D chromatin organization, strengthening topologically associating domains (TADs) and facilitating long-range enhancer-promoter communication. These changes can stabilize expression of host genes important for B-cell transformation and survival (Maestri et al., 2025).

Overall, the host and viral chromatin landscapes are key regulatory platforms in herpesvirus infection. The dynamic interplay between viral factors and host chromatin regulators determines whether the viral genome remains maintained in latency or is transcriptionally active during lytic replication. Understanding these processes offers insights into herpesvirus persistence and potential therapeutic targets.

3 AIMS OF THE STUDY

Kaposi sarcoma herpesvirus (KSHV) establishes latency in many susceptible cell types, but lymphatic endothelial cells (LECs) are uniquely permissive: they sustain high intracellular episome copy numbers and undergo spontaneous lytic reactivation that releases infectious virions. Sporadic reactivation and viral spread fuels Kaposi sarcoma (KS) progression by replenishing and expanding infected spindle cells, the hallmark KS tumor cells. What makes the lymphatic niche so supportive of the KSHV lifecycle has remained unclear.

During embryonic lymphangiogenesis, the transcription factors SOX18 and COUPTF2 promote LEC differentiation by inducing PROX1, the master regulator of lymphatic identity. This prompted us to test whether KSHV exploits this developmental circuitry to sustain persistence and drive pathogenesis. Although PROX1 induction has been linked to KSHV infection, the roles of SOX18 and COUPTF2 remained unexplored.

This thesis dissects lineage-dependent mechanisms by which KSHV hijacks the regulatory network of lymphatic endothelium to maintain infection and drive oncogenesis. The overarching aim is to define the host and viral factors that render lymphatic niche exceptionally permissive to KSHV infection, and to evaluate whether targeting these determinants can disrupt KSHV persistence and pathogenesis.

AIM 1 Define how lymphatic developmental transcription factors SOX18 and PROX1 regulate KSHV infection phases.

AIM 2 Test the translational potential of disrupting SOX18-dependent mechanisms in KSHV pathobiology using lymphatic endothelial precursor cell model.

AIM 3 Assess the impact of KSHV hijacking SOX18 to host chromatin organization and persistent infection in lymphatic endothelial cells.

4 MATERIALS AND METHODS

Table 1. List of the main methods with associated materials used in the studies of this thesis.

	Method	Study
4.1	Cell culture (primary cells, BSL2)	I, II, III
4.2	ECFC isolation (PBMC)	II
4.3	Virus production, KSHV infection and lentiviral transduction	I, II, III
4.4	Inhibitor treatments	I, II, III
4.5	Plasmid constructs and transient transfections	I, III
4.6	Luciferase reporter assay	I
4.7	Genetic RNA interference (siRNA)	I, II, III
4.8	Real time quantitative Polymerase chain reaction (RT-qPCR)	I, II, III
4.9	Quantification of intracellular viral DNA episome copies	I, II, III
4.10	Antibody concentrations	I, II, III
4.11	Immunoblotting (SDS-PAGE with WB)	I, II, III
4.12	Immunofluorescence (IF) staining	I, II, III
4.13	Immunohistochemistry (IHC) staining	I, II
4.14	Multiplex immunohistochemistry (mIHC) staining	I
4.15	Proximity Ligation Assay (PLA)	I, III
4.16	Co-immunoprecipitation (CoIP)	I
4.17	Chromatin immunoprecipitation PCR (ChIP-PCR)	I, III
4.18	Bromodeoxyuridine incorporation assay (BrdU-IP)	III
4.19	Flow cytometry (FC)	II
4.20	BioID protein interaction assay coupled with mass spectrometry	III
4.21	Cell viability assays (CTG, Trypan Blue)	II, III
4.22	Cell proliferation assay (EdU)	I, II
4.23	Soft agar assay	II
4.24	Virus release assay	I, II
4.25	Spheroid 3D assay	II
4.26	Image acquisition and analysis	I, II, III
4.27	Microscopic imaging of epigenetic landscape (MIEL)	III
4.28	Assay for Transposase-Accessible Chromatin-sequencing (ATAC-seq)	III
4.29	Global gene expression analysis with RNA-sequencing (RNA-seq)	I, II, III
4.30	*In vivo* mouse model development and SOX18 inhibition	II

4.1 Cell culture

Primary human endothelial cells LEC (juvenile, dermal) and BEC (Promocell; C-12216, C-12211), Endothelial colony-forming cells (ECFCs; isolated from PBMC) and human umbilical vein EC (HUVEC; ATCC) were maintained in EBM-2 supplemented with EGM-2 (Lonza; CC-3202, CC-4147) or Microvascular MV-2 (Promocell; C-22121) medium supplemented with 5% fetal bovine serum, basic fibroblast growth factor, insulin-like growth factor 3, epidermal growth factor, gentamicin sulfate/amphotericin, ascorbic acid, and hydrocortisone; VEGF was not added. LECs and BECs were used until passage 6, ECFCs until passage 8.

iSLK.219 (Myoung & Ganem, 2011) is an RTA -inducible renal-cell carcinoma SLK cell line, stably infected with a recombinant KSHV.219 (Vieira & O'Hearn, 2004). iSLK.BAC16-ΔORF50 cells are stably infected with a bacterial artificial chromosome (BAC) with recombinant ΔORF50-KSHV (Weissmann et al., 2025). HeLa, HEK293FT, U2OS, SLK and iSLK.219 were grown in DMEM (BioNordika; ECB7501L), supplemented with 10% FBS (Gibco; 10270-106), 1% L-glutamate (BioNordika; ECB3000D), and 1% penicillin/ streptomycin (BioNordika; ECB3001D). iSLK.219 cells were also supplied with 10µg/mL puromycin (Sigma; P8833), 600µg/mL hygromycin B (Invitrogen; 687010), and 400µg/mL Geneticin G418 (Roche; 04727878001). iSLK.BAC16-ΔORF50 cells were supplemented with 0.5µg/ml puromycin, 200µg/ml hygromycin, and 1000µg/ml G418. Cancer and HEK cell lines were used for approximately up to 15-20 passages.

All cells used in this study are listed in **Table 2**. Virus-infected cells were handled in was performed in bio-safety level 2 (BSL2) cell culture facility. All cells were propagated in a humified incubator at standard conditions. Cells were regularly tested negative for *Mycoplasma* (MycoAlert Mycoplasma Detection Kit, Lonza; LT07-705).

Table 2. The list of cells used in this study.

Cells	Source / reference	Study
LEC	Promocell C-12216	I, II, III
BEC	Promocell C-12211	I
ECFCLY	Healthy donor PBMC isolation	II
ECFCBL	Healthy donor PBMC isolation	II
HUVEC	ATCC CRL-4053	III
HeLa	ATCC CCL-2; RRID:CVCL_0030	I, II, III
U2OS	ATCC HTB-96	I
HEK293FT	Thermo Fisher, R70007; RRID:CVCL_6911	I, II, III
iSLK.219	Myoung & Ganem, 2011. A gift from Arias, C. (Biohub SF, CA, USA)	I, II, III

SLK	A gift from Schulz, T. (MHH, Hannover, GE)	III
iSLK.BAC16-ΔORF50	Weissmann et al. 2025. A gift from Grundhoff, A. (LIV, Hamburg, GE)	III

4.2 Isolation of ECFCs from PBMCs

For isolation of an adherent ECFCs, fresh blood bags were obtained from healthy donors by the Finnish Red Cross Blood Services (Helsinki, Finland) as buffy coat concentrates devoid of platelets (permission numbers 7507, 21/2020 and 6318, 14/2023). After dilution of 1:2 in PBS (Corning; 21-040-CV), the peripheral mononuclear cells (PBMCs) were isolated according to manufacturer's instructions using SepMate tubes (STEMCELL Technologies; 146138) and Cytiva Ficoll-Paque PLUS density gradient media (Fisher Scientific; 45-001-749). The final number of mononuclear cells separated from each donor's blood bag was approximately 1.5x10^7 cells/mL, yielding a total of 200 million cells. The cells were transferred onto a fibronectin 25 µg/mL (Sigma; F0895) and 15 µg/mL rat tail collagen (Merck; 7661) pre-coated cell culture 6-well plate with EGM-2 basal endothelial media (Lonza) 3 mL/well. Cultures were followed up to three weeks, washing away any non-adherent cells and changing fresh media every other day. When populations of adherent, cobblestone-like cells resembling endothelial cells formed, they were split with Trypsin-EDTA (Euroclone; ECM0920D) onto pre-coated 10 cm culture dishes without colony selection, meaning that all adherent cells were propagated. These cells were then frozen in Cryo-SFM freezing media (Promocell; C-29912) and stored in a liquid nitrogen tank prior to the phenotype analyses and using as an infection model. All experiments were performed on cells between passage 3-8.

4.3 Virus production, KSHV infection and lentiviral transduction

Virus production and handling was performed in bio-safety level 2 (BSL2) cell culture facilities. The concentrated virus preparation of recombinant KSHV.219 virus was produced from iSLK.219 (Myoung & Ganem, 2011; Vieira & O'Hearn, 2004) as described in Study II (Tuohinto et al., 2023) and the virus was precipitated with PEG-it (Systems Biosciences; LV825A-1) and spinoculated at 1500 x g for 30 min at +4°C . Cells infected with rKSHV.219 express green fluorescent protein (GFP) from the constitutively active human elongation factor 1-a (EF-1a) promoter and red fluorescent protein (RFP) under the control of RTA-responsive polyadenylated nuclear (PAN) promoter, expressed only during lytic replication. An ORF50 deletion mutant KSHV-BAC16-ΔORF50 (KSHV-ΔORF50) virus was generated as described in (Weissmann et al., 2025) and produced and concentrated from iSLK.BAC16-

ΔORF50 cells similarly as rKSHV.219. Cells infected with KSHV-ΔORF50 express green fluorescent protein (GFP) from the constitutively active human elongation factor 1-a (EF-1a) promoter. The concentrated virus was resuspended in ice-cold PBS, snap-frozen and stored at -80°C.

Lentivirus production was performed essentially as described in (Gramolelli et al., 2018). Packaging plasmids pLp1, pLp2 and pLp/VSV-G were used together with expression plasmid carrying the gene of interest. Expression plasmids used for lentivirus production are listed in **Table 3**. Heterologous coat G glycoprotein from vesicular stomatitis virus (VSV-G) was used in place of the native HIV-1 envelope, and viral enhancer and promoter sequences have been deleted from SIN vectors. These modifications increase the safety of the lentiviral vector system.

For experimental assays, cells were infected with low titers (MOI 1-2) of rKSHV.219, KSHV-ΔORF50 or transduced with lentiviruses in media with supplements in the presence of 8 μg/mL polybrene (Sigma; H9268) and spinoculation at 450 x g for 30 min, RT with the 5804R centrifuge (Eppendorf). Around 90-100% KSHV infection efficiency was achieved without selection. Virus titers were determined by infecting naïve LECs using serial dilutions of the concentrated virus and assessing the amount of GFP+ or LANA+ cells 72h post-infection with Phenix Opera 20x. Efficiency of lentiviral transduction was determined by IF staining or immunoblotting of the protein product of the expression plasmid.

4.4 Inhibitor treatments

PAA, R+, S-, R+S-Propranolol (Sigma; 284270, P0689, P8688, P0884) and small molecule SOX18 inhibitor Sm4 (#SML1999; Sigma / or a kind gift from Gertrude Biomedical Pty Ltd., Australia) was solubilized in DMSO (Sigma; D8418) to obtain a stock solutions and stored in 4°C or -80°C. R+, S-, R+S-Propranolol and Sm4 was mixed with cell media at 1-50μM.

ACBI1 (MedChemExpress; 128359) was solubilized in DMSO, stored in -80°C and mixed with cell media at 30nM. FHT-1015 (MedChemExpress; 144896) was solubilized in DMSO, stored in -80°C and mixed with cell media at 10nM. PFI-3 (Sigma; SML0939) was solubilized in DMSO, stored in -80°C and mixed with cell media at 50μM.

Bay11-7082 (Sigma; B5556) is an inhibitor of IκB-α phosphorylation, resulting in the inactivation of NF-κB pathway and decrease of NF-κB p50 and p65 expression and re-localization to the nucleus. Bay11-7082 was solubilized in DMSO as stock and stored in -80ºC, and mixed with cell media at 2.5μM.

4.5 Plasmid constructs and transient transfections

All the plasmid constructs used in the studies are listed in **Table 3**. N-terminal MYC-tagged PROX1 wild-type (PROX1wt) and DNA-binding deficient PROX1 mutant (PROX1mut) were cloned into the self-Inactivating (pSIN) lentiviral vector. Mutations N626A and N628A in PROX1 MUT were introduced by site-directed mutagenesis as described in (Petrova et al., 2002). Confirmation of mutations by sequencing (GATC Biotech, MyGATC) of the insert was performed to both PROX1wt and -mut. Also, LANA and vFLIP were cloned into the self-Inactivating (pSIN) lentiviral vector.

Reporter plasmids harbouring pGL3-7XTR and pGL3-OriA+OriLyt upstream of the firefly luciferase gene were generated using pGL3 backbone and provided by T.F. Schulz at Hannover Medical School, Germany, and pGL3-basic-luc was commercially purchased (Promega).

The BirA*SOX18 plasmid construct for BioID was generated from pFuW-myc-BirA-NLS-mCherry (a kind gift by R. Kivelä, University of Helsinki & University of Jyväskylä, Finland), used as a BirA*Cherry control. The wild-type human SOX18 insert sequence was codon optimized and synthesized by GeneArt (Thermo Fisher) to reduce G-C content, and pFuW-myc-BirA-NLS was inserted to N-terminus of SOX18. The resulting BirA*SOX18 consists of biotin-binding BirA, a nuclear localization signal (NLS), an SOX18 ORF (1152-5bp), including DNA-binding HMG domain (247-462bp), homodimerization domain (463-597bp), and transactivation domain (502-780bp).

A pFuW-myc backbone was also used to produce the Cherry, SOX18wt, and mutant plasmids C240X and HMGdel. The C240X mutant has C-terminal frameshift featuring a truncated transactivation domain that results in a transactivation deficient shortened SOX18 protein. This construct has intact HMG domain that can bind DNA, however C240X is dominant-negative mutant and causes accumulation of truncated SOX18 protein in the nucleus. The HMGdel mutant is lacking the DNA binding HMG box, resulting in a SOX18 protein that is unable to bind to DNA and causes leakage of the protein from the nucleus to the cytoplasm. The Cherry insert that enables an RFP signal, was used in a control plasmid. The codon optimized SOX18wt, C240X, and HMGdel sequences were then cloned in a pFuW-myc plasmid by Gibson Assembly. Both the backbone and gene inserts for SOX18wt, C240X, and HMGdel were assembled using NEB HiFi DNA assembly (NEB; E2611). Sanger Sequencing performed verification of the inserts while restriction analysis was performed to verify the integrity.

Table 3. Experimental plasmid constructs used in this study.

Plasmid	Backbone	Source	Study
PROX1wt	pSIN-myc > also as lentivirus (lenti)	Made in Ojala lab	I
PROX1mut	pSIN-myc (lenti)	Made in Ojala lab	I
basic control	pSIN-myc (lenti)	Made in Ojala lab	I
ORF50	pcDNA 3.1	Made in Ojala lab	I
LANA	pcDNA 3.1	Made in Ojala lab	I
3.1 control	pcDNA 3.1	Thermo Fisher	I
ORF50	pGL2	Made in Ojala lab	I
basic control	pGL2	Promega	I
7XTR	pGL3-luciferase (luc)	A gift from T.F. Schulz	I
OriA+OriLyt	pGL3-luc	A gift from T.F. Schulz	I
basic control	pGL3-luc	Promega	I
mCherry control	pFuW-myc-NLS (lenti)	Made in Ojala lab	I
SOX18wt	pFuW-myc-NLS (lenti)	Made in Ojala lab	I
SOX18 C240X	pFuW-myc-NLS (lenti)	Made in Ojala lab	III
SOX18 HMGdel	pFuW-myc-NLS (lenti)	Made in Ojala lab	III
SOX18-BirA-C	pFuW-myc-BirA-NLS (lenti)	Made in Ojala lab	III
mCherry-BirA-C	pFuW-myc-BirA-NLS (lenti)	A gift from R. Kivelä	III
LANA	pSIN (lenti)	Made in Ojala lab	+
vFLIP	pSIN (lenti)	Made in Ojala lab	+
pSIN control	pSIN (lenti)	Made in Ojala lab	+

+ = unpublished additional studies.

Transfection of semi-confluent (70-80%) cell culture dishes with cDNA was completed using a combination of OptiMEM Serum Reduced (Gibco; 31985047), FuGENE HD Transfection Reagent (Promega;), and plasmid DNA listed in **Table 3**. A mixture of OptiMEM and FuGENE HD 4 µL/1000 ng DNA was created to a total volume of 100 µL, after which an appropriate amount of plasmid DNA was added. The mixture was then vortexed at 1000 rpm for a few seconds before being incubated at RT for 20 minutes. Then, the mixture was added to the cells with 900µl of fresh DMEM media per well and incubated at 37°C for 48-72 hours.

4.6 Luciferase reporter assay

2.5x10^5 HEK293FT cells/ml were plated in 24-well plates (500mL/well). Next day each well was transfected using FuGENE XD (Promega) with 0.1µg of reporter plasmid (or the corresponding vector controls), 0.25µg of RTA (or the corresponding

vector control), 0.25 µg of the plasmid of interest (PROX1wt or -mut). Alternatively, HeLa cells were transfected with 0.1µg of reporter plasmid (or the corresponding vector controls), 0.2µg of LANA (or the corresponding vector control), 0.25, 0.5 or 1µg of SOX18-expressing plasmid or the mCherry vector control. Plasmids are listed in **Table 3**. 32-36h post-transfection cells were lysed in 1Xpassive lysis buffer (Promega). Experiments were done at least two times in duplicates, bars represent the average and the error bars the SD across the different experiments.

4.7 Genetic RNA interference (siRNA)

Transient transfection of short interfering siRNAs into a semi-confluent culture of KSHV-infected LEC was done using OptiMEM (Gibco; 31985047), 3 or 1.5µl of Lipofectamine RNAiMAX (Invitrogen; 13778075) and 150 or 75pmol siRNA per well in a 6- or 12well plate, respectively, according to manufacturer's instructions with EGM-2 or MV-2 media. Next day cells were supplied with fresh full media. The following siRNAs were used: Stealth RNAi Prox1-1 and 2 (HSS 108596; HSS 108597); COUPTF2-1 and 2 (HSS 1299001; HSS 1299002); and Stealth RNAi™ Negative Control (HSS 12935200) from Invitrogen or ON-TARGETplus SOX18 siRNA (L-019035-00); SMARCA4/BRG1 (L-010431-00), ARID1A (L-017263-00) and Nontargeting pool siRNA (D-001810-10) from Dharmacon, and pre-designed SOX18 siRNA (109098) from Ambion.

4.8 Real time quantitative Polymerase chain reaction (RT-qPCR)

Total RNA was isolated from cells using the NucleoSpin RNA extraction kit (Macherey-Nagel; 740955) according to manufacturer's protocols. The RNA concentration was measured with NanoDrop (Thermofisher). Using thermal MyCycler (Bio-Rad), total RNA was reverse-transcribed to cDNA with final reaction volume of 50µl. cDNA synthesis was achieved using 1 µg of total RNA, 2.5µl dNTP (AB 1831597), 11.0µl MgCl2 (Thermo Scientific 00292623), 5.0µl 10X RT buffer (AB 1402114), 1.0µl RNAse inhibitor (AB 566718), 10.0µl Oligo (Invitrogen 1832147), and 1.25µl MultiScribe RT (Applied Biosystems 00472355) diluted in nuclease free H2O up to volume of 19.3µl.

Transcription levels of messanger RNA (mRNA) were measured in three technical replicates using Taqman Gene Expression Assays (Applied Biosystems) with unlabelled primers and SYBR Green (2x) reaction mix (Fermentas) in the StepOnePlus Real Time PCR system (Applied Biosystems). The amplification was performed in LightCycler480 PCR 384 multiwell plates (4titude FrameStar; 4ti-0382) with total volume of 10 µl per well, of which 2 µl cDNA and 8 µl mastermix.

The PCR thermocycling included an initial denaturation at 95 °C for 10 minutes followed by 50 annealing cycles, each consisting of 15 seconds at 95 °C, 30 seconds at 60 °C and 30 seconds at 72 °C, and a final extension step at 72 °C for 7 minutes. Primer sequences used to amplify the indicated targets are listed in **Table 4**. Primers were acquired through Oligomer or Metabion. Relative abundances of human and viral mRNA were normalized by the delta threshold cycle method to the abundance of actin.

4.9 Quantification of intracellular viral DNA episome copies

Total DNA was isolated from cells using NucleoSpin Tissue Kit (Macherey-Nagel; 74098) and the KSHV genome copies were quantified by qPCR using 2XSYBR reaction mix (Fermentas; K0223) and unlabelled primers specific for LANA, K8.1, and genomic actin, listed in **Table 4**.

Table 4. Oligonucleotides used in this study.

Primer target	Sequence (Forward / Reverse)	Used in assay	Study
Actin	*TCACCCACACTGTGCCATCTACGA* *CAGCGGAACCGCTCATTGCCAATGG*	mRNA	I, II, III
PROX1	*TGTTCACCAGCACACCCGCC* *TCCTTCCTGCATTGCACTTCCCG*	mRNA	I, II, III
SOX18	*CTTCATGGTGTGGGCAAAG* *GCGTTCAGCTCCTTCCAC*	mRNA	I, II, III
COUPTF2	*GCAAGTGGAGAAGCTCAAGG* *TCCACATGGGCTACATCAGA*	mRNA	I
ETS1	*GAGCTTTTCCCCTCCCCGGAT* *TGCCGGGGGTCTTTTGGGAT*	mRNA	II
ETS2	*AGGAGTTTCAGATGTTCCCC* *GTCCCAGAATTGTTGGTGAG*	mRNA	II
VEGFC	*GCCAATCACACTTCCTGCCGA* *AGGTCTTGTTCGCTGCCTGAC*	mRNA	II
LYVE1	*CTGCATGACACCTGGATGGA* *AAGGGCTGGAAACAAGGACA*	mRNA	II
Podoplanin	*CGAAGATGATGTGGTGACTC* *CGATGCGAATGCCTGTTAC*	mRNA	II
CD44	*CCCATCCCAGACGAAGACAG* *ACCATGAAAACCAATCCCAGG*	mRNA	II
CD90 THY1	*TCGCTCTCCTGCTAACAGTCT* *CTCGTACTGGATGGGTGAACT*	mRNA	II
aSMA	*GACCCTGAAGTACCCGATAGAAC* *GGGCAACACGAAGCTCATTG*	mRNA	II

ZEB1	*GATGATGAATGCGAGTCAGATGC* *ACAGCAGTGTCTTGTTGTTGTAG*	mRNA	II
SNAI1	*GCATTTCTTCACTCCGAAGC* *TGAATTCCATGCTCTTGCAG*	mRNA	II
MMP1	*AGTCCGGTTTTTCAAAGGGAA* *CCTTGGGGTATCCGTGTAGC*	mRNA	II
CXCR4	*GCCAACGTCAGTGAGGCAGA* *GCCAACCATGATGTGCTGAAAC*	mRNA	II
IL6	*GAACCTTCCAAAGATGGCTGA* *CAAACTCCAAAAGACCAGTGATG*	mRNA	II
TGFB3	*TGAGCACATTGCCAAACAGC* *ACTCAGTGGCAAAGCTAGGG*	mRNA	II
Viperin	*GTGAGCAATGGAAGCCTGATC* *GCTGTCACAGGAGATAGCGAGAA*	mRNA	II
IFI6	*CCTCGCTGATGAGCTGGTCT* *CTATCGAGATACTTGTGGGTGGC*	mRNA	II
IL1R1	*AGAGGAAAACAAACCCACAAGG* *CTGGCCGGTGACATTACAGA*	mRNA	II
MyD88	*GCACATGGGCACATACAGAC* *GACATGGTTAGGCTCCCTCA*	mRNA	II
LANA	*CGGAGCTAAAGAGTCTGGTG* *GCAGTCTCCAGAGTCTTCTC*	mRNA	I, II, III
vFLIP	*GCGGGCACAATGAGTTATTT* *GGCGATAGTGTTGGGAGTGT*	mRNA	III
vCyclin	*AGCTGCGCCACGAAGCAGTCA* *CAGGTTCTCCCATCGACGA*	mRNA	III
ORF50/RTA	*CACAAAAATGGCGCAAGATGA* *TGGTAGAGTTGGGCCTTCAGTT*	mRNA	I, II, III
K-bZIP	*CCCGGGAACGGACAATTCTGAG* *CCACTTTGGGAAGGCGCTGTAAG*	mRNA	I, II, III
ORF45	*CCTCGTCGTCTGAAGGTGA* *GGGATGGGTTAGTCAGGATG*	mRNA	I, II, III
ORF57/MTA	*TGGACATTATGAAGGGCATCCTA* *CGGGTTCGGACAATTGCT*	mRNA	I, II, III
K8.1	*AAAGCGTCCAGGCCACCACAGA* *GGCAGAAAATGGCACACGGTTAC*	mRNA, DNA copies	I, II, III
LANA	*ACTGAACACACGGACAACGG* *CAGGTTCTCCCATCGACGA*	DNA copies	I, II, III
G. actin	*AGAAAATCTGGCACCACACC* *AACGGCAGAAGAGAGAACCA*	DNA copies	I, II, III
GAPDH	*AAGGTGAAGGTCGGAGTCAAC* *TGGAAGATGGTGATGGGATTTC*	DNA copies	I

ALU	*GGTGAAACCCCGTCTCTACT* *GGTTCAAGCGATTCTCCTGC*	DNA copies	II
ORF50 620-850	*GTGGTAGAGCCAGCAGACGTTC* *TGTAGCGCCATCTCTGCCC*	ChIP-PCR	I
ORF50 320-610	*GGGTGATTTCTTCTACCACGGTCAT* *CCGAGCGTATTCTCAGAGGTCT*	ChIP-PCR	I
ORF50 0-320	*TGGCATTTTGTTGCGCGCATGATC* *CCGAGCGTATTCTCAGAGGTC*	ChIP-PCR	I
OriA-1	*CTCCCCGGCAACAACCTG* *GGGGGTTATATGCGCGTGC*	ChIP-PCR	I
OriA-2	*CAAGCACGCGCATATAACCC* *GGGATATGCTTCCGCCTCAT*	ChIP-PCR	I
OriA-3	*CACCGTGTTAGTGTCACCCA* *CACCGTGTTAGTGTCACCCA*	ChIP-PCR	I
Orilyt-1	*ATTCAAAGGGGGCACAGAGG* *ATGCTGGGACAGAATAGCCG*	ChIP-PCR	I
Orilyt-2	*TCTGTCCCAGCATAGGCTC* *CCTGTGCCCAAATCTGTCCT*	ChIP-PCR	I
Orilyt-3	*CACGCGGGTTGTTTGAAAGT* *CCACTTGGGTGCACAGAGAT*	ChIP-PCR	I
TR-1	*CATAAATATTCCGGATACAAGGCTCG* *GACTCCTCGCACAGTAGAGAGAG*	ChIP-PCR	I
TR-2	*ACTGACAAACAAAATGCACATAACAAG* *TGGATACCTAGTCAAAATGAAGACACT*	ChIP-PCR	I
TR-3	*GAACATCAGGGATGGGTCTATGATC* *ATAACCCTCACCTACCATGGAAAT*	ChIP-PCR	I
TR-4	*GATAACCCTCACCTACCATGGAAAT* *AGAGCTACGAGTGTCATAAATACAAGA*	ChIP-PCR	I
TR-5	*TGTGTGTGAGCCTGTTTG* *TGTTCACGTAGTGTCCAG*	ChIP-PCR	III
TR-6	*TGCGAGGAGTCTGGGCTGTC* *CGTAGCAAGCACTGAGGAGGC*	ChIP-PCR	III
ORF73	*AAGTCCGTATGGGTCATTGC* *GGATGGAAGACGAGATCCAA*	ChIP-PCR	III
ORF75	*AGCGAGCACCGTCTGTATTT* *GCACCGGCGGCTACTATCTG*	ChIP-PCR	III
hsZNF268	*AATGCATTTCCACACTGCAA* *AAAGAGGTTGCTGCCAAGAC*	ChIP-PCR	III
hsZNF544	*GCCCTATGAGTGCAACCTGT* *CTCCAGTGTGAATTCGCTGA*	ChIP-PCR	III

4.10 Antibodies

Primary antibodies used in Western Blotting (WB), immunofluorescence (IF), immunohistochemistry (IHC), multiplex immunohistochemistry (mIHC) stainings, Proximity Ligation Assay (PLA), Co-immunopecipitation (Co-IP), chromatin immunoprecipitation (ChIP), bromodeoxyuridine immunoprecipitation (BrdU-IP), and flow cytometry (FC) assays of this study are listed in **Table 5**.

Table 5. Antibodies used in this study.

Antibody	Species	Source/reference	Dilution	Assay	Study
LANA	rat *mAb	Abcam, ab4103	1:1000 1:500 1:50	IF WB ChIP	I, II, III
LANA	rabbit **pAb	A gift from B. Chandran	1:1000 1:100	PLA IHC, mIHC	I, II, III
ORF50/RTA	rabbit pAb	A gift from C. Arias	1:1000 1:50 1:500	WB Co-IP PLA	I, II, III
K-bZIP	mouse mAb	Santa Cruz, sc-69797	1:1000	WB	I, II, III
ORF45	mouse mAb	Santa Cruz, sc-53883	1:1000	WB	I, II
ORF57/MTA	mouse mAb	Santa Cruz, sc-135746	1:1000	WB	I, II
K8.1	mouse mAb	Santa Cruz, sc-65446	1:1000 1:100 1:200	IF, WB IHC mIHC	I, II, III
β-actin	mouse mAb	Santa Cruz, sc-47778	1:1000	WB	I, II, III
Vinculin	mouse mAb	Santa Cruz, sc-73614	1:1000	WB	III
y-tubulin	mouse mAb	Sigma, T6557	1:1000	WB	I
A647-PDPL	mouse mAb	Biolegend, 395003	1:20	FC	II
A647-CD34	mouse mAb	Biolegend, 343617	1:20	FC	II
PE-VEGFR3	mouse mAb	Biolegend, 356203	1:20	FC	II
PE-CD31	mouse mAb	Biolegend, 303105	1:20	FC	II
A647 IgG2a	mouse mAb	Biolegend, 400239	1:20	FC	II
PE IgG1	mouse mAb	Biolegend, 400113	1:20	FC	II
Mouse IgG	mouse mAb	Santa Cruz, sc-2025	1:250 1:1000 1:100 1:50	BrdU-IP PLA Co-IP ChIP	I, II, III
Rabbit IgG	rabbit mAb	Cell Signaling, 2729S	1:1000	PLA	I, III
Rabbit IgG	rabbit mAb	Santa Cruz, sc-3888	1:50	ChIP	I
Rabbit IgG	rabbit mAb	Cell Signaling, 3900	1:100	Co-IP	I

HA.11	mouse mAb	BD Pharmingen, 16B12	1:50	ChIP	I
BrdU	mouse mAb	BD Biosciences, 555627	1:60	BrdU-IP	III
MYC	mouse mAb	Cell Signaling, 9B11	1:1000 1: 100	WB Co-IP	I, III
MYC	mouse mAb	Cell Signaling, C22276	1:50	ChIP	I
GFP	rabbit mAb	A gift from J. Mercer	1:2000	IF, WB	I, II, III
GFP	rabbit mAb	Cell Signaling, 2956	1:1000	IF, WB	I
PROX1	rabbit mAb	Abcam, ab199359	1:200 1:1000	IF WB	I, II
PROX1	rabbit mAb	Cell Signalling, D2J6J	1:200	mIHC	I, II
PROX1	rabbit pAb	Proteintech, 11067-2-AP	1: 100 1:100	Co-IP FC	I
PROX1	goat pAb	R&D Systems, AF2727	1:800	IHC	I
SOX18	mouse mAb	Santa Cruz, sc-166025	1:1000 1:500 1:100 1:200	IF, WB, PLA FC, IHC, mIHC	I, II, III
COUPTF2	mouse mAb	Perseus Proteomics, PP-H7147-00	1:500 1:100	IF, WB IHC	I
ARID1A	rabbit mAb	Abcam, ab182560	1:1000 1:500	IF, WB, PLA	III
ARID1A	mouse mAb	Santa Cruz, sc-32761	1:500	PLA	III
BRG1	rabbit mAb	Abcam, ab110641	1:1000 1:500	IF, WB, PLA	III
BRG1	mouse mAb	Santa Cruz, sc-17796	1:500	PLA	III
HP1α	mouse mAb	Santa Cruz, sc-515341	1:1000	IF	III
H2A	rabbit mAb	Cell Signaling, 12349S	1:1000	IF, WB	III
H2B	rabbit mAb	Cell Signaling, 12364S	1:1000	WB	III
NF-kB p65	mouse mAb	Santa Cruz, sc-514451	1:500	IF, WB	+
AlexaF 488	goat anti-rabbit	Invitrogen, A11034	1:1000	IF mIHC	I, II, III
AlexaF 594	goat anti-mouse	Invitrogen, A21203	1:1000	IF	I, II, III
AlexaF 647	goat anti-rat	Invitrogen, A21247	1:1000	IF	I, II, III
AlexaF 750	goat anti-rabbit	Invitrogen, A21039	1:1000	mIHC	I
HRP-IgG	Anti-rabbit	Cell Signaling, 7074	1:2000	WB	I, II, III
HRP-IgG	Anti-mouse	Cell Signaling, 7076	1:2000	WB	I, II, III
HRP-IgG	Anti-rat	Cell Signaling, 7077	1:2000	WB	I, II, III

*mAB = monoclonal, **pAb = polyclonal, + = unpublished additional studies.

4.11 Immunoblotting (SDS-PAGE with WB)

The expression of selected proteins present in the cellular lysates were detected with Sodium dodecyl sulphate polyacrylamide gel electrophoresis (SDS-PAGE) followed by Western blotting (WB).

Cells were lysed with RIPA buffer (150mM-NaCl; 1%-Igepal CA630-0.5% Na-deoxycholate-0.1% SDS-50mM; Tris-HCl-PH 7.8) supplemented with proteinase and phosphatase inhibitors (Pierce; 88666, 88667), and cleared by centrifugation. The concentration of protein from each cleared sample was measured with Protein assay dye reagent concentrate (Bio-Rad) and BioPhotometer (Eppendorf), and accordingly used to obtain equal amount of protein in all the samples included in the experiment. Loading buffer 5XLaemmli was mixed with 2-mercaptoethanol and added to the cell extracts, which were boiled 5 min in 99℃. After cooling down at RT, samples and PageRuler Plus Prestained protein ladder (Thermo Scientific) were loaded on Criterion TGX precast polyacrylamide gel (Bio-Rad), and run at 55mA for approximately 40 min. After the electrophoresis run, proteins in the gel were transferred to nitrocellulose membrane using trans-blot Turbo Transfer system (Bio-Rad).

Membranes were blocked in 5% non-fat dry milk in Tris-buffered saline with 0,1% Tween (TBS-T) solution for 1h in rocking table. Primary antibody incubations were performed in the blocking solution overnight (O/N) at 4℃. After three rounds of washing in TBS-T, membranes were incubated in the appropriate HRP-conjugated secondary antibody diluted in blocking solution for 4h RT. All the primary and secondary antibodies used for human and KSHV are listed in **Table 5**. After washes luminescent signal was revealed with Wester-Bright Sirius detection Kit (Advansta) and ChemiDoc MP imaging system (Bio-Rad). Experiments were done at least two independent times, representative experiments are shown. Multiple independent blots were used to represent one experiment requiring multiple antibodies for detection. Equal loading of the independently generated blots was ensured by Ponceau-S staining. The Fiji software (https://imagej.net/Fiji) was used to quantify the intensity of the bands. β-actin, gamma-tubulin or vinculin was used as a loading control.

4.12 Immunofluorescence (IF)

Cells were plated on a 96-well PhenoPlate (Revvity; 6055300) and infected with rKSHV.219 and treated or cells were seeded on fibronectin (from human plasma, Sigma; F0895) -coated glass coverslips on 24-well plate, and treated. Cells were fixed with 4% PFA, permeabilized with Triton X-100 (Sigma; T9284) and stained

for KSHV and human proteins with antibodies indicated in **Table 5**. Nuclei were visualized with Hoechst 33342 (Sigma; 14533).

4.13 Immunohistochemistry (IHC)

Formalin-fixed, paraffin-embedded (FFPE) Kaposi sarcoma tissue sections were kindly provided by Justin Weir (Charing Cross Hospital and The London Clinic, London, UK). The study (Kaposi Sarcoma Herpes Virus Infection and Immunity; REC reference: 04/Q0401/80) was approved by the Riverside Research Ethics Committee, and written informed consent was obtained from all participants. FFPE Kaposi sarcoma-negative skin biopsies were retrieved from the archives of the Department of Pathology, Helsinki University Hospital (Helsinki, Finland), in accordance with Finnish laws and regulations, and with permission from the director of the health care unit. All samples were de-identified and analyzed anonymously.

After deparaffinization in xylene and rehydration, and antigen retrieval, sections were stained with Hematoxylin (Merck Millipore; 1092530) and Eosin Y (Sigma; HT110132), and some sections were treated in a PreTreatment module (Lab Vision Corp) in Tris-HCl (pH 8.5) and in Tris-EDTA (pH 9.0) buffer for 20 minutes at 98°C. Sections were stained in an Autostainer 480 (Lab Vision). Tissues were incubated with the antibodies listed in **Table 5** O/N at 4°C in humidified chambers. For detection, ImmPRESS HRP Polymer Detection Kit, Peroxidase, (Vector Laboratories) was used. Samples were imaged in a Panoramic 250 viewer (Genome Biology Unit, University of Helsinki).

4.14 Multiplex immunohistochemistry (mIHC)

Multiplex IHC was performed essentially as described in (Blom et al., 2017), with some modifications. Briefly, paraffin was removed from 3.5-µm FFPE sections and heat-induced epitope retrieval (HIER) was performed. After HIER, endogenous peroxide activity and protein blocking was performed in 0.9% H2O2 and in 10% normal goat serum, respectively. The first primary antibody (K8.1) was detected using HRP-conjugated secondary antibody and a tyramide signal amplification (TSA; AlexaFluor488; Life Technologies, see manufacturer´s instructions). Another TSA reaction was done for the second primary-secondary antibody complex (PROX1). Then, after HIER denaturation, a pair of primary antibodies raised in different species was used to detect additional two targets (SOX18 and LANA) using AlexaFluor647 and AlexaFluor750 fluorochrome-conjugated secondary antibodies (**Table 5**), respectively. Nuclei were counterstained using DAPI and slides were mounted and coverslips applied.

4.15 Proximity ligation assay (PLA)

Proximity ligation assay (PLA) was performed using Duolink PLA technology (Sigma-Aldrich). LECs and KLECs were plated on a PhenoPlate (Revvity; 6055300) and infected with rKSHV.219. Cells were fixed with 4% PFA, permeabilized with Triton X-100 (Sigma; T9284) and 1µg/mL of Hoechst 33342 (Fluka Biochemicka) in PBS. Blocking with Duolink Blocking Solution in a 37ºC humidity chamber for 60 minutes and then stained with antibodies against rabbit or mouse anti-protein of interest or normal mouse or rabbit IgGs, listed in **Table 5**. Wells were washed five times with 1x wash buffer A and then treated with PLA probe solution composed of anti-mouse PLUS (DUO92001) and anti-rabbit MINUS (DUO92005) probes diluted in Duolink antibody diluent and incubated in a 37ºC humidity chamber for 60 minutes. Probes were detected with *in situ* far-red detection reagent (DUO92013). Ligation was performed by treating cells with 1:40 dilution of Ligase in 1x Ligation Buffer and incubating and 37ºC humidity chamber for 30 minutes. Wells were washed five times with 1x wash buffer A and Amplification was performed by treating cells with 1:80 dilution of Ligase in 1x ligation buffer and incubating and 37ºC humidity chamber for 100 minutes. Wells were washed five times with 1x wash buffer B and a 0.01x wash buffer B was added. Imaging of interaction PLA dot signals were accomplished using Opera Phenix (PerkinElmer) and quantified using Harmony high-content imaging and analysis software.

4.16 Co-immunoprecipitation (Co-IP)

For immunoprecipitations, cells were lysed in the IP lysis buffer (150mM-NaCl; 50mM Tris-HCl-pH 7.8; 0.2%-NP40 Igepal; 1% glycerol; 0.5mM-EDTA) supplemented with complete proteinase and phosphatase inhibitory cocktails, and the whole cell extracts were cleared by centrifugation for 20min at 4°C. Next, aliquots were taken for inputs and the rest of the extracts were incubated with antibody against protein of interest, or a control IgG antibodies (**Table 5**) O/N at 4°C rotating. Protein G sepharose beads (Abcam; ab193259) or Strep-tactin sepharose beads (IBA; 2-1201-002) were washed with IP buffer and added (50µl) into the samples for 2h 4°C with rotation, followed by 3x washes with cold IP buffer. Immunoprecipitated and total proteins were subjected to SDS-PAGE and transferred to nitrocellulose membranes for WB.

4.17 Chromatin immunoprecipitation PCR (ChIP-PCR)

HeLa cells transfected with Cherry, SOX18, C240X, or HMGdel cDNAs, or LECs were infected with rKSHV.219, and after 72 hours, the infection efficiency was

confirmed by GFP signal. For KLEC, cells were treated with inhibitors or DMSO control and incubated for another 24 hours. For each ChIP, one or three 10-cm dish for HeLa and KLEC, respectively, was cross-linked and protocol according to SimpleChIP Enzymatic Chromatin IP Kit (Cell Signaling; 9003S) was used. Antibodies against viral and host proteins were used, and listed in **Table 5**. Chromatin was eluted and de-crosslinked and DNA was purified using a DNA Clean & Concentrator kit (Zymo Research; D5205). The purified DNA was amplified with qPCR with sets of KSHV ORF50 promoter, OriA, OriLyt and TR primers, and controls primers for KSHV genome as well as additional primers for human genome as negative controls listed in **Table 4**, and differences in samples is shown as % of input as individual values for each biological replicate.

4.18 Bromodeoxyuridine incorporation assay (BrdU-IP)

HeLa cells transfected with Cherry, SOX18, C240X, or HMGdel cDNAs, or LECs were infected with rKSHV.219, and after 72 hours, the infection efficiency was confirmed by GFP signal. For KLEC, cells were treated with inhibitors and incubated for another 72 hours. Cell culture media with 100μM of BrdU (Sigma; B-5002) was added and incubated for 2 hours for HeLa and 4 hours for KLECs before cell samples were trypsinized and collected. The samples were centrifuged for 5 minutes at 1500 rpm to collect a cell pellet. The cell pellet was then used for DNA extraction using the Nucleospin Tissue kit (Macherey-Nagel; 740952) with T1 lysis buffer and Proteinase K. DNA samples were eluted and sonicated for 3 cycles for 30 seconds, with the samples cooling on ice between each cycle. For BrdU pulldown, DNA was first denatured at 95ºC for 10 minutes and cooled on ice. For an input samples, 10% of each sample was aliquoted and stored. Following, 4μL of mouse monoclonal BrdU antibody (BD Biosciences; 555627) or normal mouse IgG (Santa Cruz; sc-2025) was added to the remaining samples and incubated overnight at 4ºC while rotating. Additionally, a total of 130μL of DynabeadsTM Protein G magnetic beads (Invitrogen; 10003D) were washed twice with 1mL IP wash buffer (50mM HEPES-NaOH pH 7.55, 250mM LiCl, 1mM EDTA, 1% NP-40, 0.7% sodium deoxycholate) and once with IP buffer (10mM HEPES-NaOH pH 7.9, 100mM NaCl, 1mM EDTA, 0.5 mM EGTA, 0.1% sodium deoxycholate) with the magnetic rack (Bio-Rad). The beads were then blocked with 1mg/mL of BSA and 0.25mg/mL of Salmon sperm DNA (Fisher; 10605543) overnight at 4ºC, rotating. The next day, the blocking buffer in the magnetic beads were removed using the magnetic rack and washed once with IP buffer. Then, 130μL of IP buffer were mixed by pipetting up and down and 15μL of the beads were added to each sample and mixed. The samples were then incubated for 3 hours at RT, rotating. Following, the beads in the samples were washed 5 times with IP wash buffer using 1mL for each sample. The samples were then eluted in 200μL of elution

buffer (50mM Tris-HCl pH 8, 10mM EDTA, 1% SDS) at 65ºC for 1 hour. Following elution, the samples were added to the magnetic stand and the supernatant was transferred to new, clean tubes. The samples, and the inputs, were then purified with the ChIP DNA Clean and Concentrator kit (Zymo Research; D5205). A total of 40µL of elution buffer was used for the final DNA product for a subsequent qPCR run conducted using primers for KSHV and the human housekeeping genes of interest listed in **Table 4** and differences in samples is shown as % of input. The workflow is presented in **Figure 8**.

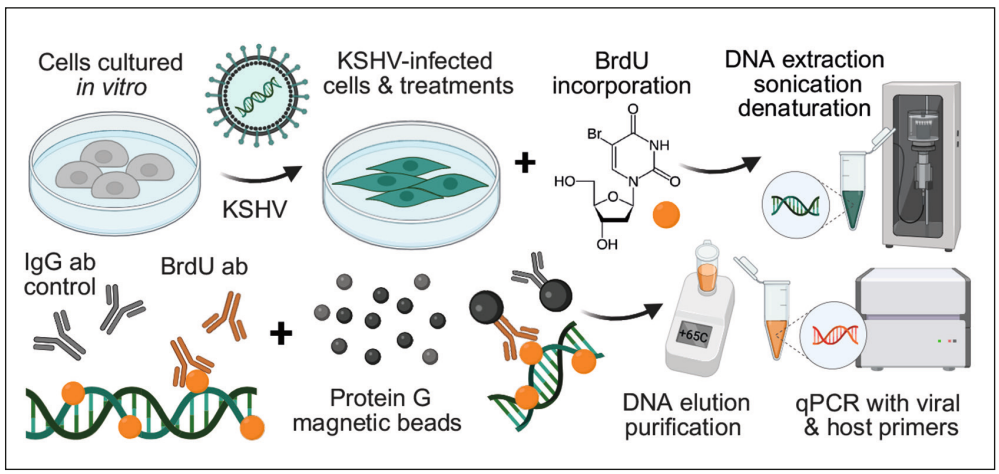

Figure 8. Shematic workflow of BrdU incorporation and precipitation assay to measure efficiency of nascent viral latent DNA replication normalized to human BrdU analysed via qPCR. Created with Biorender.

4.19 Flow cytometry (FC)

The cells were analyzed by FC using the fluorescently conjugated antibodies for endothelial surface markers or corresponding IgG isotypes (Biolegend). For the nuclear EC markers, cells were fixed and permeabilized with MetOH and stained with anti-PROX1 (Proteintech) and anti-SOX18 (Santa Cruz) antibodies, followed by staining with secondary antibodies conjugated to Alexa Fluor stains (Invitrogen). All antibodies are shown in **Table 5**. Samples were analyzed with BD Accuri C6 flow cytometer using unstained cells and conjugated IgG isotypes, or secondary antibody only treated controls.

4.20 BioID coupled with mass spectrometry

Protein-protein interaction screen BioID (Roux et al., 2018) was performed from stably KSHV-infected iSLK.219 and parental non-infected SLK cell line, transduced

with BirA*SOX18 or BirA*mCherry construct containing lentiviruses (**Table 3**). iSLK.219 was not induced, thus KSHV infection was strictly latent. Following transduction, cells were incubated and expanded for 72h before 80% full cultures were incubated with 50μM biotin (Pierce; B4639) for 24 hours. Cells were washed with PBS before scraping and pelleted before snap-frozen with liquid nitrogen and stored in -80°C. Next, the 1ml pellets were resuspended in 3x volume (3ml) of ice cold BioID lysis buffer (wash buffer (see below) with 0.1% SDS) and 1:3000 benzonase nuclease was added. The samples were vortexed and kept on ice for 15 min and sonicated with low output settings 45s on ice for 3 cycles, 5 min on ice in between. After, samples were centrifuged at 16.000g for 15 min at 4°C, and supernatants were transferred to new tubes and spin was repeated. From final supernatant, 50 μl inputs were removed for Western blot to check the expression of transduced plasmids. The supernatant samples were transferred through Bio-Spin chromatography columns (BioRad; 7326008), containing 200μl of Strep-Tactin Sepharose beads (IBA; 2-1201-002, 50% suspension), prewashed 3x 1ml with wash buffer (HENN-buffer with 0.5% IGEPAL, 1mM DTT, 1mM PMSF, 1,5mM Na_3VO_4, protease inhibitors; Sigma) for affinity purification. After supernatants were drained under gravity flow, the columns were washed four times with HENN-buffer (50mM HEPES pH 8.0, 5mM EDTA, 150mM NaCl, 50mM NaF, stored at 4°C in the dark). Then, the columns were closed, and biotin-bound proteins were eluted from the beads in the column with 300μl of fresh Biotin-HENN buffer (HENN-buffer with 0.5mM biotin) by incubating 5 min before opening the columns and flow-through was collected, and these steps were repeated. Final elution (600μl) was then frozen in -80°C before further processed and analysed in Proteomics Unit (Institute of Biotechnology, University of Helsinki). Briefly, reduction of the cysteine bonds with 5mM Tris(2-carboxyethyl) phosphine (TCEP) for 30 mins at 37°C and alkylation with 10mM iodoacetamide was performed. The proteins were then digested to peptides with sequencing grade modified trypsin (Promega, #V5113) at 37°C overnight. After quenching with 10% TFA, the samples were desalted by C18 reversed-phase spin columns according to the manufacturer's instructions (Harvard Apparatus). The eluted peptide sample was dried in vacuum centrifuge and reconstituted to a final volume of 30μl in 0.1% TFA and 1% CH_3CN. BioID was performed with liquid chromatography-mass spectrometry (LC-MS) and analysed as described in (Liu et al., 2018) by Proteomics Unit (Institute of Biotechnology, University of Helsinki). The mechanism and workflow of BioID is depicted in **Figure 9**. The high-confidence interacting proteins were identified by first filtering the data using Contaminant Repository for Affinity Purification (CRAPome) and Significance Analysis of INTeractome (SAINT)-express version 3.6.0. Then, only interacting proteins with ≥2 found unique peptides were selected, and finally BirA*SOX18 interacting proteins were bait-normalized to BirA*Cherry interacting proteins using the PSM (peptide spectral match) values.

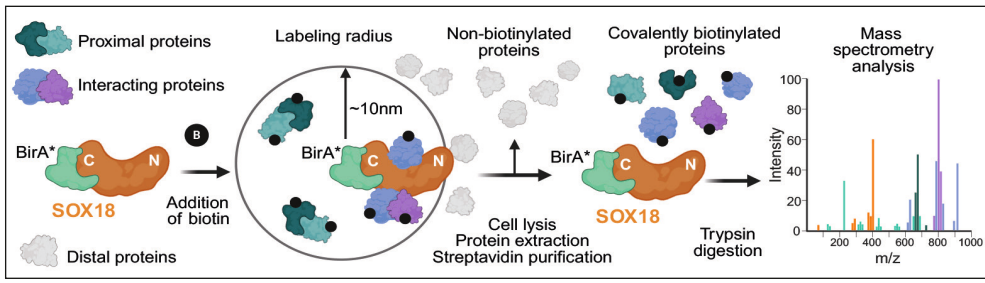

Figure 9. Schematic workflow of BioID coupled with mass spectrometry analysis.

4.21 Cell viability assays

For measuring the viability of cells, CellTiter-Glo (Promega; G7572) luminescent viability assay was performed on black 96-well ViewPlates (Revvity; 6005182) for 10 min and the luminescence from live cells were measured with FLUOstar Omega microplate reader (BMG Labtech). The viability % was calculated as an average of luminescent signal from triplicates comparing to DMSO treated cells considered as control with 100% viability.

Potential toxicity of treatments to cells *in vitro* was evaluated with Trypan Blue staining of cells after six days. First, growth media with possible floating cells was collected, after which adherent cells were detached and collected using Trypsin-EDTA, after which all cells were centrifuged and resuspended. The cell suspension was mixed 1:1 with 0.4% Trypan Blue solution (Sigma; T8154) and counted in a TC20 automated cell counter (Bio-Rad) to acquire % of viable cells.

4.22 Cell proliferation assay

To compare the proliferation rates, low number of cells were plated on 96-well ViewPlates (Revvity; 6005182) and the next day the cells were treated with 10μM 5-ethynyl-2'-deoxyuridine EdU (Thermo Fisher) for 4 h with ECs, and 2 h with HeLa cells, and fixed in 4% PFA in PBS. The proliferating cells were visualized using Click-iT EdU Alexa Fluor 647 (Molecular Probes; C10340) staining according to manufacturer's instructions, and Hoechst 33342. Images were taken using Phenix Opera 20x and the portion of EdU-containing cells was quantified with Harmony software.

4.23 Soft-agar assay

Mock- and KSHV-infected blood or lymphatic ECFCs ($3x10^4$ cells/well) were mixed 48h or 7 days post infection with 0.4% agarose as single cell suspension

in growth medium and plated on top of a solidified layer of 0.5% agarose in EGM-2 in 6-well dishes. Fresh media was replenished every 2-3 days and wells were imaged each week using a BZ-X800 (Keyence) or Eclipse Ts2 (Nikon) fluorescent microscope.

4.24 Spheroid 3D assays

3D spheroid cultures mock- or KSHV-infected ECs were seeded into 0.5% agarose precoated, round-bottom 96-well plates (Greiner Bio-One; 650180) at $4x10^3$ cells per well. After 16-24h incubation at 37°C, the preformed spheroids were transferred into the fibrin gel consisting of plasminogen-free human fibrinogen (final concentration 3 mg/mL; Millipore; 341578) and human thrombin (final concentration 2 U/mL; Merck; 605190) in 50 µL Hank's Balanced Salt Solution HBSS (Gibco; 14025) supplemented with 400 µg/mL aprotinin (Calbiochem; 616370). The gels were cast onto the bottom of 12-well plates (Greiner; 665180) and incubated for 1 h at 37°C to allow complete gelling followed by addition of EGM-2 culture medium. The next day, inhibitors (Sm4 or DMSO as a control) was added to the culture media, replenished at day 3 and followed until day 6. Phase contrast images were taken with the Eclipse Ts2 (Nikon) microscope and the spheroids were fixed with 4% PFA for 1 h RT. The spheroids were then stained by anti-rabbit GFP, and Hoechst 33342 as described in (Cheng et al., 2011) and analyzed by confocal microscopy.

4.25 Virus release assay

One day prior to titration, $8x10^3$ naïve cells/well were plated on the viewPlate-96black (Revvity). Cells were spinoculated in the presence of 8 µg/mL of polybrene using a serial dilution of precleared supernatant from the infected cells. 48h later, cells were fixed with 4% PFA, permeabilized with Triton X-100 and stained with antibodies against GFP (gift) to detect the rKSHV.219-infected cells or LANA (Abcam) and Hoechst 33342 (Sigma). Images were taken using the automated cell imaging system ImageXpress Pico or Phenix Opera and KSHV+ cells were quantified using pipeline created in CellProfiler or Harmony softwares.

4.26 Image acquisition and analysis

High-throughput images
From 96-well plates (Revvity), images were taken using an automated cell imaging system ImageXpress Pico (Molecular Devices) with 10x objective or Opera Phenix

(PerkinElmer) with either 20x or 40x objectives with z-stack of 5 images. Images of the spindling phenotype and GFP was taken with 20x and intranuclear LANA speckles or PLA dots were imaged with 40x.

Cells were quantified using pipelines created in CellProfiler and Harmony softwares. Briefly, LANA speckles were quantified as mean number of nuclear objects from 10 fields (n > 200 nuclei) for each biological replicate (n = 3) shown as individual values ±SD. Signal from PLA dots were quantified as mean number of nuclear objects from 10 fields (n = 100 nuclei) combined from (n=3) biological replicates shown as violin plots with median and quantiles. The number of positive cells in virus release assay were quantified over the total amount of cells (number of nuclei) using Cell Profiler (http://cellprofiler.org). The graph shows the average of virus titres or positive cells per each condition, error bars indicate SD across at least two experiments. The virus titres were calculated as IU/ml.

Confocal images

Coverslips (Study I, II, III), spheroids (II) and the *in vivo* whole mount sections (II) were imaged with LSM 780 and LSM 880 (Zeiss) microscopes provided by Biomedicum Imaging Unit (BIU, University of Helsinki).

Coverslips in Study I and II were imaged with Zeiss LSM 780 confocal microscope equipped with a Plan-Apochromat 63x objective (NA 1.40), and DAPI/ Hoechst FITC/Alexa Fluor 488/ GFP TRITC/ Cy3/ Alexa Fluor 546 filter sets. Coverslips in Study III were imaged with LSM 880 with a PMT confocal and was used with Plan-Apochromat 63x oil objective with 405, 561 and 633nm lasers. Average signal intensity in Study I was calculated with appropriate cell profiler pipeline, the graph shows the average intensity per condition and the error bars indicates the SD across n>100 cells/condition/staining. Co-localization was assessed by Pearson´s co-localization coefficient calculated using Coloc2 plug-in in Fiji software package. Signal intensity in nuclei in Study III were quantified using macro pipeline created in Fiji-imageJ. Briefly, maximum image projections (MIP) were created from z-stack of 15 images for each channel. Signal intensity thresholds were acquired for 16-bit depth MIP images with default settings, and particles (nuclei) were analyzed for mean arbitrary unit (a.u.) intensity within each nucleus (n = 100 or 200) shown as individual values ±SD. LANA speckles were quantified as mean number of nuclear objects in each nucleus (n = 100) shown as violin plots with median and quantiles.

The 3D spheroids and *in vivo* section images (Study II) were taken with LSM 780 as a Z-stack, and tiling was chosen to image the whole section area when needed. GFP was imaged with a 20x objective using laser Argon 488nm and LANA was imaged with a 63x objective using laser HeNe 633nm. The images were quantified for GFP by the integrated ZEN 3.5 analysis program (Zeiss) and a pipeline was

generated for the images to measure the relative GFP intensity normalized to the section area and the comparable coverage of the GFP signal in the cells showing an elongated spindling phenotype. Images of similarly prepared and stained histological samples from the implanted, mock infected lymphatic ECFC plugs, which do not express GFP, were used to subtract the autofluorescence for quantification.

HUVEC cells (Study III) were seeded on 0.5% gelatin coated 8-well microscope slide (Ibidi; 80827) at a density of 50,000 cells/well in EGM-2 media overnight. HUVEC cells were then treated overnight with either DMSO or Sm4 (30μM). The next day cells were stained with SiR-DNA (Spirochrome) at a 1:2000 dilution for 1 hour prior to imaging. Cells were imaged on a Leica TCS SP8 (Leica Microsystems GmbH) microscope at 37°C and 5% CO_2 using a 93x 1.30NA glycerol immersion objective and a tunable white light laser unit.

Slide scanner images

Digital, whole-slide fluorescence images of mIHC slides (Study I) were acquired at 0.24 μm/pixel resolution using Zeiss Axio Scan.Z1 equipped with Plan-Apochromat 20x objective (NA 0.8), Hamamatsu Orca Flash 4.0 K3 camera, Solid-State Light Source Colibri 7 LED, and DAPI, FITC, CY3, CY5, and CY7 filter sets. After image acquisition, images were exported as single channel 16-bit monochrome TIFF images. For mIHC image analysis, red blood cell and tissue-derived autofluorescence was detected and removed by machine learning (Ilastik 1.3.3, Pixel classification). For this, RGB color images were generated from DAPI, FITC (K8.1), and CY3 (SOX18) channel images using CellProfiler GrayToColor module. All subsequent image analyses were performed using CellProfiler. Cells were segmented using Identify-PrimaryObjects for DAPI channel with Global threshold, minimum cross entropy, and 0.5 smoothing scale. All channels with a specific marker were thresholded using either manual cut-offs (K8.1) or Adaptive Otsu defined cut-offs (PROX1, SOX18, LANA). Cell classes were determined using MaskObjects modules. H&E sections (Study II) were imaged with automatic Panorammic250 slide scanner with 20x microscope through services from Genome Biology Unit (GBU, University of Helsinki).

4.27 Microscopic imaging of epigenetic landscape (MIEL)

Preparation

HUVEC cells were seeded at a density of 50,000 cells/well in an 8-well chamber slide (Ibidi; 80827). Cells were then treated with either DMSO or Sm4 overnight. LECs were seeded at a density of 100,000 cells/well in a 12-well plate and the next day either left non-infected or infected with rKSHV.219. The next day cells

were moved to fibronectin (from human plasma, Sigma; F0895) coated glass coverslips on 24-well plate. After 72 hours post infection, cells were then treated with either DMSO or Sm4 for 24 hours. The following day both ECs were fixed with 4% PFA for 10 mins at room temperature, then washed with PBS. Cells were then permeabilized with 0.3% Triton X-100/PBS for 5 minutes, followed by washing with PBS and blocking with 0.5% BSA/PBS for 1 hour. Cells were then stained with 5 ug/ml of DAPI for 3 minutes and then washed with PBS. LECs and KLECs were additionally stained with mouse monoclonal anti-HP1α (Santa Cruz; sc-515341) overnight, washed with PBS and Alexa Fluor anti-mouse 596 (Invitrogen; A21203) was used as secondary antibody. Coverslips were washed with PBS and dH2O before mounting to microscope slides.

Confocal acquisition

HUVEC cells were acquired on a Nikon A1R confocal microscope using the 20x 0.75 NA air objective and LECs/KLECs were acquired on a Zeiss LSM880 confocal microscope using the 63x oil objective.

Data Processing

Image features for each cell were extracted using the MIEL pipeline (Farhy et al., 2019), explained also in **Figure 10**. Feature values were normalized using z-score transformation. For each experimental condition, individual cell profiles were condensed into an averaged center representing the population-level feature vector. The number of cells used to compute each averaged center was determined through bootstrap analysis, as described in Bootstrap analysis. The condensed centers were then subjected to principal component analysis (PCA), using four principal components, to construct a reduced-dimensional representation of cellular behavior.

Distance Matrix

To assess phenotypic similarity between conditions, the Euclidean distance between all pairwise centers was calculated. To evaluate within-condition variability, the average distance between all centers belonging to the same experimental condition was computed, providing a measure of dispersion in cellular behavior across replicates.

Confusion Matrix

Support vector machine (SVM) classification was performed using Python's scikit-learn library (version 1.2.2) to evaluate the separability of the condensed centers. Eighty percent of the data from each condition were used as a training set, while the remaining 20% served as the test set. Classification accuracy was assessed on the test set, and results were summarized in a confusion matrix to visualize performance across conditions.

Bootstrap Analysis

To determine the optimal number of cells required to generate a representative averaged center, we conducted a bootstrap-based optimization. First, PCA was performed using all available cells from all conditions. From this analysis, we selected conditions that exhibited clear separation in the PCA space. Using these separable conditions, 1,000 bootstrap iterations were performed. In each iteration, 80% of the total cell count per condition was randomly sampled with replacement. These subsampled datasets were condensed into centers, and PCA followed by SVM classification was applied. Classification accuracy was recorded for each iteration. The optimal condensation number was defined as the smallest number of cells that achieved ≥95% classification accuracy in ≥95% of the bootstrap iterations. This ensured robust and reproducible discrimination of experimental conditions while minimizing cell input requirements.

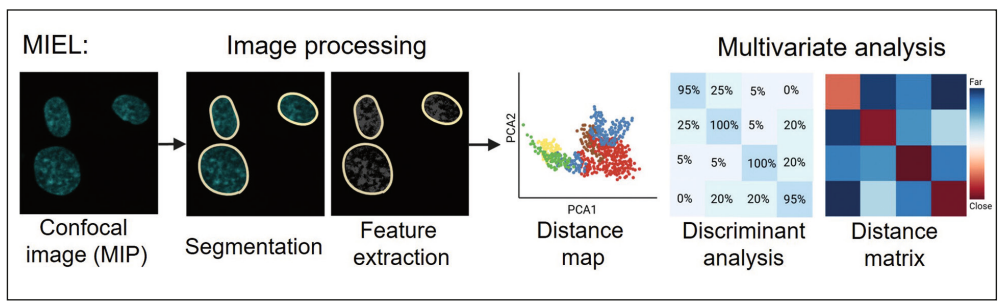

Figure 10. Representative pipeline of unsupervised MIEL analysis from confocal images. Individual nuclei are segmented using DAPI and texture- and edge-based fluorescent features are extracted at the pixel level. These features are computed using the intensity relationships between each pixel and its surrounding neighbors, capturing spatial variation in signal distribution. The variation in the extracted nuclear features is quantified across all nuclei, and dimensionality reduction is performed using PCA. The top two principal components are used to visualize data structure and spread in a 2D PCA plot. To classify cell populations, a SVM algorithm is applied, enabling the identification of distinct clusters based on feature signatures. The average pairwise distances points in PCA space are then computed and represented as a similarity matrix.

4.28 Assay for Transposase-Accessible Chromatin -sequencing (ATAC-seq)

Cell preparation

LECs infected with rKSHV.219 display a unique infection program harboring a high number of intracellular KSHV copies and spontaneous lytic reactivation initiated by viral ORF50/RTA, leading to production of viral progeny, as shown in Study I (Gramolelli et al., 2020). These viral particles contain nascent DNA that upon lysis of the host cell releases cell free viral DNA that interferes with the ATAC-seq analysis resulting in high background signal. To avoid this, we opted to infect LECs with a KSHV-BAC16-ΔORF50 strain that has ORF50/RTA stop-codon prohibiting

spontaneous lytic reactivation, and production of new viral particles (Weissmann et al., 2025). Notably, although KSHV-ΔORF50 is an optimal viral strain for ATAC-seq, most of the infection assays in the studies of this thesis are carried out using rKSHV.219 strain as it better recapitulates the natural infection of KSHV in LECs. Briefly, non-infected LEC and ΔORF50-KLEC infected for 24h were treated for another 24h with DMSO or 20μM Sm4, or infected for 72h and treated for another 72h with DMSO or 20μM Sm4, or 10nM FHT.1015. Cells were then trypsinized, pelleted and frozen O/N in FBS +10% DMSO in a cell freezing box.

Library preparation for sequencing

ATAC-seq libraries for 24h trearted cells were prepared in B. Sahu lab as previously described in (Buenrostro et al., 2015; Corces et al., 2017). Briefly, 50,000 cryopreserved cells were washed with ice-cold PBS and resuspended in 50μl of ATAC-seq lysis buffer and incubated for 3 min on ice. Nuclei were centrifuged at 500 x g for 10 min at 4°C, followed by transposition with Tn5 transposase (Illumina; 20034197). Tagmentation was carried out on a thermomixer at 37°C for 30 min at 1,000 rpm. The reaction was purified using MinElute PCR Purification Kit (Qiagen; 28004) and eluted in nuclease-free water. The samples were amplified for a total of 8 cycles and purified with AMPure beads (Agencourt; A63881). Libraries were paired end sequenced on Illumina Novaseq 6000. ATAC-seq for ΔORF50-KLEC treated for 72h with DMSO, Sm4 or FHT-1015, was performed in A. Grunhoff lab using the Omni-ATAC-seq protocol (Corces et al., 2017). Briefly, 50,000 cryopreserved cells were thawed, treated with DNase I (200U/ml, Worthington) at 4°C for 5 min and DNAse was inactivated by addition of EDTA (1.5mM final). Cells were washed with cold wash buffer (PBS + 0.04 % BSA) twice and $1x10^5$ cells were resuspended in 1ml cold RSB buffer (10mM Tris-HCl pH 7.4, 10mM NaCl, 3mM $MgCl_2$). Cells were pelleted again at 500 x g for 5 min and resuspended in 50μl of cold ATAC-NTD lysis buffer (RSB Buffer + 0.1% NP40, 0.1% Tween20, 0.01% Digitonin). Lysed cells were diluted in 1ml cold ATAC-T buffer (RSB + 0.1% Tween20) and inverted three times. The resulting nuclei were pelleted at 500 x g for 10 minutes and the supernatant was removed. Cell pellets were transposed with 50μl of transposition mix containing 25μl 2xTD Buffer (20mM 1M Tris-HCl pH 7.6, 10mM $MgCl_2$, 20% Dimethyl Formamide) 2.5μl transposase (custom made, 100nM final), 16.5μl PBS, 0.5μl 1% digitonin, 0.5μl 10% Tween-20 and 5μl H2O) at 37°C and 1000 rpm on a thermomixer for 30 min. The reaction was stopped by adding 250μl of DNA Binding Buffer and DNA was isolated using the Clean and Concentrator-5 Kit (Zymo; D4013). Libraries were produced by PCR amplification of tagmented DNA and sequenced on a NextSeq 2000 sequencer 50bp Paired End.

Bioinformatic analysis

The ATAC-seq data processed as previously described (Fei et al., 2023). Briefly, for mapping of ATAC-seq data to both human genome and virus genome,

we constructed a hybrid genome that included the hg38/GRCh38 version of human genome and Kaposi sarcoma virus genome (GenBank id: HQ404500.1) (referred as hybrid genome from now on). This hybrid genome included human chromosomes 1-21, X, Y and KSHV genome. The hybrid genome was used for all the ATAC-seq analysis steps. Briefly, Pearson correlation between the samples was calculated and visualized using deeptools (v.3.1.3) with outlier removal. Differential analysis of the chromatin accessibility in the ATAC-seq samples was done in R using Diffbind (v3.16.0). The analysis was conducted using alignment files and narrowPeak files. Sites with a false discovery rate (FDR) value of less than 0.05 were defined as differentially accessible. Differential site locations were compared using bedtools and visualized as heatmaps using deeptools with bigwig files. ATAC-seq signal in the viral genome was visualized using pyGenomeTracks (v3.9) with bigwig files. For the visualization of the human genome sites, the bigwig files were converted into bedGraph format using bigWigToBedGraph (v377) and the genomic coordinates were plotted using Spark (v2.6.2). Homer v4.10.4 was used to perform de novo motif analysis on the differential ATAC-seq sites. The chromatin accessibility loss and gain sites were ranked according to their log2FoldChange and up to 1000 differential accessibility sites with the highest fold change were selected for the motif analysis. findMotifsGenome.pl script was used to run de novo motif analysis with the hybrid genome using default parameters. Transcription factor Occupancy prediction By Investigation of ATAC-seq Signal (TOBIAS, v0.13.3) was used to predict transcription factor binding differences as previously described in (Fei et al., 2023). Motifs were retrieved from Jaspar database: (https://jaspar.elixir.no/download/data/2024/CORE/JASPAR2024_CORE_vertebrates_non-redundant_pfms_jaspar.txt) and the results were visualized using ggplot2 (v3.5.1). ATAC-seq raw and processed data are deposited in NCBI's Gene Expression Omnibus and are accessible through GEO series accession number GSE303435.

4.29 Global gene expression analysis with RNA-sequencing (RNA-seq)

Study I

Cell preparation and sequencing

RNA from iSLK.219 cells and KLECs from three independent experiments, was extracted using NucleoSpin RNA extraction kit (Macherey Nagel). Ribosomal RNA was depleted using Ribo-zero rRNA Removal Kit (Illumina) and the RNA quality was monitored with Bioanalyzer RNA Kit (Agilent). Libraries were prepared using NEB Next-Ultra-Directional RNA library-Prep Kit for Illumina (NEB) and sequencing was done with NextSeq High-Output 1 × 75 bp.

Bioinformatic analysis

FASTQ data was aligned to the annotated human reference genome hg38 and using STAR with the build in gene quantification function. Differential gene expression (DGE) of the quantified genes was performed using DeSeq2. Significantly DGE (FDR < 0.1 and log2FoldChange >= +/- 1) were subjected to Kyoto Encyclopedia of Genes and Genomes (KEGG) pathway analysis to identify regulated pathways (FDR < 0.1). Concerning viral gene expression differences FASTQ data was aligned to the rKSHV.219 reference sequence which is identical to BAC16 (Genbank Acc.: GQ994935) using STAR. We inserted the panPromoter-RFP, GFP and PuroR cassette according to the original publication into the reference for analysis (, since it was not part of the deposited Genbank sequence. Read counting of viral ORFs was performed using FeatureCounts. KSHV specific counts were normalized using the estimated size factors generate for the human dataset to correct for sequencing depth-based bias. DGE for KSHV genes was performed using DeSeq2. To detect KSHV- encoded circular RNAs, FASTQ files were aligned using STAR to the human (hg19) + KSHV hybrid genome file. CIRCexplorer2 was used to detect back-spliced junctions in the KSHV genome. All back-spliced junctions were mapped in 200 nucleotide-sized bins and plotted. The raw data is deposited in the European nucleotide Archive (ID code: ena-STUDY-UNIVERSITY OF HELSINKI-13-02-2019-22:25: 30:309-452; accession number: PRJEB31253).

Study II

Cell preparation and sequencing

Total RNA was isolated from three independent experiments mock- and KSHV-infected blood or lymphatic ECFCs using the NucleoSpin RNA kit (Macherey-Nagel; 740955). RNA was further concentrated and purified using the RNA Clean and Concentrator kit (Zymo Research; R1017). Purity and concentration was determined with NanoDrop spectrophotometer (Thermo Scientific). Purified RNA samples were processed either at the Fred Hutchison Cancer Research Center Genomic Resources core facility (Seattle, WA) and sequenced using an Illumina HiSeq 2000 or processed in University of Helsinki and sequenced with Illumina Novaseq 6000 (150 bases, paired end) by Novogene (Cambridge, UK).

Bioinformatic analysis

Briefly, RNA-seq performed in Seattle, image analysis and base calling were performed using RTA v1.17 software (Illumina, San Diego, CA). Reads were aligned to the Ensembl's GRCh37 release 70 reference genome using TopHat v2.08b and Bowtie 1.0.0. KSHV reads were aligned to ViralProj14158 Strain GK18 reference genome. Counts for each gene were generated using htseq-count v0.5.3p9. Differentially expressed genes were determined using the R package EdgeR (Bioconductor). Genes were called significant with a |logFC| > 0.585 and

a false discovery rate (FDC) of <0.05. Gene Ontology enrichment was performed using Cytoscape and BINGO. Using cytoscape software and the Gene Ontology classification application BINGO, we determined the Gene Ontology terms that were highly enriched among the blood and lymphatic specific expressed genes. Gene Set Enrichment Analysis (GSEA) was also performed using the web app available through the Broad institute.

For RNA-seq performed in Helsinki, original image data was transformed to sequenced reads by CASAVA base recognition. Raw data were cleaned from low quality reads and reads containing adapter and poly-N-sequences in FASTP. Clean reads were mapped to the human genome (GRCh38.p12) using HISAT2 with parameters-dta-phred33. Read counts were generated by FeatureCounts. Differentially expressed genes were determined using the R package DESeq2. The resulting P values were adjusted using Benjamini and Hochberg's approach for controlling FDR. Genes with adjusted P value <0.05 were assigned as differentially expressed. The raw data is deposited in NCBI's Gene Expression Omnibus and are accessible through GEO Series accession number GSE54416, GSE207589 and GSE207657.

4.30 In vivo mouse model development and SOX18 inhibition

All animal work, including maintenance and procedures, was carried out in authorized facilities at the Laboratory Animal Center, HiLIFE, University of Helsinki, by certified personnel. The experiments were approved by the Finnish National Animal Experiment Board under licenses ESAVI/10548/2019 (tumor growth) and ESAVI/22896/2020 (oral gavage administration).

Female NSG mice (Nonobese diabetic (NOD)/severe combined immunodeficiency (SCID); NOD.Cg-Prkdc^{scid} Il2rg^{tm1Wjl}/SzJ) used in this study were provided by Jackson Laboratory and acquired through Scanbur (Germany). The mice were acclimatized for 7 days in isolation. After the isolation period, mice were trained for handling, weighing and finally to oral gavage tube feeding with clean water to reduce stress for the animals during the experimental procedures. The maintenance and all procedures with the mice were performed in authorized facilities, at the Laboratory Animal Center, HiLIFE, University of Helsinki (Finland), by trained certified researchers, and under a license approved by the national Animal Experiment Board, Finland (license number ESAVI/10548/2019 for tumor growth and ESAVI/22896/2020 for the oral gavage administration).

When the majority (about 90%) of the rKSHV.219 -infected lymphatic ECFCs expressed GFP, with some (about 5%) expressing RFP, the cells were collected

and mixed with KLECs, almost fully infected with rKSHV.219, with a substantial part (20-30%) expressing RFP. The combined cell preparation consisted of 90-95% of KSHV-infected lymphatic ECFCs and 5-10% of KLECs. KLECs were included to provide the more spontaneously lytic cells that can contribute to the inflammatory microenvironment and produce more infectious virus than the ECFCs. 5x10^6 cells/ 100 µL of cells were embedded in media containing ice-cold growth-factor reduced Matrigel (Corning; 356231) at 3 mg/mL concentration. 100 µL of the cell-Matrigel suspension was injected subcutaneously to both sides of the flanks of NSG mice, using total of 14 mice/ group. Additionally, mock infected ECs were mixed in the same ratio and implanted into NSG mice (n = 4) as a control.

For *in vivo* studies, Sm4 (a kind gift from Gertrude Biomedical Pty Ltd., Australia) was freshly prepared in the vehicle solution of 80% Kollisolv PEG-400 (Sigma; 06855), 10% MilliQ water and 10% Kolliphor ELP/Solutol HS-15 (Sigma; 42966) for each treatment dosing day at a concentration of 8 mg/mL. One day after subcutaneous implanting of the cell-Matrigel suspension a dose of 25 mg/kg of body weight was administered to mice daily for 10 sequential days as described in (Overman et al., 2017) using disposable polypropylene 20 ga x 38 mm feeding tubes (Instech; FTP-20-38) optimal for safe intragastric (IG) administration. The bioavailability of Sm4 was not measured during the treatment in this study, as the drug has been shown, when using a similar dose and administration route of Sm4, to be consistently detected in plasma of the treated mice, indicating a good systemic delivery of the drug (Overman et al., 2017). The gait, piloerection, type of breathing, alertness, skin tone, eye condition and abdomen were all normal on handling, and no signs of dehydration, diarrhea, or other adverse reactions were observed during the treatment period. After the 10-day Sm4 or Vehicle control treatment, and 24h after the last dose, the mice were euthanatized under anesthesia by cervical dislocation. In the autopsy, no abnormal swelling, colorization, or internal bleeding was observed. The injected cells (appearing as visible/palpable Matrigel plugs) were quickly removed from each mouse for either histological sampling and embedded in 10% neutral buffered formalin solution (Sigma; HT501128) or stored in -80C for DNA extraction performed by NucleoSpin Tissue Mini Kit (Macherey-Nagel) according to manufacturer's instructions and quantified for relative KSHV DNA. The histological samples were carefully cleaned of the mouse fat and skin and enclosed to tissue cassettes (Leica) for dehydration and processing with an overnight program in Tissue-Tek VIP 5Jr. (Sakura). The next day, the processed samples were embedded in paraffin (Sakura Tissue-Tek) and solidified into blocks at +4°C until cut. The blocks were cut with a Microtome (Leica) to sections and dried overnight on glass slides until stored at +4°C. The IHC and IF staining and imaging was performed as described above.

4.31 Statistical analysis

Graphical presentations and statistical analysis were generated with GraphPad Prism Software v9.0 (Dotmatics). For statistical evaluation of the RT-qPCR data for relative KSHV genome copies, the logarithmic values were converted to linear log2 scale values by using the double delta CT (2-ΔΔ CT) method. Human genomic actin when measuring DNA, and actin when measuring mRNA were used as internal control and accounted in the calculations to correct differences in the RNA and DNA amount from *in vitro* experiments. Human ALU-sequences were used as internal control and accounted in the calculations to correct differences in the DNA amount, quality, and PCR synthesis efficacy between the samples from *in vivo* experiments. The data is presented as individual values ± standard deviation (SD) between biological replicates unless otherwise reported. Statistical differences between groups were evaluated with either Student's *t*-test (two-tailed) or Welch's *t*-test, or ordinary one-way ANOVA followed by Dunnett correction for multiple comparisons. Further details can be found from original publication figure texts with exact p-values or when considered significant indicated by asterisk.

5 RESULTS & DISCUSSION

5.1 Lymphatic developmental factors contribute to unique KSHV-infection program in LECs and are expressed in KS tumors (I)

While KSHV establishes latency in virtually all susceptible cell types, LECs are uniquely permissive to KSHV infection, with high intracellular viral episome burden and spontaneous reactivation releasing infectious virus. Sporadic lytic reactivation and subsequent spread of infectious virus may be required for the progression of KS via replenishing and expanding the population of infected SCs, the charasteristic KS tumor cells.

We hypothesized that LEC-restricted or enriched host factors enable spontaneous lytic replication, given that the lymphatic, but not the blood, endothelial environment supports the spontaneous lytic replication of KSHV (**Fig 1A-C, S1A in I**). We assessed the contribution of the infectious virus released from KLECs to the spread of infection with phosphonoacetic acid (PAA), an inhibitor of viral but not cellular DNA polymerase, to block the production of infectious virus. KLEC-derived virus readily infected and spread in naïve LECs but failed to spread in the presence of PAA or within the blood endothelial cell (BEC) culture (**Fig 1D-E in I**). PAA being effective to block virus spread within LEC culture argues for a virus-mediated route rather than proliferation of cells that are already infected. These results indicate that efficient spontaneous reactivation and progeny virion production in KLECs likely sustains and expands the SC population in KS lesions. KSHV-infected BECs (KBECs) do not spontaneously reactivate and therefore fail to spread the infection in naïve cultures, underscoring the importance of an LEC-specific environment for sporadic lytic reactivation and virus dissemination.

The factors that render the lymphatic environment uniquely supportive for the KSHV life cycle were unclear. We therefore examined the roles of key developmental lymphatic transcription factors SOX18, COUPTF2 and PROX1 in driving the KSHV infection program in KLECs. Following *de novo* infection, *PROX1* mRNA transcripts increased in BECs and decreased in LECs within 14 days (**Fig 2A,C in I**), consistent with previous reports (Hong et al., 2004; Carroll et al., 2004; Yoo et al., 2012; Cancian et al., 2013). Despite transcriptional downregulation, PROX1 protein levels in KLECs were comparable to uninfected LECs by immunoblotting (**Fig 2D in I**). COUPTF2 expression remained unchanged. Notably, KSHV induced

SOX18 transcripts and protein in both KBECs and KLECs, a previously unreported observation that suggested a role in KSHV infection (**Fig 2A-E in I**). Overall this may indicate that KSHV infection is skewing the identity of LECs and BECs toward a lymphatic-embryonic program in which SOX18, COUPTF2, and PROX1 initiate LEC differentiation.

To investigate whether these three TFs were expressed in KS tumors, consecutive sections of biopsies from patients with AIDS-KS and HIV-negative KS were stained for SOX18, COUPTF2, and PROX1 and compared to normal skin from KSHV-negative donors. PROX1 has been previously shown to be expressed in KS (Hong et al., 2004, Yoo et al., 2012; Miettinen & Wang, 2012; Gramolelli et al., 2018). Accordingly, widespread and prominent expression of PROX1, but also SOX18, and to a lesser extent COUPTF2, were observed in both AIDS-KS and HIV-negative tumors colocalizing with latent and lytic viral proteins, LANA and glycoprotein K8.1, respectively (**Fig 7A; S5A,D in I**). By contrast, in KSHV-negative skin the expression of these three TFs was largely confined to vascular or lymphatic vessels, as expected (**Fig S5B-C in I**). Additionally, multiplex IHC analysis of over 8000 tumor cells across a KS skin cohort (n=19) further showed that SOX18 expression significantly correlated with latent LANA, whereas PROX1 correlated with both LANA and K8.1 (**Fig 7B-D; S5E in I**). These patterns link LEC lineage-specific TF expression to infection stage and suggest distinct roles for each factor in the viral program, with SOX18 acting during latency and PROX1 also contributing to the lytic cycle. Together with the observation that KLEC-derived virus spreads via spontaneous reactivation, the presence of K8.1-positive tumor cells underscores that lytic protein expression is important for the KS pathogenesis. These data further indicate that KS progression likely depends on recurrent seeding of the SC compartment via lytic reactivation and virus production, in addition to clonal expansion of pre-infected cells. In this view, sporadic lytic events are not bystanders, instead they are a sustaining engine for lesion maintenance.

Overall, lymphatic SOX18 and PROX1 are expressed in SC of KS lesions, supporting their relevance for the oncogenic KSHV infection cycle. To further investigate the role and connection of SOX18, COUPTF2 and PROX1 in lymphatic environment upon KSHV infection, we used genetic interference approach (siRNA). Interestingly, we observed that the reciprocal regulation of SOX18 and PROX1 is partially uncoupled during KSHV infection. During LEC specification, SOX18 and COUPTF2 positively regulate PROX1; accordingly, their depletion reduced PROX1 in uninfected LECs (**Fig S2J-K in I**). In KLECs, however, the effect on PROX1 was modest (**Fig 3B in I**), indicating that, unlike in uninfected LECs, SOX18, COUPTF2, and PROX1 are not strictly interdependent once cells are infected with KSHV. This proposes that KSHV drives alternative regulation that relieves PROX1 from its dependence on SOX18 during KSHV-induced reprogramming and, conversely, redirects SOX18 for

functions uncoupled from the PROX1 control. Functionally, this decoupling allows the virus to redirect the roles of normally interdependent developmental TFs, and likely introduces new infection-specific genomic targets, interaction partners and regulatory axes for both SOX18 and PROX1.

5.2 KSHV exploits SOX18 and PROX1 to promote viral persistence through different mechanisms (I)

To define how SOX18, COUPTF2 and PROX1 shape the distinctive KSHV program in KLECs, we examined loss-of-function effects on viral gene expression and output. Knockdown of SOX18 or PROX1 significantly reduced both gene and protein expression of key lytic factors ORF50, ORF45 and K8.1, and additionally SOX18 depletion decreased latent LANA protein level. In contrast, COUPTF2 depletion modestly increased lytic and LANA transcripts, without a corresponding change at the protein level (**Fig 3A-B in I**). Consequently, infectious virion production was reduced by approximately half upon SOX18 or PROX1 depletion, whereas COUPTF2 silencing had no effect (**Fig 3C in I**). Co-depletion of SOX18 and PROX1 suppressed virus release more strongly than individual knockdowns and achieved similar effect to the inhibition by PAA treatment (**Fig 3E-F in I**).

Notably, SOX18 knockdown also reduced intracellular viral episomes by 65%, while PROX1 had only a modest effect, and COUPTF2 had none (**Fig 3D in I**). Consistent with this, SOX18 silencing lowered LANA protein level, which is required for episome replication and maintenance. These data indicated a potential role for SOX18 in episome replication and maintenance in KLECs. Gain-of-function experiments supported this model: ectopic SOX18 expression increased episome numbers in KBECs, which normally express low SOX18 (**Fig 5A in I**). Moreover, in a non-endothelial background of iSLK.219 cells, ectopic SOX18 induced a dose-dependent increase in episomes (**Fig 5B in I**), even at SOX18 levels comparable to endogenous levels observed in KLECs and without affecting the overall cell proliferation (**Fig S3A in I**). iSLK.219 is a cancer cell line stably infected with rKSHV.219 and harboring a doxycycline-inducible KSHV-ORF50 that drives lytic reactivation from otherwise latent cells (Myoung & Ganem, 2011). The episome increase was not attributable to global LANA elevation as LANA levels were comparable between SOX18- and mCherry (mock control)-transduced iSLK.219 cells (**Fig S3B-C in I**).

Next, we used the SOX18 inhibitors Sm4 and R(+) propranolol enantiomer to further probe the SOX18 dependence on the high number of KSHV episome copies in LECs. Pharmacological inhibition of SOX18 in KLECs led to a dose-dependent reduction in both intracellular episomes and progeny virus release (**Fig**

4A-D in I). In contrast, the racemic mixture and the S(−) enantiomer triggered lytic reactivation (**Fig 4C-D in I**), likely through cell cycle disruption rather than specific SOX18 inhibition (McAllister et al., 2015). Additionally, Sm4 and R(+) propranolol treatments reduced episome copies in iSLK.219 ectopically expressing SOX18, but not in the SOX18-negative controls, supporting the specificity of the SOX18 inhibition (**Fig 4E in I**). These results provide a proof-of-principle that SOX18 is a druggable host factor with antiviral potential.

To investigate the mechanism by which SOX18 positively regulates the KSHV episome copy numbers, we tested its activity at KSHV replication origins. First, we used reporter plasmids harboring either seven copies of the *TR* region (*7XTR*) or the *OriA* fused to a firefly luciferase reporter. SOX18 expression increased the activity of the *7XTR*-luc reporter in a dose-dependent manner in the presence of LANA, while the increase in the *OriA*-luc reporter activity occurred independent of LANA expression (**Fig 5C-D, S3E in I**). Importantly, chromatin immunoprecipitation followed by qPCR (ChIP-qPCR) demonstrated SOX18 occupancy near the KSHV replication origins (*TR* and *OriA*) in both KLECs and SOX18-transduced iSLK.219 cells (**Fig 5E-G in I**). SOX18 targets promoters via IR5 motifs (Moustaqil et al., 2018), and one such motif lies adjacent to the *TR* region. These findings underscore SOX18 as a key regulator of KSHV genome maintenance and persistence.

While SOX18 primarily regulates latent episome numbers, PROX1 influenced the lytic cycle. To study the role of PROX1 on lytic infection further, we performed RNA-seq of KLECs upon *PROX1*- or control-targeting siRNA treatment. *PROX1* depletion in KLECs significantly reduced the expression of all KSHV genes, especially those expressed during the lytic cycle, indicating important role in supporting the complete lytic cycle. Additionally, RNA-seq was also performed with doxycycline (dox)-induced iSLK.219 cells ectopically expressing a Myc-tagged PROX1wt from a lentivirus. Ectopic PROX1wt expression in otherwise PROX1-negative iSLK.219 cells led to an increase in viral gene expression when induced to lytic cycle with dox (**Fig 6A in I**). Analysis of differentially expressed genes also revealed several cellular pathways involved in oncogenesis altered by *PROX1* silencing in KLECs (**Fig S4B in I**). Together, these data indicate that *PROX1* supports the KSHV lytic gene expression.

In KBECs, which lack endogenous PROX1, ectopic PROX1wt, but not a transactivation-deficient mutant (PROX1mut; Petrova et al., 2002), significantly increased expression of lytic genes *ORF50, ORF45, ORF57* and *K8.1* (**Fig 6B in I**). Correspondingly, dox-induced ORF50 in iSLK.219 yielded a larger fraction of lytically reactivating, virus-producing cells in the presence of PROX1wt versus PROX1mut (**Fig S4C-F in I**). Because KSHV ORF50 can trigger the full lytic cascade, we investigated whether PROX1wt would act synergistically with ORF50 to

increase the lytic gene expression. We performed a luciferase reporter assay using the *ORF50* promoter fused upstream of a luciferase gene, indicating that PROX1wt but not PROX1mut, significantly enhanced the ORF50-induced autoactivation (**Fig 6C, S4I in I**). Then, a physical interaction between PROX1 and ORF50 was confirmed with co-immunoprecipitation in both KLECs with endogenous PROX1 and spontaneously expressed ORF50 and in iSLK.219 with ectopic PROX1 and dox-induced ORF50 (**Fig 6D, S4J in I**). The PROX1-ORF50 interaction was further confirmed by PLA, and they also colocalized in the nuclear viral replication and transcription compartments (**Fig 6E-F in I**), a characteristic feature of DNA viruses to facilitate viral replication (Schmid et al., 2014). Importantly, PROX1 bound to the proximal regions of the *ORF50* promoter during the lytic cycle in KLECs and dox-induced iSLK.219 cells, shown by ChIP-qPCR (**Fig 6G in I**). Concurrently, another group reported that PROX1 activity promotes the KSHV lytic phase in the lymphatic context, binding the RTA promoter and interacting with RTA to co-regulate lytic genes (Choi et al., 2020), supporting our findings. They also proposed that PROX1 expression supports KLECs to sustain a productive *de novo* infection.

Together, these results reveal marked differences between BECs and LECs and further argue that the lymphatic developmental program provides a uniquely permissive context for KSHV. This study identifies LEC-enriched SOX18 and PROX1 as key host regulators of KSHV infection. SOX18 maintains high episome loads to promote persistence, whereas PROX1 amplifies lytic gene expression through ORF50 regulation. The limited impact of COUPTF2 on viral output further supports a model in which only a subset of lymphatic lineage factors are co-opted by KSHV. The summary of the study I main findings are presented in **Figure 11**.

Most SCs in KS lesions harbor latent KSHV, however a minority of cells are undergoing spontaneous lytic reactivation (Gramolelli & Schulz, 2015). Both latent persistence and lytic reactivation likely collaborate to sustain KS tumorigenesis *in vivo* (Grundhoff & Ganem, 2004). KSHV episomes are lost during cell division unless efficiently replicated, tethered and segregated upon mitosis, whereas sporadic lytic reactivation and release of infectious virus is required to replenish infected cell population. This also boosts the expression of angiogenic and inflammatory viral oncogenes that are essential for KS tumor progression. SOX18 and PROX1 provide a duality in the LEC environment co-opted by the virus to balance the two main imperatives of oncogenic herpesvirus infection.

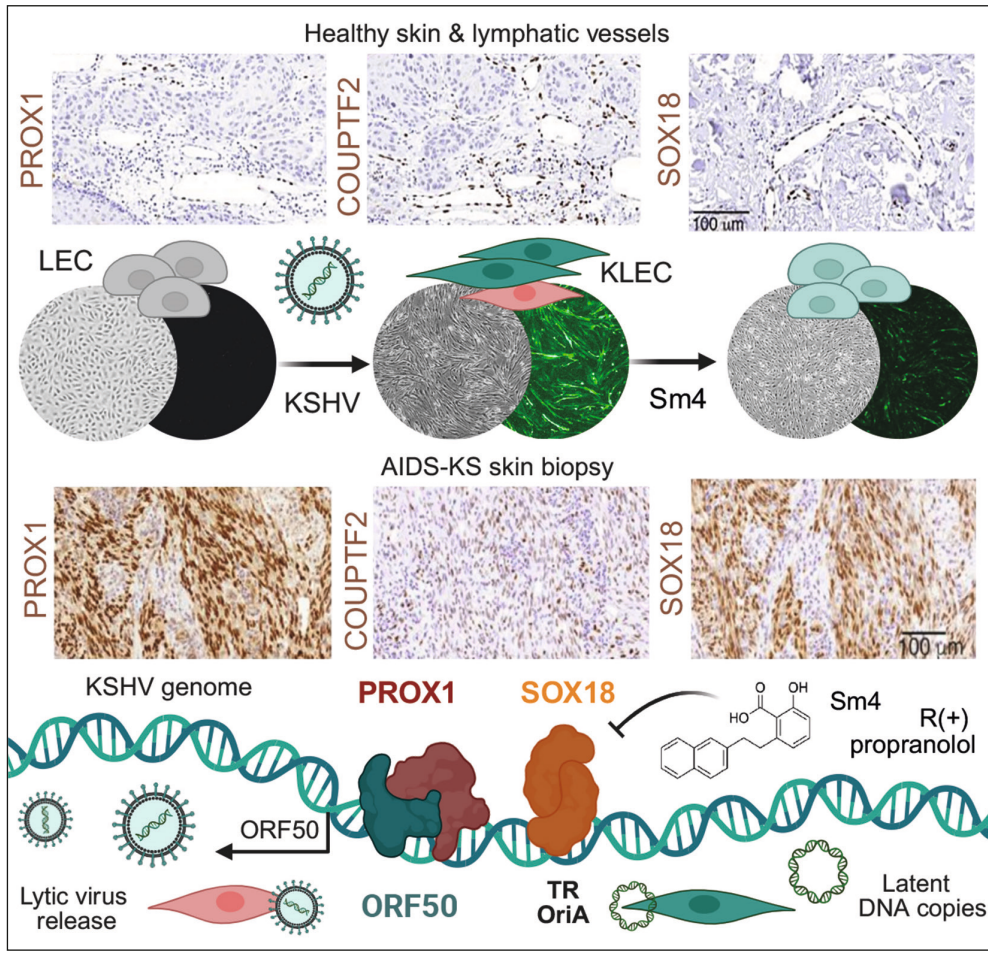

Figure 11. Schematic of the study I main findings. Lymphatic TFs PROX1, COUPTF2 and SOX18 are normally expressed in the LECs (grey) of vessel linings, whereas in KS lesions PROX1 and SOX18 are widespread. KSHV infection of LECs (grey) leads to spindle cell phenotype with majority of infected KLECs in latency (GFP signal from the recombinant KSHV strain: green) and small population of cells in lytic cycle (RFP signal: red). PROX1 regulates ORF50 -dependent lytic cycle and boosts release and spread of infectious virus. SOX18 is needed for efficient latent viral episome duplication from TR/OriA replication origin. Pharmacological SOX18 targeting with Sm4 or R(+)propranolol hampers KSHV episome persistence and spindling phenotype. Created with BioRender.

5.3 Lymphatic ECFC isolates are more permissive for KSHV than blood ECFCs (II)

Prior studies suggest that in addition to mature ECs, KSHV-infected endothelial colony-forming cells (ECFCs) may contribute to SC formation and KS lesion development (Cancian et al., 2013; Della Bella et al., 2008; Yoo et al., 2011).

ECFCs are rare circulating precursors of endothelial lineages that home to sites of angiogenesis (Asahara et al., 1997; Le Ricousse-Roussanne et al., 2004). However, their role in KS-associated neoangiogenesis is poorly understood.

Our collaborators previously isolated two ECFC phenotypes from whole blood, termed blood endothelial-like (BL) and lymphatic endothelial-like (LY) ECFCs (DiMaio et al., 2016). In this study, we isolated ECFCs from healthy donors, characterized, and assessed their susceptibility to KSHV infection. We isolated ECFCs from four healthy donors and identified isolates expressing markers of the lymphatic endothelium. Flow cytometry analysis revealed that these cells expressed high levels of CD34, VEGFR3, podoplanin, CD31/PECAM-1, SOX18 and PROX1 (**Fig S1 in II**), indicating a lymphatic ECFC phenotype (hereafter referred to as ECFCLY), rather than blood vascular endothelial ECFCs (hereafter referred to as ECFCBL).

We observed that, similar to LECs, ECFCLYs are more susceptible to KSHV infection than the ECFCBLs identified by our collaborators. By using the same amount of virus (multiplicity of infection; MOI), the infected ECFCLYs (K-ECFCLYs) had significantly more LANA-positive infected cells, compared to the K-ECFCBLs (**Fig 1A-C in II**). The latent infection efficiency can also be observed with GFP signal recombinant rKSHV.219. Notably, ECFCLYs from all donors developed evident KSHV-induced spindling phenotype resembling KLECs, whereas their blood type counterparts did not (**Fig 1C, E, S2 in II**). Next, we analyzed if either population of ECFCs could support spontaneous lytic replication and production of new infectious viruses, a phenotype typically observed only in KLECs, but not in KBECs. As seen by immunofluorescence and -blotting, K-ECFCLYs had spontaneously lytic cells expressing K8.1, in contrast to the strictly latent K-ECFCBLs (**Fig 1C-D in II**). We also confirmed that the reactivation, also indicated as RFP signal from recombinant rKSHV.219 in lytic cycle (Myoung & Ganem, 2011), produced infectious virus particles in K-ECFCLYs, albeit significantly less than KLECs (**Fig 1E-F, S2C in II**). Similar to K-BECs, K-ECFCBLs did not produce any infectious virus.

Previous data from us and others using neonatal ECs showed that LECs were able to maintain the KSHV episome but BECs lost the genome relatively rapidly over the course of cell passaging (Choi et al., 2020; DiMaio et al., 2020; Gramolelli et al., 2020). Using LANA staining to monitor infection, we observed that while both lymphatic and blood ECFCs showed comparable initial infection rates, fewer than 40% of ECFCBLs retained punctate LANA staining by 10 days post-infection. In contrast, nearly 100% of ECFCLYs remained LANA-positive, indicating more efficient viral maintenance and spread of infection (**Fig 1G-H in II**). In summary, similar to LECs, ECFCLYs maintain the viral episome over time, unlike BECs and ECFCBL, which gradually lose the viral genomes. Importantly, KSHV-infection led to a marked increase in SOX18 protein levels in ECFCLYs (**Fig 1D in II**), consistent

with previous findings in LECs (**Fig 2A-E in I**). The high SOX18 expression likely supports the maintenance of high copy number of KSHV genomes in K-ECFCLYs, analogous to KLECs.

Together, these data support a model in which ECFCLYs act as circulating reservoirs for KSHV and potential founders of SCs (Cancian et al., 2013; Della Bella et al., 2008; Yoo et al., 2011). K-ECFCLYs collectively mirror key features of KSHV-infected LECs, however, as CD34+ endothelial precursors, they can circulate systemically and are recruited to microenvironments of injury, inflammation, or angiogenic remodeling (Asahara et al., 1997; Le Ricousse-Roussanne et al., 2004), where they could potentially initiate or amplify KS lesions. Such a dissemination route offers an explanation for the multifocal pattern of KS across skin and visceral sites. These findings may have clinical implications; the frequency of KSHV-positive ECFCLYs in peripheral blood could serve as a biomarker for an elevated KS risk.

5.4 Lymphatic ECFCs gain tumorigenic properties upon KSHV-infection (II)

To understand why lymphatic and blood ECFCs diverge after KSHV infection, we profiled host transcriptional responses during primary infection (**Fig S3 in II**), and compared them with published transcriptomes of mature LECs and BECs. The results suggest that lymphatic and blood ECFCs exhibit distinct gene expression responses to KSHV infection, mirroring innate immune differences observed in neonatal LECs and BECs. Interferon-induced genes enriched in BECs upon infection are shown to be viral restriction factors (Crameri et al., 2018), potentially contributing to the reduced susceptibility to KSHV or accelerated episome loss in KBECs. Notably, genes involved in lymphatic endothelial identity, including LYVE1, podoplanin, and VEGFR3/VEGFC, were significantly upregulated (**Fig S3F-G in II**). Interestingly, Erythroblast Transformation Specific (ETS) TF family members ETS1 and ETS2 were strongly induced by KSHV-infection in ECFCLYs, which is in line with previous studies by our collaborators showing that KSHV leverages ETS via latent vFLIP induction of angiogenic phenotypes of KS-SC (Gutierrez et al., 2013). Because ETS factors regulate the PROX1-VEGFR3 axis during lymphatic specification and ETS2 enhances inflammatory lymphangiogenesis (Ducoli & Detmar, 2021; Yoshimatsu et al., 2011), these data nominate ETS1/2 as potential additional drivers of the lymphatic-biased infection program.

Furthermore, a subset of mesenchymal genes, such as αSMA, SNAI1, ZEB1, THY1, CD44, PDGFRA, and MMPs implicated in endothelial-to-mesenchymal transition (EndMT) were modestly but significantly induced (**Fig S3F-G, Text S2 in II**). Also, pathways driving EndMT such as TGFB and Wnt were enriched in K-ECFCLYs,

as well as several chemokines. MMP matrix metalloproteinases are mediators of EndMT and invasive properties of tumorigenic cells (Verma & Hansch, 2007). Prior studies showed that KSHV triggers MMP-dependent invasion and EndMT in LECs via Notch activation (Cheng et al., 2011; Gasperini et al., 2012). Additionally, we have shown that PROX1 modulates MMP14 activity in ECs (Gramolelli et al., 2018). Notch signaling is tightly regulated developmental pathway, however its aberrant regulation is showed to be involved in several pathogenic conditions, such as infections and cancer. Recently, it was discovered by Ojala group that Notch3 is also involved in LEC-melanoma cross-talk supporting the metastatic processes (Alve et al., 2024; Pekkonen et al., 2018). It is plausible that infected LECs and ECFCLYs share Notch-centric rewiring that promotes the invasive SC phenotype, similar to LECs in tumor microenvironment promoting melanoma metastasis. A time-course of single cell RNA-seq post infection of ECFCLYs would better map trajectories toward SC-like states and subpopulations undergoing tumorigenic changes during the dynamic KSHV-infection.

To determine if KSHV-induced transcriptional changes would confer ECFCs tumorigenic properties, we studied their growth and survival capacities. KSHV modestly inhibited proliferation irrespective of lymphatic vs blood origin (**Fig 2A in II**). However, K-ECFCLYs exhibited superior survival under growth factor-reduced and serum-deprived conditions compared with uninfected counterparts, K-ECFCBLs, and KLECs (**Fig 2C in II**). Notably, only K-ECFCLYs formed small multicellular colonies in soft agar within one month, whereas infected ECFCBLs and all uninfected ECFCs did not (**Fig 3 in II**). Across experiments, around 10% of K-ECFCLYs formed colonies, indicating virus-induced acquisition of anchorage-independent growth, enhanced survival and transforming potential. Consistently, lymphatic ECFCs showed higher basal proliferation and greater survival under serum- and growth factor-limited conditions than mature LECs (**Fig 2B, D in II**). This growth advantage under restrictive conditions further supports their heightened transformative potential relative to LECs, which have not been shown to transform *in vitro* despite efforts. This difference likely reflects the progenitor-like plasticity of ECFCLYs, enabling greater phenotypic change upon KSHV-infecton.

Although proliferating SCs in KS tumors specifically express lymphatic markers such as SOX18 and PROX1, they also display certain BEC and mesenchymal features. Consistent with this, KSHV infection of BECs drives lymphatic-like differentiation, including induction of PROX1 and VEGFR3 (Carroll et al., 2004; Hong et al., 2004; Wang et al., 2004). SCs have been shown to exhibit EndMT, accounting for the mesenchymal markers in the complex SC phenotype (Cheng et al., 2011; Gasperini et al., 2012). Thus, while LECs are considered the most likely cell of origin for SCs, the progenitor-like plasticity of circulating ECFCLYs may represent viral reservoirs that seed multifocal KS lesions and explain SC heterogeneity.

5.5 Lymphatic ECFCs represent a translational model for testing potential KS therapies (II)

We leveraged the SOX18-expressing ECFCLYs as a physiologically relevant KSHV-infection model to further test SOX18's role in KS pathogenesis. As in KLECs (**Fig 3 in I**), siRNA-mediated SOX18 depletion in ECFCLYs significantly reduced intracellular viral genome copies, the fraction of LANA-positive cells, and titers of infectious viral progeny (**Fig 4A-E in II**). We then evaluated pharmacologic inhibition with the small-molecule SOX18 inhibitor Sm4. At non-toxic concentrations, Sm4 decreased GFP and RFP signals from rKSHV.219, indicating latent and lytic cells, respectively, and diminished the spindle morphology of infected cells. K-ECFCLYs were more sensitive to Sm4 than uninfected ECFCLYs, consistent with elevated SOX18 levels (**Fig 4E-F in II**). Importantly, Sm4 led to dose-dependent reductions in KSHV episome copies, LANA-positive cells, and released infectious virions (**Fig 4G-I in II**). These data demonstrate that SOX18 is required to sustain high intracellular episome loads and infectious output in KSHV-infected ECFCLYs, mirroring its role in KLECs.

Given prior evidence from Ojala group that KSHV enhances sprouting and invasion of mature LECs in three-dimensional (3D) fibrin matrices (Cheng et al., 2011), we interrogated ECFC behavior in an analogous 3D organotypic assay. KSHV robustly induced sprouting in lymphatic ECFC spheroids, and this response was completely abrogated by Sm4 (**Fig 5A, C in II**). In contrast, blood ECFC spheroids exhibited sprouting independent of viral infection, highlighting their intrinsic angiogenic capacity. Sm4 had no impact on KSHV-infected blood ECFCs, which lack SOX18 expression, further confirming the specificity of the response in lymphatic ECFCs (**Fig 5B, D in II**). Together these data support that the lymphatic ECFCs represent a viable *in vitro* model for KSHV infection and for preclinical evaluation of KS-relevant host targets.

Because KLECs do not exhibit progressive transformation, or persist *in vivo*, they are unsuitable for translational anti-tumor efficacy studies. However, as K-ECFCLYs complete the lytic infection program, proliferate, and show emerging transformation features, we decided to test their long-term persistence *in vivo* (**Fig 6A in II**). K-ECFCLYs were subcutaneously implanted into immunocompromised NSG mice as Matrigel plugs, which remained visible after 30 days, indicating sustained *in vivo* survival (**Fig 6B, S5 in II**). Although no tumorigenic growth was observed within this time period, the xenografts recapitulated the spindling phenotype of KS tumor cells in the lesions and expressed GFP, RFP (latent and lytic rKSHV.219) and LANA. This contrasts with KLECs, which fail to survive and are therefore unsuitable as an *in vivo* infection model. The propensity of KLECs toward the lytic program, shown in **study I** (Gramolelli et al., 2020) and by others (Choi et al., 2020), is a necessary

component of infection program. However, the sporadic lytic reactivation tends to make KLECs more susceptible for environmental stressors and cytopathic effect owing to lytic cell lysis upon release of viral progeny.

To assess the effect of SOX18 inhibition, a cohort of mice (n=8 per group) bearing K-ECFCLY plugs was treated orally with Sm4 for 10 consecutive days, as described in (Overman et al., 2017). Additionally, KLECs (5-10%) were mixed with K-ECFCLYs (90-95%) to provide more spontaneously lytic cells that could contribute to the inflammatory microenvironment, and to better recapitulate the complex KS lesions in patients (**Fig S4 in II**). In the vehicle-treated group, strong GFP expression and characteristic spindle cell morphology (hallmark of KS) were observed again. In contrast, K-ECFCLY plugs from Sm4-treated mice exhibited significantly reduced GFP signal, fewer spindle-shaped cells, and markedly lower KSHV genome copy numbers (**Fig 6C-G in II**). These results further support SOX18 inhibition as a promising therapeutic strategy for KS. The workflow and summary of the study II findings are presented in **Figure 12**.

Collectively, our data suggest that circulating lymphatic ECFCs can act as viral reservoirs and progenitors for KS initiation, potentially explaining the multifocal nature of KS lesions. In K-ECFCLYs, the expression of the lymphatic TFs SOX18 and PROX1 expression supports both viral episome maintenance alongside a low yet persistent level of lytic replication – processes that are essential for sustaining oncogenic KSHV infection. Their progenitor-like plasticity confers enhanced survival and EndMT-linked adaptability, promoting transformative potential and positioning ECFCLYs as potential contributors to KS pathogenesis. Importantly, lymphatic ECFCs provide a physiologically relevant platform to dissect KSHV-host interactions and to evaluate lymphatic-specific antiviral strategies *in vivo*.

Recently, an *in vivo* model was generated in which the complete KSHV genome was inserted in transgenic immunocompetent mice (Sin et al., 2024). This differs from most earlier models that examined the effects of individual viral oncogenes, such as vGPCR, in genetically engineered mice (Medina et al., 2020). vGPCR has been identified as a major KSHV oncogene, promoting cell transformation and angiogenesis (Bais et al., 1998; Ma et al., 2010; Montaner et al., 2003), and it can immortalize human HUVECs via constitutive activation of the VEGF signaling (Bais et al., 2003). The key limitation in such models is the absence of the full KSHV infection program, as both latent and lytic phases have been shown to be important for KS tumorigenesis. Another approach utilizes transfection of BAC-KSHV in mouse to induce KS-like tumors *in vivo*, however these were reversible and lost the KSHV episomes over time. The model by Sin et al. produced growth of LANA-positive, aggressive angiosarcomas that mirror KS (Sin et al., 2024). These spontaneously arising vascular tumors expressed lymphatic markers and KS hallmark pathways

with SC phenotype, and importantly, exhibited both latent and lytic gene expression programs. This constitutes the most faithful and reproducible KS preclinial model by far for diessecting of the stepwise molecular pathogenesis of KS and to evaluate potential virus or host-targeted therapeutic avenues for KS, also in immuno-competent context. A caveat, however, is that the KSHV genome is integrated into the mouse genome rather than maintained as an episome tethered to the host genome. While this enables expression of full KSHV genome under viral promoters in mouse and allows the interplay of several oncogenic KSHV factors to induce angiosarcomas, it does not fully recapitulate the natural infection mechanisms. Due to integration, LANA is not confined as nuclear speckles binding as oligomers on viral episomes; instead, it displays more diffused pattern in nucleus and cytoplasm (Sin et al., 2024). Although the K-ECFCLY presented in this thesis does not show clear tumorigenic growth *in vivo*, it provides a fast translational model for preclinical target testing. In this system the full KSHV infection program occurs naturally, with most cells in latency and a minority undergoing spontaneous lytic reactivation. Notably, K-ECFCLYs express the key lymphatic factors that drive both phases of KSHV infection, enabling the assessment of how the human lymphatic nexus modulates responses during testing of novel KS therapies. In sum, multiple complementary animal models are needed to achieve a comprehensive understanding of the KSHV pathogenesis and to map potential vulnerabilities for KS.

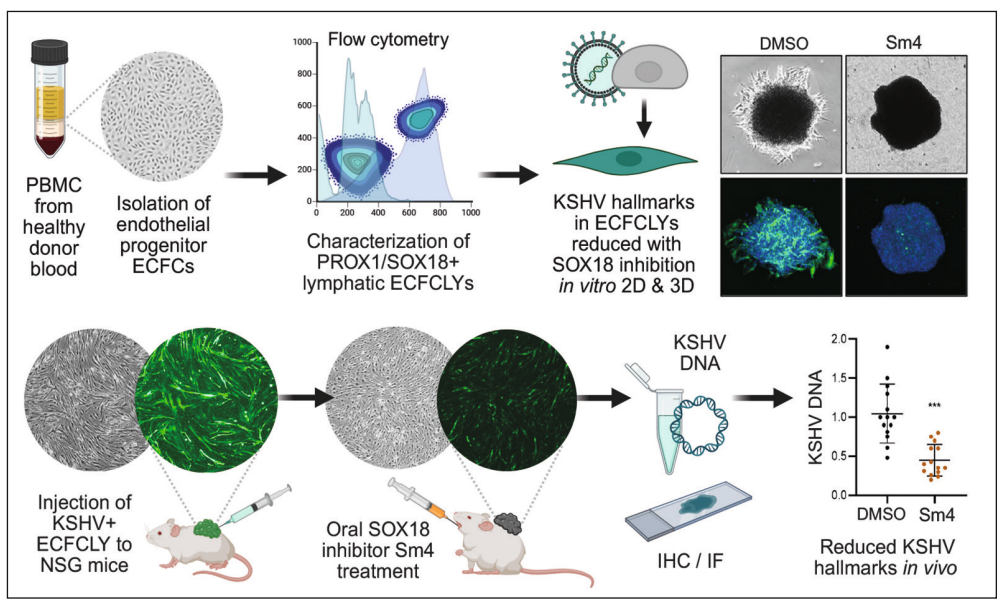

Figure 12. Schematic of the study II workflow and main findings. Progenitor ECFCs were isolated from healthy donor blood and subpopulation was characterized to express lymphatic markers, such as SOX18 and PROX1. Upon KSHV-infection, lymphatic ECFCLYs acquired enhanced survival, spindle cell features, high KSHV load and spontaneous production of viral progeny. These KSHV infection hallmarks could be blocked via SOX18 inhibition with Sm4 in vitro and in vivo. Created with BioRender.

5.6 Latent KSHV-infection upregulates SOX18 by activation of the host NF-κB pathway (III & additional results)

Given SOX18's central role in KSHV infection, we asked how the virus upregulates SOX18 and whether this occurs during latency or depends on lytic replication. Because rKSHV.219 undergoes spontaneous lytic reactivation in KLECs driven by ORF50/RTA and PROX1, we compared rKSHV.219 infection with KSHV-BAC16-ΔORF50 strain, which carries a stop codon in ORF50 and thus cannot reactivate or produce progeny virions (Weissmann et al., 2025). ΔORF50 was produced from iSLK.BAC16-ΔORF50 cells and used to infect LECs alongside rKSHV.219 (Myoung & Ganem, 2011). Notably, both strains induced SOX18 upregulation (**Fig S4A in III**), indicating that latent infection is sufficient for this. Consistently, viability assays with the SOX18 inhibitor Sm4 showed that infection with either of the two strains sensitized LECs, similar to ECFCLYs, likely reflecting elevated SOX18 levels (**Fig S4B in III**). Both strains caused prominent spindling cell phenotype, and yielded similar intranuclear episome levels, which were reduced by Sm4 treatment (**Fig S4C-D in III**). Speckled LANA staining, a marker for nuclear episomes, showed comparable levels for both strains, and Sm4 likewise reduced them (**Fig S4E-F in III**). These results confirm that the SOX18-related enhanced infection phenotype occurs during latency, and is not dependent on the lytic cycle.

We next investigated whether NF-κB signaling mediates SOX18 upregulation. Prior work in endothelial models showed that NF-κB activation increases SOX18 and that the IκBα phosphorylation inhibitor Bay11-7082 reduces SOX18 in a dose-dependent manner (Basilio et al., 2013). NF-κB pathway typically signals through p50/p65 (RelA) dimers, with nuclear translocation of p65 marking activation (Brown et al., 2003; Schmitz & Baeuerle, 1991). Interestingly, KSHV activates NF-κB during *de novo* infection to regulate host and viral genes and promote survival (Grossmann & Ganem, 2008; Sadek et al., 2020). We first established a non-toxic Bay11-7082 concentration (2.5 μM by CellTiter-Glo) for LECs and KLECs (**Fig 13A in additional results**). Infection with ΔORF50 or rKSHV.219 again upregulated SOX18 protein expression or stability (**Fig 13B-C**), consistent with our previous results (**Fig S4A in III**). When treated with Bay11-7082 for 72h, SOX18 protein reduced to near baseline levels and concomitantly lowered LANA levels (**Fig 13B-C**). This reflects the decreased KSHV episome copies upon SOX18 loss (**Fig 3D in I**) or protein inhibition (**Fig 4A, C in I**). These results implicate that activation of NF-κB pathway could be inducing SOX18 protein expression or stability during latency.

Because the latent proteins LANA and vFLIP can engage NF-κB pathway by interacting with IKKγ leading to activation of the IKK complex (Konrad et al., 2009; Liu et al., 2002), we tested their individual contributions. To this end, LECs transduced

with lentiviral LANA or vFLIP were analyzed for NF-κB activation and SOX18 expression. LANA expression was verified by IF (**Fig 13D**), and vFLIP, for which no functional antibody is available, was confirmed by RT-qPCR (**Fig 13E**). The latent vFLIP has also been shown to drive primary ECs towards spindle cell morphology (Alkharsah et al., 2011), by acting as a sustained activator of the NF-κB pathway (Liu et al., 2002). In line with prior reports, vFLIP, but not LANA, induced a spindle morphology, seen with both phase contrast microscopy images and VE-cadherin staining (**Fig 13F**). NF-κB activation, measured by RelA/p65 nuclear translocation and nuclear signal intensity, was robust with vFLIP but minimal with LANA (**Fig 13G**). Quantification of both the percentage of RelA p65 positive nuclei and the nuclear RelA p65 signal intensity showed that vFLIP activated NF-κB signaling, whereas LANA expression did not significantly induce re-localization of RelA p65 (**Fig 13H**). Indeed, in LECs, the expression of vFLIP significantly upregulated the expression of SOX18 protein (**Fig 13G-J**). Also, LANA moderately increased SOX18 protein levels in LECs, though less strongly than vFLIP. Overall, these results indicate that the KSHV-encoded latent protein vFLIP, and more modestly LANA, upregulate SOX18 by activating the host NF-κB pathway in LECs during KSHV latent infection.

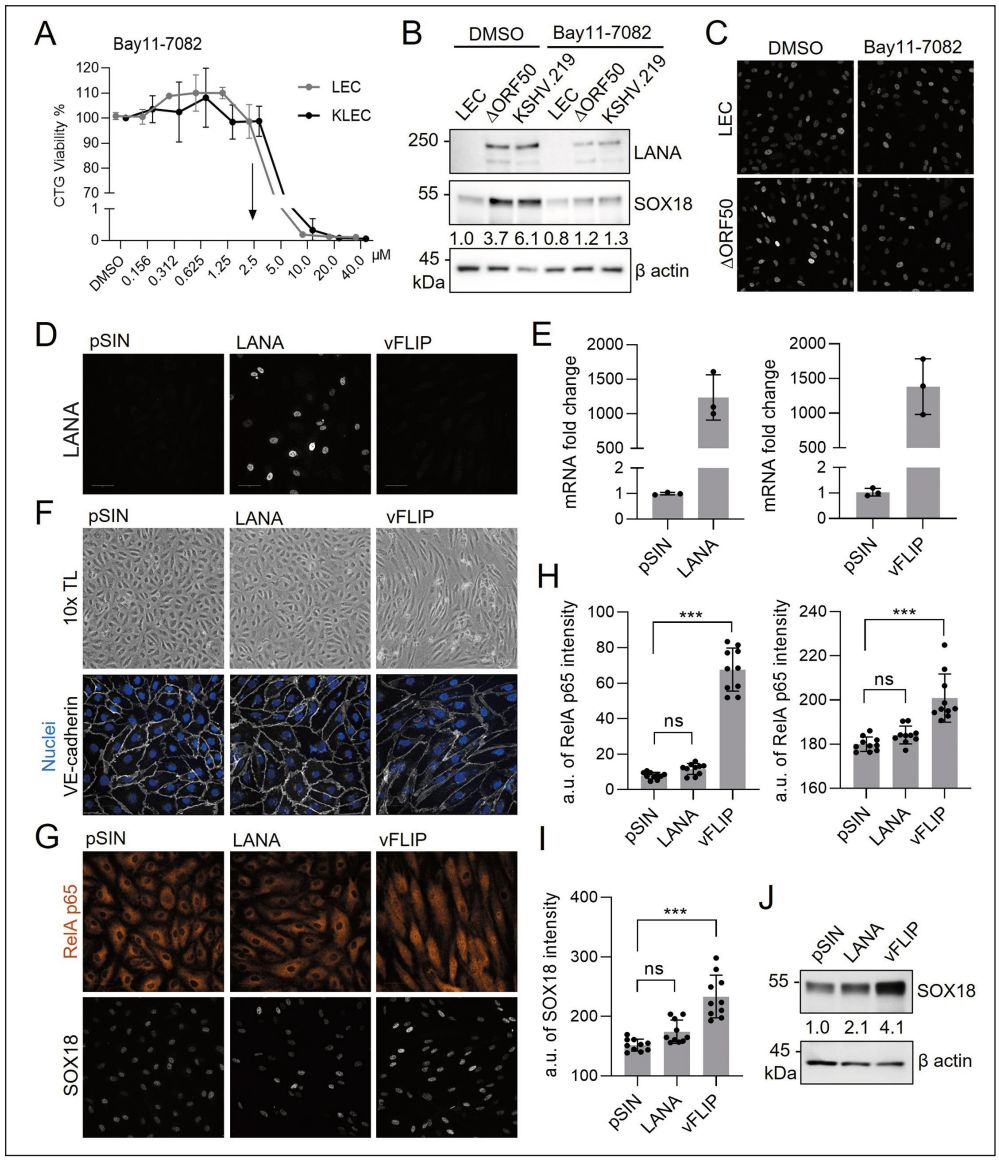

Figure 13. Additional results: latent KSHV-infection induces SOX18 via activation of the host NF-kB pathway. A. Uninfected LECs or infected with rKSHV.219 (KLEC) were treated with DMSO or increasing concentrations of the NF-kB inhibitor Bay11-7082 for 72h and viability measured with CTG assay. The chosen experimental concentration 2.5μM is indicated by an arrow. **B-C.** Uninfected LECs or infected with ΔORF50 or rKSHV.219 for 24h treated with DMSO or Bay11-7082 at 2.5μM for 72h were analyzed for SOX18 by immunoblotting (quantified using β-actin for normalization) and by IF. D-J. LECs transduced with vector control (pSIN), LANA or vFLIP expressing lentiviruses for 72h. **D.** IF images of LANA, and E. RT-qPCR analysis of LANA and vFLIP in relation to the pSIN control. **F.** Phase contrast images of transduced LECs (upper panels) and IF images of VE-cadherin staining (lower panels). Nuclei were counterstained with Hoechst (33342). **G.** IF of RelA p65 (upper panels) and SOX18 (lower panels) and **H.** quantified from n=10 replicates and n=9 fields for % of RelA p65+ nuclei and mean nuclear RelA p65 and **I.** mean SOX18 intensity. **J.** Immunoblotting with anti-SOX18 antibody and quantified using β-actin for normalization. ***p < 0.001, ns = non-significant.

Mechanistically, our results implicate the host NF-κB pathway via vFLIP as the primary driver of SOX18 induction in latency. A non-toxic dose of the NF-κB pathway inhibitor Bay11-7082 reduced SOX18 to near-baseline seen in LECs. Concomitantly, this lowered LANA levels, consistent with reduced episome numbers seen in the previous studies of this thesis (**Fig 3D, 4A, C in I**), when SOX18 activity was genetically or pharmacologically hindered. Together, these findings show that vFLIP activates NF-κB, which in turn upregulates SOX18, promoting episome stability and KS-like cellular reprogramming, whereas LANA may provide a minor, auxiliary input. Of note, broad NF-κB inhibition is likely to carry on-target toxicities, thus it is better to target downstream SOX18. In addition to SOX18, vFLIP has been shown previously to upregulate ETS1 in EC context (Gutierrez et al., 2013), indicating that vFLIP can induce multiple central host EC TFs. This also further supports the earlier notion that ETS factors may play an underexplored role in KSHV infection of LECs, in addition to SOX18 and PROX1.

5.7 SOX18 recruits SWI/SNF chromatin remodeling complex upon KSHV infection (III)

KSHV persists in LECs by maintaining high numbers of episomal viral genomes, and previous findings of this thesis implicated SOX18 is upregulated by the virus (**Fig13 in additional results**) and acts as a critical player in this process (**Fig 3D, 4A, C in I**). The third original study of this thesis further investigates the molecular mechanism through which SOX18 supports KSHV latency and persistent infection.

As SOX18 is known for its function as TF, we first investigated whether SOX18 transactivation activity would be responsible for an increase in episome copies by activating expression of viral genes. To this end, we generated plasmid constructs, and produced lentiviruses to transduce wild-type (wt) SOX18, two SOX18 mutants: a transactivation deficient dominant negative mutant (C240X) and a DNA-binding HMG box deletion mutant (HMGdel) (**Fig S1A in III**), or a Cherry expressing mock control, into HeLa cells inherently lacking SOX18 expression (**Fig S1B in III**). Overexpression of SOX18wt or the mutants in KSHV-HeLa cells had no effect on initiation of viral transcription, and inhibition of SOX18 by Sm4 in KLECs did not alter viral gene expression significantly (**Fig S1C-D in III**). This data is in line with our previous findings in SOX18wt and mCherry control transduced iSLK.219 cells where upon dox-induction LANA and lytic expression remained similar at least within 24 hours post infection (**Fig S3B-C in I**). This indicated that SOX18 does not directly promote KSHV gene expression and its function in supporting episome maintenance operates independently of direct transcriptional activation.

SOX factors often rely on protein-protein interactions with partner TFs, coactivators, or chromatin regulators to modulate gene expression effectively. Through these interactions, SOX proteins act as versatile architectural factors, rather than functioning as stand-alone activators, enabling them to regulate diverse developmental and cell fate programs in a cell type-dependent manner (Kamachi & Kondoh, 2013; Wilson & Koopman, 2002). Therefore, we sought to investigate this alternative mode of action. We transduced a lentivirus expressing BirA*-fusion of SOX18wt or mCherry control into iSLK.219 and uninfected, parental (SLK) cells to differentiate interactions specific for KSHV-infection. An unbiased BioID proteomics-based screen coupled with mass spectrometry (MS) revealed that SOX18 notably interacts with components of the SWI/SNF chromatin remodeling complex (CRC), specifically ARID1A and BRG1, but only in KSHV-infected cells (**Fig 1A-D in III**). Most of the top SOX18 interactors in infected cells are components of this same CRC complex, also known as cBAF, generating chromatin accessibility via nucleosome eviction (Centore et al., 2020). The detection of SOX18 interaction with itself, due to tendency to dimerize, in both conditions served as an internal positive control for successful pull-down efficiency.

The interactions between SOX18 and ARID1A or BRG1 were confirmed by PLA and were significantly reduced by pharmacological inhibition of SOX18 with Sm4 (**Fig 1E-G in III**), without reducing the overall protein expression (**Fig S1E-F in III**). Interestingly, also ETS2 has been shown to form complex with SWI/SNF (Baker et al., 2003). Thus, it is plausible that ETS factors, upregulated upon KSHV-infection in LECs (Gutierrez et al., 2013) and ECFCLYs (**Fig S3F-G in II**), co-operate with SOX18 in episome maintenance. The caveat of BioID in this study is the lack of LEC background, that could have also uncovered interaction changes between different lymphatic specific factors with SOX18 upon KSHV-infection. As the interaction between SOX18 and SWI/SNF subunits was pronounced in infected cells, we investigated whether a viral protein mediates this. We found that LANA, essential for episome maintenance, also interacted with BRG1 and ARID1A by using PLA, and these interactions were mainly SOX18-dependent in KLECs (**Fig 1H-J in III**). In a non-endothelial context, a previous report demonstrated a direct interaction between SWI/SNF complex subunits and LANA (Zhang et al., 2016), supporting our findings. These data gave the first pieces of evidence that LANA facilitates SOX18 to recruit SWI/SNF as a virus-engaged pioneer factor.

5.8 SOX18 activity orchestrates chromatin accessibility as a pioneer factor (III)

To test if KSHV infection engages SOX18 to function as a pioneer factor, we first set out to address whether SOX18 can influence chromatin organization independently

of KSHV. To assess SOX18's chromatin-regulating capacity beyond infection, we collaborated with Dr. Mathias Francoís group (University of Sydney, Australia), who studies human umbilical vein endothelial cells (HUVECs), where endogenous SOX18 expression could be manipulated and activity inhibited by Sm4. SOX18 inhibition increased distribution and intensity of the heterochromatin properties (**Fig 2A-C in III**). This observation was confirmed using a high-content, image-based, multi-parametric method known as microscopic imaging of epigenetic landscapes (MIEL; **Fig S2A in III**)) (Farhy et al., 2019). Our collaborators examined HUVECs with ectopic over-expression of SOX18wt to mimic the increase in SOX18 levels upon KSHV infection in LECs, and upon SOX18 inhibition by Sm4 with MIEL. This cell population analysis revealed significant changes in chromatin compaction upon SOX18wt ectopic expression, whereas the opposite effect on compaction was observed after SOX18 inhibitor Sm4 treatment, when compared to DMSO treated baseline population (**Fig 2D in III**).

This is in line with SOX18 having strong intrinsically disordered region (IDR; **Fig S2F in III**), which allows dynamic partner interactions to remodel chromatin or activate transcription through phase-separation. IDRs are stretches of amino acids in a protein that do not fold into a stable 3D structure on its own, but instead, stay flexible and are potent at recruiting transcriptional coactivators, such as SWI/SNF (Boija et al., 2018; Erdos & Dosztanyi, 2024; Sabari et al., 2018). Additionally, live-cell imaging with number and brightness (N&B; **Fig S3A in III**) (Digman et al., 2008) analysis showed that in addition to monomer and dimer states, SOX18 forms higher-order oligomers (**Fig 3A-D in III**), that can bind DNA co-operatively increasing residence time and form a scaffold for recruiting transcriptional coactivators. Trichostatin A (TSA) treatment opened chromatin and promoted dimer and higher-order oligomer assemblies with residual monomers, while Actinomycin D (ActD) treatment compacted chromatin, suppressing dimers/oligomers and shifting the population toward monomers. Single molecule tracking (SMT; **Fig S3B in III**) (Chen et al., 2014) measured the mobility and chromatin binding dynamics of labeled SOX18 in real-time, showing more stable and prolonged chromatin occupancy under open chromatin conditions by using TSA treatment (**Fig 3E-I in III**). These properties were lost when chromatin was compacted, confirming that SOX18's activity is tightly coupled to chromatin accessibility. In summary, pharmacological inhibition of SOX18 changes the chromatin organization and in turn chromatin organization alters SOX18 nuclear navigation.

To investigate whether inhibition of endogenous SOX18 influences chromatin accessibility also in LECs in the absence of KSHV infection, we performed ATAC-seq from Sm4 or DMSO control treated LECs. The data shows that SOX18 regulated global chromatin organization and accessibility, especially at SOX motif-enriched sites (**Fig 2F-G, S2G in III**). Together, these observations demonstrate that SOX18

dimerization helps to maintain an open chromatin state, while its inhibition by Sm4 leads to a significant loss of chromatin accessibility. This shows that SOX18 can influence chromatin organization, indicating potential for pioneering activity.

TFs with pioneer capacity can recognize DNA wrapped in nucleosomes and initiate local chromatin opening, thereby licensing downstream regulatory programs. A widely known factor SOX2 helps to sustain embryonic stem cell pluripotency through pioneer activity (Hagey et al., 2022). Beyond development, SOX18 has demonstrated lineage-instructive potential as its expression in stromal and adipose-derived cells induces endothelial markers (PECAM-1, VE-cadherin, CD34) and can bias hemogenic endothelial progenitors toward other lineages (Fontijn et al., 2014; Jung et al., 2023). Although individual SOX proteins govern distinct developmental processes, several can partially substitute for SOX2 during cellular reprogramming, albeit far less efficiently, implying shared structural and functional features within the family (Nakagawa et al., 2008). Consistent with this, the HMG domain that enables pioneer-type DNA engagement in SOX2 is structurally conserved across multiple SOX paralogs, including SOX18 (Dodonova et al., 2020). These studies support the findings in this thesis that SOX18 could function as a pioneer factor, likely via recruiting SWI/SNF to evict nucleosomes for more accessible chromatin.

5.9 KSHV hijacks SOX18 pioneer activity to increase chromatin accessibility in LECs during latency (III)

Pathological settings such as cancer or infection can confer pioneer-like behavior on TFs that are not pioneers at physiological levels; occurring through mutations or overexpression that alter DNA binding and cofactor interactions (Bulyk et al., 2023). Our data showing upregulated SOX18 in latency fits in this pathological-pioneer framework in the context of KSHV infection. Results from the previous studies in this thesis show that KSHV hijacks SOX18 to positively regulate the episome maintenance and consequently infection hallmarks, such as the spindling phenotype during latency. We therefore proceeded to investigate how SOX18 affects viral and host chromatin organization and accessibility via its pioneering activity.

To circumvent the released viral DNA from spontaneous reactivation in KLECs, that interferes with ATAC-seq by generating high background on viral genome, we used the strictly latent KSHV-BAC16-ΔORF50 strain. As shown above (chapter 5.6), ΔORF50 infection was validated to yield similar intranuclear episome levels and infection hallmarks as rKSHV.219, including SOX18 upregulation (**Fig S4 in III, Fig13 additional data**). As we have previously shown that SOX18 binds to the proximity of KSHV DNA replication origins (*TR* and *OriA*; **Fig 5E-F in I**), we hypothesized that SOX18 pioneer activity would primarily render viral chromatin

more prone for replication initiation events. To our surprise, ATAC-seq showed only minor changes on the viral chromatin (**Fig S5C in III**) after 24h of inhibitor treatment. However, this further supports that SOX18 does not contribute to high numbers of KSHV episomes in KLECs primarily by altering the transcription of viral genes at early stages (**Fig S1C-D in III**). Of note, previous studies in this thesis and by others have shown that KLECs are unique hosts due to spontaneous reactivation, which does not happen with KBECs, possibly as regulatory regions of ORF50/RTA and other lytic genes were more open and accessible in KLECs compared with those in KBECs (Choi et al., 2020). Such a difference was not found for the promoter of LANA, supporting our results that there were no significant accessibility changes in the latent viral genome.

In contrast, our results showed that ΔORF50-KSHV infection in LECs significantly increased chromatin accessibility across the host genome (**Fig 4A,C in III**). This effect was largely reversed by SOX18 inhibition by Sm4, with more than 75% of KSHV-induced accessible regions reverting to a more closed state (**Fig 4B-C in III**). We hypothesize that the stronger increase of SOX18-mediated LEC chromatin accessibility observed in infected KLECs is due to significant upregulation of SOX18 upon KSHV infection. Enhancers and SOX binding motifs became more accessible upon infection and less so upon SOX18 inhibition (**Fig 4D-E in III**). We next determined through HOMER analysis that KSHV infection causes an enrichment for *de novo* motifs from bZIP (FRA1) and ETS (ETV2) TF families, in addition to SOX factors, while Sm4 treatment reciprocally reduced accessibility in the regions of corresponding TF family motifs (**Fig 4F in III**). This further indicates that ETS factors potentially have a role via co-operation with SOX18 in the development of KSHV hallmarks in LECs. The accessibility increase in KLECs and reciprocal decrease upon Sm4 can be seen in several enhancer regions, which are enriched for SOX18 binding motifs (**Fig 4G in III**).

Moreover, supporting ATAC-seq, heterochromatin marker HP1α foci in the nucleus were decreased upon KSHV-infection of LECs and appeared more intense and widespread following Sm4 treatment (**Fig 4H-I in III**), indicating that SOX18 is required for KSHV-induced chromatin accessibility. We also performed MIEL with rKSHV.219 infected LECs, to ensure a more natural, full infection cycle. MIEL confirmed that KLECs have a distinctly different HP1α distribution and chromatin organization compared to uninfected LECs (**Fig 4J-L in III**). This distribution of LECs and KLECs reflects the Anna Karenina principle (Zaneveld et al., 2017), which posits that healthy systems tend to be similar, whereas each dysfunctional system is abnormal in its own way. This principle is evident in the broader distribution of chromatin features observed in DMSO-treated KLECs, where KSHV infection is asynchronous, cells occupy different phases of infection, and oncogenic effects are highly variable, in contrast to the more

compact, homogeneous populations of uninfected LECs (**Fig 4L, Fig S5I in III**). However, SOX18 inhibition rescues the phenotype towards uninfected LECs, and also Sm4 treated KLEC and LECs are more similar to each other than their respective DMSO controls. In summary, we have identified a pioneer function for SOX18, driving genome-wide changes in chromatin accessibility under both physiological and pathological conditions, supported by multiple complementary approaches.

Many DNA viruses, including herpesviruses, exploit host TFs to regulate viral gene expression for replication and persistence (Neugebauer et al., 2023). In contrast, we show that SOX18 does not directly control viral genes; rather, KSHV redirects SOX18 to remodel host chromatin, revealing a novel mechanism in which a host TF is hijacked to support latent infection. Similarly, EBV, a related oncogenic gammaherpesvirus, reprograms the host epigenome by altering chromatin accessibility (Ka-Yue Chow et al., 2022). During KSHV infection, SOX18 pioneer activity opens host chromatin, likely contributing to the reprogramming of ECs towards KS-SC phenotype (Aguilar et al., 2012; Carroll et al., 2004; Cheng et al., 2011; Gasperini et al., 2012; Hong et al., 2004; Wang et al., 2004). Chromatin state serves as a gatekeeper of cell identity, and increased accessibility enhances plasticity, facilitating identity shifts and transformation. Our finding that SOX18 recruits SWI/SNF complex components in KSHV-infected cells (**Fig 1 in III**) highlights a previously unrecognized role for SOX18 in promoting host chromatin remodeling via pioneer activity. However, the precise mechanisms driving the spindle phenotype in KLECs remain unclear. One way to address this would be single-cell RNA sequencing of KLECs with and without inhibition of SOX18-BRG1 axis to map transcriptional trajectories across infection and identify the gene programs that precede or accompany the spindle cell morphological change.

5.10 SWI/SNF ATPase activity is required for the hallmarks of KSHV infection in LECs (III & additional results)

To further investigate whether targeting the virus-induced host genome remodeling is a viable molecular strategy to reduce KSHV episomes and hallmarks of infection, we set out to target the SWI/SNF complex recruited by SOX18 in infected cells, using either genetic interference or pharmacological approach.

First, we depleted top SOX18 interactors, ARID1A and BRG1, individually in KLECs with siRNA to assess impact on KSHV infection hallmarks. Efficient knockdown of either BRG1 or ARID1A (**Fig 5A in III**) resulted in a clear decrease in cell spindling (**Fig 5B in III**) and reduced the relative intracellular KSHV episome load in KLECs (**Fig 5C in III**). We did not pursue complementary experiments with ectopic

expression of ARID1A or BRG1, as individually highly expressed subunits are often unstable or incorrectly folded without their appropriate binding partners and thus do not represent endogenous, physiologically relevant complexes in cells (Singh et al., 2023). Knockdown experiments revealed that BRG1 plays a more critical role in maintaining KSHV episome numbers than ARID1A, mirroring the preferential binding of LANA to BRG1 observed in interaction assays (**Fig 1H-I, S1G-H in III**). Nevertheless, the decrease in viral episomes following BRG1 depletion was less striking than the loss seen upon inhibition of SOX18 with Sm4 (**Fig S4D in III, Fig 4A in I**). This discrepancy likely reflects functional redundancy within the SWI/SNF complex, as BRM can act as the second ATPase subunit, also detected among SOX18-associated proteins by BioID (**Fig 1A, C in III**), and has previously been shown to substitute for BRG1 in chromatin remodeling (Hoffman et al., 2014).

To directly test whether BRM can compensate against BRG1 depletion, we turned to chemical approaches targeting the SWI/SNF ATPase module. For this, we employed three complementary inhibitors with distinct modes of action. ACBI1, a PROTAC degrader, simultaneously eliminates BRG1 and BRM by directing them to the proteasome, whereas FHT-1015, in contrast, blocks the catalytic activity of both subunits through allosteric inhibition (Battistello et al., 2023; Farnaby et al., 2019). Finally, PFI-3 disrupts bromodomain-mediated chromatin engagement without interfering with ATP hydrolysis (Singh et al., 2023; Wanior et al., 2021). Cell viability assays highlighted a clear vulnerability of KLECs to the ATPase-targeting compounds ACBI1 and FHT-1015, while uninfected LECs were comparatively resistant. This selective sensitivity was not observed with the bromodomain inhibitor PFI-3 (**Fig S6A-C in III**). The infected cell viability did not greatly vary when using rKSHV.219 (**Fig S6A-B in III**) or the latent ΔORF50 strain (data not shown) in the inhibitor assays. This suggests that the sensitization of KLEC to the SWI/SNF ATPase inhibitors was the result of latent infection rather than the infected cells turning lytic and bursting to release virus more readily. These data indicate that KSHV may require SWI/SNF ATPase activity for persistent infection and survival of the host cells. Immunoblotting validated the function of inhibitors as ACBI1 treatment led to depletion of BRG1 protein, while FHT-1015 caused an accumulation of BRG1 (**Fig 5D in III**). The increase in BRG1 levels upon FHT-1015 treatment likely reflects a common, inhibitor-induced stabilization of the protein, reduced proteasomal turnover, and possibly compensatory upregulation in response to blocked ATPase activity.

Treatment of KLECs with relatively low doses of the ATPase inhibitors ACBI1 (30 nM) and FHT-1015 (10 nM) was sufficient to reverse the spindle-like morphology typically induced during infection, restoring the cells to the characteristic cobblestone appearance of EC monolayers. In contrast, even substantially higher concentrations of the bromodomain inhibitor PFI-3 did not lead to a comparable morphological reversion (**Fig 5E in III**). Notably, only inhibition of the ATPase subunits caused

a marked reduction in the number of KSHV episomes maintained within the cells (**Fig 5F in III**), while cell proliferation remained unaffected under these treatment conditions (**Fig S6D in III**). This decline in viral episome numbers was accompanied by a pronounced decrease in LANA protein expression after 72 hours of exposure to the ATPase inhibitors, indicating overall weaker infection. Interestingly, PFI-3 treatment led to a modest reduction in LANA protein levels, but this effect was not accompanied by a measurable loss of KSHV episomes. BRG1 bromodomain can direct the complex to the regions of active transcription via recognizing acetylated histone tails (Singh et al., 2023). Thus, PFI-3 may disrupt the recruitment of SWI/SNF complex at certain chromatin regions (Lee et al., 2021; Wanior et al., 2021), however, it does not inhibit the ATPase function of BRG1 once it is already recruited to chromatin. Additionally, the function of the bromodomain may be redundant in KSHV latency, given that LANA or SOX18 likely recruit BRG1 to the chromatin. Taken together with the earlier observation that siRNA-mediated depletion of ARID1A had a weaker impact on infection compared to knockdown of BRG1 (**Fig 5A-C in III**), these pharmacological findings underscore the critical role of the BRG1/BRM ATPase activity in supporting KSHV persistence, whereas disruption of ARID1A appears less consequential.

Immunofluorescence analysis revealed that heterochromatin marker HP1α staining was markedly weaker in DMSO-treated KLECs compared with cells exposed to the BRG1 ATPase inhibitors (**Fig 5G in III**). Inhibition with ACBI1 or FHT-1015 led to a clear increase in the intensity of HP1α-associated heterochromatin foci, whereas PFI-3 treatment did not (**Fig 5H in III**). Since HP1α is a central component of heterochromatin and functions as a marker of transcriptionally repressive domains (Bartkova et al., 2011; Larson et al., 2017; Strom et al., 2017), these findings suggest that BRG1 ATPase actively counteracts the formation or stabilization of heterochromatic regions in KLECs. Inhibiting this activity therefore favors a shift toward a more compact chromatin state, reinforcing the idea that SOX18 relies on BRG1 to maintain chromatin accessibility during infection. Interestingly, the enhancement of heterochromatin formation observed with FHT-1015 treatment closely mirrored the phenotype previously seen with SOX18 inhibition by Sm4 (**Fig 4H-I in III**).

To directly test whether SOX18 and BRG1 shape the chromatin landscape through a shared mechanism, we profiled chromatin accessibility (ATAC-seq) in KLECs treated with the SOX18 inhibitor Sm4 or the BRG1 ATPase inhibitor FHT-1015 (**Fig S6E-F in III**). Strikingly, the analysis revealed a strong convergence, with 61.5% of same genomic regions displaying reduced accessibility in both treatment conditions. This shared signature suggests that BRG1 ATPase activity and SOX18 function converge on common regulatory elements that shape the chromatin architecture of KLECs, thereby maintaining an open chromatin landscape that is permissive for viral persistence.

To connect chromatin accessibility to transcriptional output, we performed RNA-seq after prolonged (72h) inhibition. Both compounds produced a repression of host gene expression, with significantly more genes down- than upregulated (**Fig 14A, C in additional results**). Consistent with the ATAC-seq overlap, 63% of the genes reduced by SOX18 inhibition were likewise downregulated by FHT-1015. Additionally, FHT-1015 affected the transcription more broadly due to the possible BRG1's roles beyond the SOX18-BRG1 axis in KSHV-infection in LECs. This data supports a model in which SOX18-BRG1 activity maintains an open, transcription-permissive landscape in KLECs. Notably, ETS1 and ETS2 transcripts were significantly diminished under both treatments. Given the role as lymphatic TFs, this points to potential co-dependencies of the SOX18-BRG1 program in infected LECs and again highlights an underexplored contribution of ETS factors to KSHV permissivity. In line with their ability to reduce the overall infection phenotype (**Fig S4C, 5E in III**), both inhibitors also markedly decreased KSHV transcript levels during this prolonged treatment period (**Fig 14B, D in additional results**). We view the viral transcript reduction as a downstream consequence of diminished chromatin accessibility, lower KSHV episomal copy numbers, and overall slower infection progression, rather than a direct effect on viral transcription machinery per se.

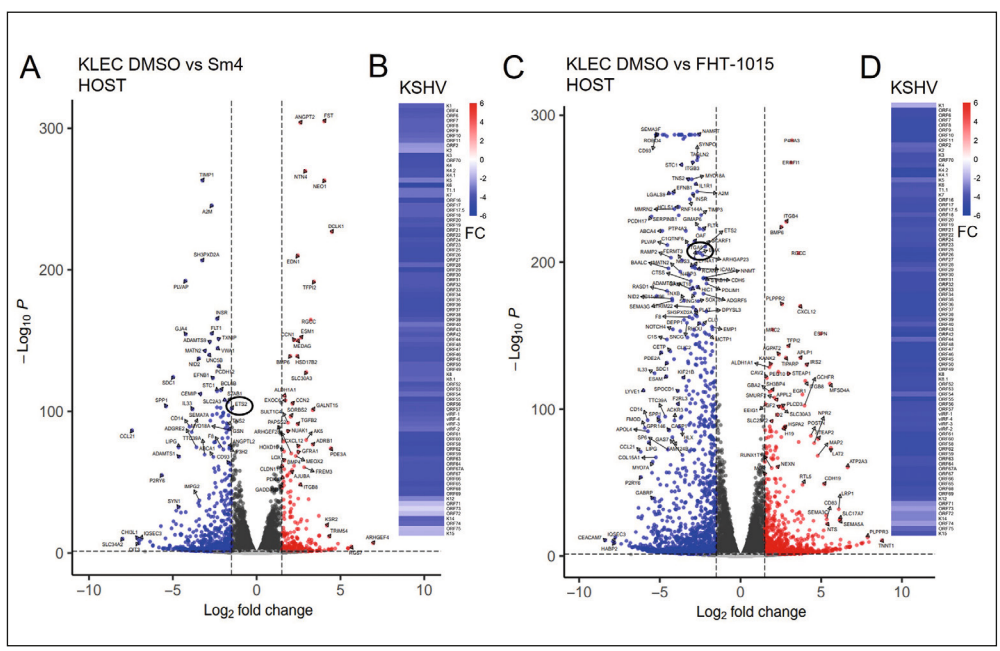

Figure 14. Additional results: inhibition of SOX18-BRG1 axis with either Sm4 or FHT-1015 causes global downregulation of host and viral transcripts in KLECs. RNA-seq analysis (n=3) of LECs infected with rKSHV.219 and treated for 72h with Sm4 or FHT-1015 and shown as **A**, **C**. volcano blots of significantly downregulated (blue) and upregulated (red) host genes, and as **B**, **D** heatmaps showing global downregulation (blue) over KSHV gene transcripts. ETS2 as example of shared downregulated host gene is indicated with circles in A and C.

5.11 Effective KSHV episome maintenance relies on a functional SOX18-BRG1 axis (III)

To define SOX18's role in KSHV episome maintenance, we further examined its mechanism of action in regulating intracellular viral DNA. We compared the effects of SOX18wt and the two mutant variants – transactivation-deficient C240X and DNA-binding-deficient HMGdel – on episome abundance in KSHV-infected HeLa cells. Quantitative analysis revealed that only SOX18wt significantly increased episome copy number relative to the Cherry control, whereas both mutants failed to elicit this effect (**Fig 6A in III**). Confocal microscopy further corroborated these findings: SOX18wt -expressing cells displayed an elevated number of nuclear LANA speckles (**Fig S7A in III**), which is an established proxy for episome count (Adang et al., 2006).

Given our earlier observation that SOX18 associates with DNA sequences adjacent to the KSHV terminal repeat (TR) replication origin (**Fig 5E-G in I**), we next examined whether SOX18 influences LANA recruitment to these regions. Chromatin immunoprecipitation followed by qPCR (ChIP-qPCR) targeting canonical LANA-binding sites within the TR revealed a marked increase in LANA occupancy in cells expressing SOX18wt, but not in those expressing the mutants or the control (**Fig 6B in III**). To determine whether this enhanced LANA binding translated into greater viral DNA replication, we performed BrdU incorporation and pulldown assays to detect nascent viral DNA. Only SOX18wt expression significantly promoted new viral DNA synthesis, normalized to host DNA (**Fig 6C in III**). Importantly, since KSHV episomes replicate once per cell cycle using the host DNA replication machinery, we excluded increased proliferation as a confounding factor (**Fig S7B in III**). Collectively, these results demonstrate that SOX18 enhances episome copy number in a manner dependent on both its DNA-binding and transactivation domains, which together facilitate increased LANA loading at the TR and more efficient replication and accumulation of intracellular episomes.

The strong correlation between SOX18 expression and enhanced LANA occupancy prompted us to assess whether SOX18 physically interacts with LANA. PLA in KLECs confirmed an interaction between SOX18 and LANA, which was abolished upon Sm4 treatment (**Fig 6D-E in III**). These results indicate that SOX18 not only binds near the TR but also engages with LANA, a dual mechanism likely underpinning the observed increase in LANA occupancy at the latent origin of replication.

We next aimed to assess the functional role of BRG1 within the SOX18-LANA complex, since LANA interacts with both SOX18 (**Fig 6D-E in III**) and BRG1 (**Fig 1H-I in III**) in KLECs. ChIP-qPCR revealed that inhibition of BRG1 or SOX18

(via FHT-1015 and Sm4, respectively) significantly reduced LANA occupancy at the TR within 24 hours, without affecting negative control loci on the viral or host genome (**Fig 6F, S7C in III**). Immunoblotting confirmed that the reduced LANA binding was not due to lower levels of LANA protein in the inhibitor-treated cells (**Fig S7D-E in III**). Consistent with this, BrdU pulldown assays demonstrated that both inhibitors significantly impaired nascent viral DNA synthesis in KLECs (**Fig 6G in III**). Together, these findings establish that SOX18 promotes episome maintenance primarily by enhancing LANA binding at the TR in a BRG1-dependent manner, which subsequently leads to a more efficient viral DNA synthesis, and that chemical disruption of the SOX18-BRG1 axis diminishes both episome replication and accumulation. These findings are supported by previous studies showing interaction between SWI/SNF complex subunits and LANA (Zhang et al., 2016), as well as BRG1 and TR (Si et al., 2006).

Further analysis revealed that inhibitor treatment not only reduced LANA binding but also altered its nuclear distribution. Upon inhibition, the number of LANA speckles, that corresponds to higher-order LANA oligomers at TRs (Hellert et al., 2013), was markedly reduced, and the remaining signal appeared more diffuse (**Fig 6H-I in III**). This suggests that disruption of the SOX18-BRG1 axis destabilizes LANA clustering on episomes. Finally, since LANA tethers viral episomes to host chromatin through histone H2A and H2B binding (Ballestas & Kaye, 2001; Barbera et al., 2006; Verma et al., 2013), we examined whether inhibitor treatment affected histone expression. IF analysis showed that Sm4 or FHT-1015 treatment led to a significant concurrent reduction in both LANA speckles and H2A intensity in KLECs (**Fig 6H-J in III**), while immunoblotting confirmed decreases in both H2A and H2B protein levels (**Fig S7F in III**). Inhibition of the SOX18-BRG1 axis appears to compromise episome stability by reducing chromatin accessibility and downregulating canonical histone gene transcription, thereby impairing nucleosome assembly. As a result, LANA has fewer stable binding sites and reduced affinity for chromatin, leading to weaker tethering, fewer speckles, and compromised episome stability. In line with this, LANA has been shown to generally bind to open or active chromatin (Hu et al., 2014; Kumar et al., 2022; Lotke et al., 2020; Lu et al., 2012; Mercier et al., 2014; Ye et al., 2024). In parallel, alterations in the post-translational modification landscape of H2A and H2B may further disrupt chromatin structure and reduce LANA's binding capacity, but these were not further studied. Together, these effects highlight that SOX18-BRG1 activity safeguards viral persistence not only by maintaining accessible chromatin but also potentially by ensuring sufficient levels and appropriate modification states of core histones essential for stable LANA and chromatin interactions.

Previous studies established that the SWI/SNF complex is essential for ORF50/RTA-mediated KSHV lytic reactivation. It was showed that SWI/SNF facilitates

RTA-dependent transcriptional activation (Gwack et al., 2003), and that this occurs through remodeling of a stably positioned nucleosome at the ORF50 promoter (Lu et al., 2003), a critical regulatory step for initiating the switch from latency to lytic replication. Both studies were conducted in B-cell lines, the cellular background relevant to KSHV-related primary effusion lymphoma (PEL), where SWI/SNF activity appears to be primarily linked to the lytic program. This is no surprise as SWI/SNF typically functions as an activator of gene promoters, and because viral lytic gens are tightly chromatinized during latency, they need nucleosome remodeling for activation. In contrast, our findings in KLECs reveal that SOX18 recruits SWI/SNF during latency to support episome maintenance through a mechanism independent of lytic reactivation. This reflects the endothelial context relevant to KS, where SOX18 is highly expressed, whereas SOX18 expression has not been reported in PEL. Taken together, these observations suggest a cell-type-specific exploitation of SWI/SNF by KSHV.

Additionally, Choi et al. showed that in the absence of ORF50/RTA, LECs progressively lose viral episomes. This suggests that PROX1-dependent ORF50 activity is indispensable for long-term viral persistence and excluded enhanced episome replication or segregation as potential mechanisms underlying episome stability in KLECs (Choi et al., 2020). In contrast, this thesis demonstrates that the persistent infection and episome maintenance in KLECs is supported by SOX18 and occur during latency, independent of the lytic cycle. Still, it remains possible that over extended culture periods, KLECs gradually start to lose episomes despite the initial SOX18-mediated increase in episome copy number. This would highlight the complementary importance of spontaneous lytic reactivation in KLECs, driven by PROX1, for sustaining population of infected SCs *in vivo*. Importantly, the SOX18-mediated elevation in episome load may still confer a more progressed infection phenotype, as higher number of virus copies increases the likelihood of reactivation followed by dissemination of new infectious virions. Together, this thesis suggests that episome maintenance is not a static process but rather a dynamic balance between SOX18-mediated episome maintenance and PROX1-driven lytic turnover, both of which are important for oncogenic viral persistence.

In conclusion, this work uncovers a previously unrecognized mechanism of host–pathogen interaction between oncogenic KSHV and its preferred host cells, LECs. The findings in **Study II** add a new dimension to our understanding of virus–host crosstalk that supports persistent latency. At the molecular level, we show that KSHV-induced upregulation of SOX18 in LECs drives a functional shift from a lineage-determining TF to a pioneer factor that remodels chromatin accessibility. This switch is essential for KSHV genome replication and the maintenance of long-term infection. Mechanistically, SOX18 mediates this pioneering activity by

recruiting BRG1, the core ATPase subunit of the SWI/SNF chromatin-remodelling complex, thereby stabilizing chromatin occupancy and promoting viral persistence. To our knowledge, this is the first example of a virus repurposing a lineage-restricted TF to secure and maintain its latent state. The main findings of the study III are presented in **Figure 15**.

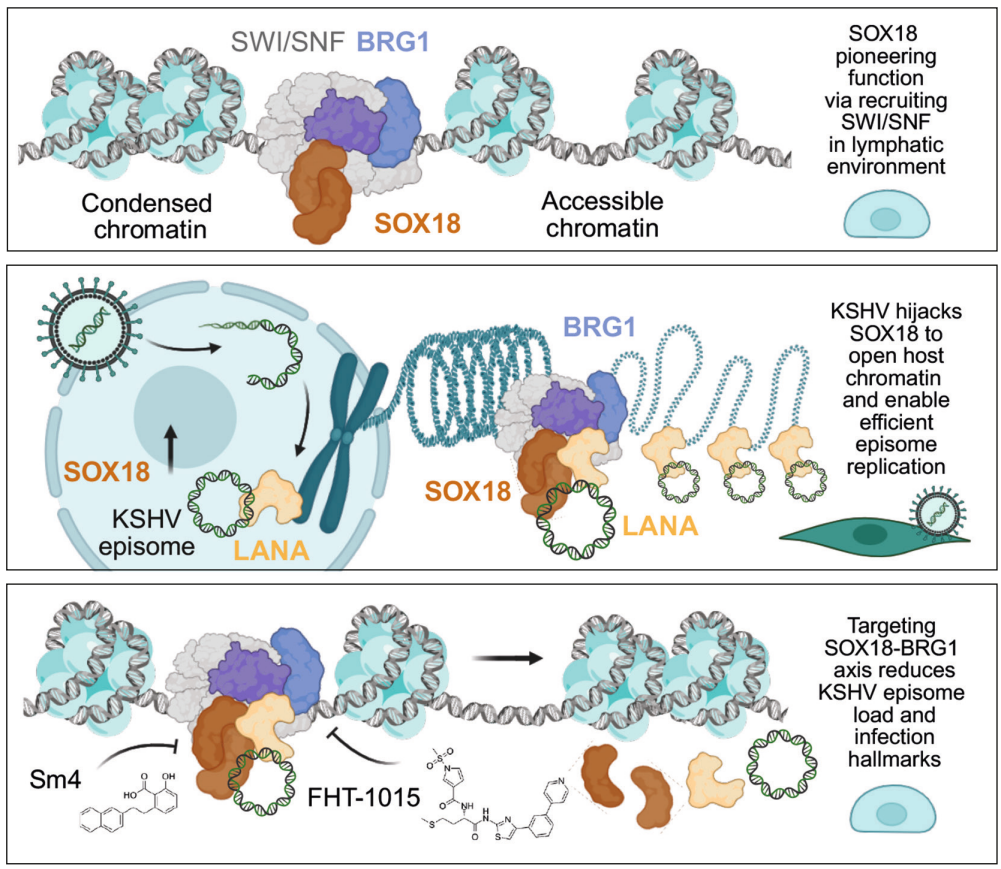

Figure 15. Schematic of the study III main mechanistic findings. Top panel: the SOX18 transcription factor exhibits a pioneering role through its interaction with the SWI/SNF complex, shaping chromatin accessibility and genome organization in LECs. Middle panel: upon KSHV infection, SOX18 is upregulated, and the viral LANA protein hijacks the SOX18/BRG1 pioneer complex to anchor viral episomes onto the host genome. This LANA–SOX18–BRG1 axis establishes a chromatin environment conducive to latent viral genome replication. Bottom panel: pharmacological disruption of the host chromatin machinery impairs SOX18 or BRG1 function and consequently inhibits viral genome duplication. This highlights previously unrecognized host-derived therapeutic targets for the treatment of KSHV infection and the associated diseases. Created with BioRender.

5.12 Translational implications of SOX18 targeting (I, II, III)

The findings of this thesis suggest that SOX18 represents an attractive therapeutic target for KS, demonstrated both *in vitro* (**Study I**) and *in vivo* (**Study II**). SOX18 inhibition can be achieved by small molecule inhibitor Sm4 and R(+) enantiomers of an FDA-approved propranolol and atenolol. In addition to this thesis, SOX18 activity has been shown to be directly modulated as part of the off-target effects of R(+) propranolol or R(+) atenolol (Holm et al., 2025; Overman et al., 2019; Seebauer et al., 2022), particularly in the context of infantile hemangioma, another vascular anomaly.

The link between SOX18 and KSHV is further supported by a recent case study in which a six-month oral propranolol treatment in a patient with classic KS led to a marked reduction in the size of skin lesions, accompanied by decreased KSHV infection (Salido-Vallejo et al., 2022). During 2025, the AIDS Malignancy Consortium (AMC) is launching a phase II clinical trial in partnership with hospitals in Africa and South America to assess the efficacy of orally administered propranolol in treating AIDS-associated KS (ClinicalTrials.gov Identifier: NCT05797662). It is noteworthy that the trial will use FDA-approved commercial propranolol, a racemic mixture containing both R(+) and S(-) enantiomers. While R(+)-propranolol reduces KSHV episome levels and inhibit virus release, the S(-) form may paradoxically promote lytic reactivation and inflammation. Given these concerns, the development of more specific SOX18 inhibitors would be a more targeted and potentially safer therapeutic option with less side-effects for SOX18-associated diseases. Although compounds such as Sm4 and its derivatives require further preclinical evaluation, the enantiopure R(+) propranolol has already demonstrated a favorable safety profile and could, in principle, be repurposed for KS treatment and other SOX18-associated vascular anomalies. Until the selective SOX18 inhibitors become clinically available, commercial propranolol remains an accessible, affordable, and logistically practical option, especially in low-income countries bearing the highest KS burden. However, the high production cost and IPR (Intellectual property rights) issues of enantiopure R(+) propranolol presents a major challenge, and manufacturing processes will need to be optimized for broader clinical use.

The fact that the SOX18 inhibitor Sm4 is an analogue of a natural product from brown seaweed – first identified through high-throughput screening of marine extracts – highlights a timely issue in conservation of natural chemical reservoirs (Fontaine et al., 2017). Preserving natural ecosystems safeguards a vast, living chemical library that underpins modern therapeutics. Plants, microbes, and marine organisms continue to yield first-in-class drugs and provide scaffolds for potent semi-synthetic medicines. Globally, estimates suggest that more than half of approved drugs derive from natural sources; in oncology, roughly two-thirds of small-molecule approvals since the 1980s are natural products, their derivatives,

or nature-inspired (Haque et al., 2022; Newman & Cragg, 2020). As biodiversity declines, so do the prospects for future medicines, including promising leads against cancers, HIV, and other diseases. Protecting nature is therefore as much a public-health strategy as it is a conservation imperative, as emphasized in IPBES Nexus Assessment: Summary for Policymakers 2024 (McElwee, 2024). This thesis exemplifies how repurposed medicines and newly discovered natural compounds can offer unforeseen treatment options for emerging health challenges.

This thesis further identifies the SOX18-BRG1-LANA axis as a key regulator of viral latency maintenance in LECs, with significant implications for therapeutic strategies targeting host chromatin regulators to manage both KSHV infection and KS (**Study III**; Tuohinto et al., under review). This redefines the current dogma for anti-viral therapies that mostly relies on targeting viral effectors rather than host targets. Unlike direct inhibition of LANA, which has proven difficult, targeting the chemically druggable SOX18-BRG1 axis may destabilize episome maintenance indirectly, potentially reducing latent reservoirs.

As critical regulators of gene expression and key drivers of cancer and other diseases, components of the SWI/SNF chromatin remodelling complex have emerged as promising therapeutic targets. Preclinical studies have demonstrated the efficacy of therapeutic targeting of the canonical BAF (cBAF) complex using catalytic inhibitors or proteolysis-targeting chimeras (PROTACs) in various cancer models (Battistello et al., 2023; Centore et al., 2020; Farnaby et al., 2019). Encouragingly, several of these agents have already advanced into clinical trials, highlighting progress toward effective therapeutics targeting cBAF and its sub-complexes (Dreier et al., 2024; Malone & Roberts, 2024). We did not proceed to test the efficacy of BRG1 ATPase inhibitors or PROTACs, similar to Sm4, in a preclinical KS *in vivo* model utilizing a transplant of K-ECFCLYs, since this was not in the scope of this study. Also, biopsies obtained from KS lesions could be used to assess the expression and localization of SOX18 and SWI/SNF components through multiplexed IHC. These approaches could strengthen the translational relevance of the findings of this thesis.

This work provides proof for the therapeutic utility of drugging a TF, an emerging field in the biotechnology sector. This is the first study to investigate a key developmental TF as a potential therapeutic target for KS. We unveil a mechanism by which SOX18 inhibition disrupts persistent KSHV infection, a prerequisite for KS development. Our findings reposition SOX18 as a pioneer transcription factor in chromatin remodeling, with broad implications for the development of therapies targeting not only developmental TFs, but also chromatin regulators, to treat viral infections, virus-induced malignancies, and SOX18-driven vascular anomalies.

6 CONCLUSIONS & FUTURE PERSPECTIVES

This thesis defines a lineage-dependent strategy by which KSHV exploits the regulatory circuitry of lymphatic endothelium to survive and drive oncogenesis. The studies presented here have uncovered a fundamental duality in the KLEC transcriptional landscape, where the lymphatic fate-determining factors SOX18 and PROX1 are co-opted by the virus to balance two imperatives – latent persistence and intermittent reactivation – thereby sustaining the infected spindle-cell population, the pathological hallmark of KS.

The central finding establishes that KSHV latency is not a passive state but an actively maintained condition reliant on a dynamic interplay of host-viral axis. We identified SOX18 as an indispensable host factor for genome maintenance in latency. Mechanistically, SOX18 binds the viral genome near replication origins, enhances LANA-mediated episome tethering and replication, and crucially, partners with the BRG1-containing SWI/SNF chromatin remodeling complex to maintain an open host chromatin architecture. This SOX18-BRG1 axis actively preserves the viral episomes, creating a stable latent reservoir. Through a feed-forward loop in which the viral latent protein vFLIP activates NF-κB to induce SOX18, the virus amplifies the very host factor that secures its persistence.

Complementing this mechanism of persistence, this thesis defined PROX1 as a key regulator of lytic competence. By engaging the promoter of the master lytic transactivator, ORF50, PROX1 primes the system for reactivation. This finding resolves a long-standing question, revealing how KSHV can maintain a persistent latency while retaining the capacity for spontaneous reactivation, a requirement for replenishing infected cells and spreading the infection within KS lesions. Together, these discoveries present a powerful model: SOX18 safeguards the latency, while PROX1 renders KLECs poised to the lytic cascade.

Extending this thesis beyond mature endothelium, we identified circulating lymphatic endothelial progenitor cells as a previously unrecognized, highly permissive reservoir for KSHV. These ECFCLYs, expressing both SOX18 and PROX1, not only harbor high number of latent episomes but also exhibit spontaneous lytic activity and acquire oncogenic properties, such as anchorage-independent growth. Their ability to survive as *in vivo* transplants with spindle cell phenotype positions them as a physiologically relevant model for dissecting viral pathogenesis and for preclinical evaluation of novel KS therapeutics.

In sum, this work reframes KSHV pathogenesis as an outcome of viral engagement with lymphatic lineage factors, modulating cellular microenvironment for its own persistence. By defining the molecular machinery that sustains latency in KLECs, we identify compelling therapeutic targets. Pharmacologic inhibition of SOX18 or its partner BRG1 destabilizes the latent reservoir, lowers viral load, and reverses KS-like spindle phenotype. This reframes KSHV pathogenesis as strategic co-option of SOX18-BRG1-LANA module as the engine of latency and the PROX1-ORF50 axis as the ignition for reactivation, and provides a blueprint for host-directed, mechanism-based therapies to disrupt viral persistence and treat KS.

Building on the framework established in this thesis, there are several compelling avenues for future investigation. A deeper mechanistic dissection of the identified host-viral complexes and their role in both host and viral epigenetic landscape is warranted. Key questions remain regarding the precise molecular interfaces governing the SOX18-BRG1-LANA interaction and whether additional lymphatic TFs contribute to this regulatory nexus. It will be crucial to determine how the balance between the SOX18-driven latency program and PROX1-mediated lytic competence is dynamically regulated by the tumor microenvironment and during the progression from early to advanced KS lesions. In parallel, repurposing efforts should optimize SOX18 or BRG1-directed agents and evaluate their efficacy not only as monotherapies but also in combination and with existing antivirals. Such approaches hold the potential to move beyond viral suppression towards a curative strategy aimed at the complete eradication of the latent KSHV reservoir, with the goal of translating these insights into host-directed therapies for patients with Kaposi sarcoma.

7 COLLABORATION AND FUNDING DETAILS

Mathias Francois (I, III)
The University of Sydney, School of Medical Sciences, Sydney, New South Wales, Australia.

Adam Grundhoff, Thomas Günther & Simon Weissmann (I, III)
Leibniz Institute of Virology, Germany.

Tara Karnezis (II, III)
Gertrude Biomedical Pty Ltd., Melbourne, Queensland, Australia.

Mark Bower (I)
National Centre for HIV Malignancy, Chelsea and Westminster Hospital & Imperial College London, United Kingdom.

Joseph M. Ziegelbauer (I)
HIV and AIDS Malignancy Branch, Center for Cancer Research, NCI, NIH, Bethesda.

Caj Haglund (I)
Department of Surgery, University of Helsinki and Helsinki University Hospital.

Teijo Pellinen (I)
Institute for Molecular Medicine Finland (FIMM), Helsinki Institute of Life Science (HiLIFE), University of Helsinki.

Michael Lagunoff & Terri A. DiMaio (II)
Department of Microbiology, University of Washington. Seattle WA, United States of America.

Pipsa Saharinen & Elina A. Kiss (II)
Translational Cancer Medicine Research Program, Faculty of Medicine, University of Helsinki.

Pirjo Laakkonen (II)
Translational Cancer Medicine Research Program, Faculty of Medicine, University of Helsinki.
Wihuri Research Institute, Biomedicum Helsinki.

Biswajyoti Sahu, Ville Tiusanen & Fei Liangru (III)
Applied Tumor Genomics Research Program, Faculty of Medicine, University of Helsinki.
Norwegian Center for Molecular Biosciences and Medicine, University of Oslo, Norway.
Institute for Cancer Research, Oslo University Hospital, Norway.

Matthew S. Graus, Susav Pradhan, Yew Yan Wong, Justin Wong, Quintin Lee (III)
The University of Sydney, School of Medical Sciences, Sydney, New South Wales, Australia.

Elizabeth Hinde & Jieqiong Lou (III)
The University of Melbourne, School of Physics, Melbourne, Victoria, Australia.

Alexey Terskikh & Martin Alvarez-Kuglen (III)
Harry Perkins Institute of Medical Research, The University of Western Australia, Australia.

Conflicts of interest

Gertrude Biomedical Pty Ltd. participated in the study II and III design.
The authors declare no other competing interests.

Funding and grants

Doctoral program in Biomedicine salaried position
Finnish Cultural Foundation working grant
Magnus Ehrnrooth foundation working grant
The Gertrude Biomedical Pty Ltd. comission salaried position
K. Albin Johanssons Foundation young investigator grant
Biomedicum Foundation young investigator grant
Virustutkimussäätiö VITUS young investigator grant
Finnish Cancer Foundation young investigator grant
Finnish Cancer Foundation travel grants
UH dsHealth Medicine Fund travel grants

8 AKNOWLEDGEMENTS

This thesis was carried out in the Translational Cancer Medicine Research Program, part of the Research Programs Unit within the Faculty of Medicine at the University of Helsinki. I am grateful to the Doctoral Programme in Biomedicine for academic support during my doctoral studies and for the four-year salaried position. I also warmly thank the Finnish Cultural Foundation, Magnus Ehrnrooth Foundation, Cancer Foundation Finland, K. Albin Johanssons Foundation, the Biomedicum Foundation, and Virustutkimussäätiö VITUS for financial support. This project was additionally supported by funding granted to the Ojala group.

This study would not have been possible without the core facilities at the University of Helsinki: the Laboratory Animal Center (LAC) HiLIFE, the Biomedicum Imaging Unit (BIU), the Finnish Institute of Molecular Medicine (FIMM), and the Genome Biology Unit (GBU) for expert support in animal care, imaging, sequencing, and data analysis. I also want to thank the Citylab Biomedicum personnel for brightening my days whenever I came downstairs, whether it was laughter, insights, ice cream, or that one reagent I really needed at exactly the right moment.

Here comes my grandiloquent aknowledgements, as there are numerous parties and people that have contributed to this work directly or via supporting me, and I truly appreciate all their efforts.

First and foremost, I owe my sincere gratitude to my supervisor, mentor, and custos, Päivi M. Ojala. Working with you for a decade has been both a joy and essential to becoming the scientist I am. I admire your bold, vivid way of engaging with science, and how you constantly challenge and inspire me. Thank you for taking me along into the world of KSHV, encouraging me to present our work widely, and trusting my skills through many challenges. Our travels gave me invaluable opportunities to discuss science, to meet KS patients, and to connect with remarkable researchers as you opened your network and welcomed me into the broader herpesvirus community. I am grateful that I have always been able to ask for your guidance and to find you either in the lab, at Villa Ojala, or in the middle of the dancefloor. Your passion for both fun and science is truly unparalleled.

I am deeply grateful to my opponent, Erle S. Robertson, and I look forward to discussing this thesis with you. Over the years we met at KSHV conferences, and then one evening in Dar es Salaam I happened to sit next to you at a dinner only to find ourselves debating world topics, despite essentially agreeing. Since then, we

have become friends and considered you a worthy opponent. I am happy to share this experience with you, and I truly value your calm, steady, and firm presence, always accompanied with a wink.

Sincere thanks to the pre-examiners of this thesis, Lea Sistonen and Miikka Vikkula, for taking the time to evaluate this work. Miikka, thank you also for organizing the vascular anomalies meetings, which deepened my understanding of the clinical side of our research and what it may ultimately mean for patients. Lea, your thorough insights and comments strengthened the thesis significantly. From both of you, I received encouragement to be proud of this work.

I thank Kari Vaahtomeri for agreeing to act as the faculty representative in my thesis defense. Many years ago you evaluated my Master's thesis, and since this dissertation continues that path, it feels especially meaningful to share the defense with you.

Thank you to Biswajyoti Sahu and Sinem Karaman for serving as my thesis committee members and for supporting my growth as a scientist. I truly appreciate our discussions over the years; they have guided this thesis into what it is today. I admire your passion and dedication to science, even through the struggles that come with it.

I am grateful to all my co-authors and collaborators for their contributions to the work included in this thesis. In particular, I thank Mat Francois and Matt Graus (Sydney) for sustaining a strong and open collaboration through an exceptionally complex and demanding project. It has been exciting to see our science refine in synergy and to solve problems together along the way. At its core, science is about sharing: to lift one another for the good of all. Huge thanks to Biswa, Ville Tiusanen and Fei Liangru for excellent discussions, technical skills and consistent high-quality work. It has been a privilege to collaborate with people I can truly rely on, and I wish you the very best in your own scientific journeys.

I also value the experience of working both collaboratively and through commissioned research with Gertrude Biomedicals Ltd., especially with Tara Karnezis. Our shared work offered me a welcome glimpse into industry and many rewarding scientific discussions. It was a pleasure to do science with Michael Lagunoff and Terri A. DiMaio (Seattle); thank you for the professional advice and Michael for the many funny moments shared within the KSHV community. I also thank Pipsa Saharinen and Elina Kiss for a collaboration that was both interesting and rewarding. Pirjo Laakkonen, your professional excellence and great sense of humor were always close by and deeply appreciated. Thank you to Vadim Le Joncour for help and guidance in academy and with animal work. Huge thanks to Antti Hassinen (FIMM) for all the trouble-shooting and learning experiences with imaging. Finally, I thank

Adam Grundhoff, Thomas Günther, and Simon Weissmann (Hamburg) for tackling complex, mind-bending technical discussions, analysis, and guidance over the years around the mysteries of herpesviruses.

A special thank you to my mentor Silvia Gramolelli as this thesis would not exist without your ideas and efforts. Your work laid the foundation for this thesis. Working with you accelerated my learning curve immensely, and I admire your determination. Your mentoring struck a rare balance between demanding and supportive, and it carried me through this project even after you embarked on your independent path. Thank you, Endrit Elbasani, for your calm presence, patience, and technical expertise. At the time, I could always rely on you in the lab, and I learned so much from you across many projects. Thank you, Giuseppe Balistreri, for acting as my first hands-on mentor. From day one you had my back, supporting me, pushing me forward, and fueling my confidence. Your enthusiasm for science still inspires me, and it lit that passion in me, too. Because of that, I will always be the Fireball. Thank you Pirita Pekkonen, for being another early mentor and for giving me the chance to study melanoma in such intelligent and fun company, and please never stop dancing, even with a broken arm.

Hearty thanks to our lab manager and technician, Nadezhda Zinovkina, for all these years. Your guidance, organization, kindness, and warmth made the lab a genuinely pleasant place to work, and your precision and quality are exceptional. I am truly happy to have you back with us. I also thank our other lab managers for sharing responsibilities and always offering a helping hand: Julia Härme (my dear friend, the horrors persist, but so do we), Elina Hurskainen (you emit rays of light where ever you go), Minttu Kaloinen, and Veronika Rezov. Huge thanks to Tapio Tainola, without you the department would be in chaos, alarms and desperate researchers everywhere. Your knowledge and steady support are deeply valued. Thank you to the Wihuri personnel for sharing the BSL2 room and for keeping an eye out when there were unwanted peeping sounds. And especially thank you, Maija, for sharing your love for the outdoors and reminding me of life beyond the lab.

To my researcher co-workers: Kerttu Kalander (Keke), I still wonder how you manage to stay so cool and collected through it all. You handle everything with elegance, even with your strong will. You are like Markl (Howl's Moving Castle): always there, keeping things running with a sharp eyes and mind. Katri Oksa (Kake), thank you for the laughter and the tears (often at the same time) during thetime of our lives. Apologies for the occasional embarrassing oversharing. I admire your unapologetic attitude: you are like Calcifer, and a Pitbull at the same time. I never want to be on your bad side, but always on your team, even when I don't fully catch your sarcasm. Just ask and I will give you everything, including my best attempt at being your riverdance companion. You're on fire!

Peyton Staab, the amount of work you poured into the last publication means a great deal. You have been my lab companion for years like Robin to my Batman, or steady Turnip Head to my old and tired granny Sophie (again Howl's Moving Castle). I honestly don't know if I would have survived the amount of pipetting without you. Thank you for sharing both the struggles and the victories with me, and I wish you all the best as you continue this project in my footsteps. Your technical skills and quick mind will take you far. And as always, do not hesitate to contact me.

To all the other students: Elisabeth (Lisi) Pottendorfer, I miss your lively company and all our laughs. Lorenza Cutrone, thanks for our deep-dive discussions on psychology, and my favorite red wine these days is from Puglia. Micaela Haapanen, your sharp eye for details impressed me greatly. Miro Nylén, I appreciated your steady hands and professional manner. Shadi Azam, thank you for your delightful company and precision. And most recently, Adela Mäkilä I admire how you are the positivity and the calm in our KSHV team.

To Ojala lab alumni: Joonas Jukonen (double JJ), thank you for your unfiltered company and commentary, both in professional and personal matters. Your dark humor andsarcasm gave perspective during the gonahdus: not to take everything so personally or seriously. I'm still searching for a box big enough to fit into so I can be shipped away. I also thank Sanni Alve for the guidance and your wisdom, and sharing many tedious protocols and moments with LECs. See you in the country(flip)side! Hector Monzo and Veijo Nurminen thank you for the fun and thoughtful discussions, both in the lab and outside of it.

I am grateful for the new challenges and opportunities that came through The Science Basement community full of inspiring researchers who taught me how to communicate my science. Katja, Rhiannon, Usha, Dina, Ainhoa, Jamie, and the rest of the crew, thank you.

To my friend who has struggled through every step of the same path: Mariel. No words can capture what you mean to me, or the unconditional love and support you have given me. You've been by my side from the very first day of university to the final stretch of my studies. Sometimes it felt like "piupiu please help," but we always made it through. I promise to be there for you too. Remember, if I can do it, you can do it too. By extension, thank you Antti, for being the calm voice of reason, and for having "my own room" at your place.

Warm thanks to Joonas (Thor) for supporting me for years, as I supported you. Thank you for your endless curiosity about science and the world, and for being there after long hours in the lab, grounding my restless electricity with your calm

patience. I hope I transmitted some energy to you along the way. Keep the coffee brewing and the theories flowing!

Dear BBE, with you I see life through a kaleidoscope: Annika, Anniina, Helena, Rusty, Hannu, and Roope, I thank you all for supporting me and also kicking my butt when needed, both professionally and personally. You are my chosen second family, and I'm excited to see us grow together and new butts to emerge.

Ylva, I salute your courage and almost inhuman ability to withstand all the elements. How many times have I wished I could join your adventures when stuck in the lab. Ibrahim, Cem, and the rest of the big Biomedicum PhD family, thank you for showing what fun can be. Your energy is relentless and contagious. Thank you to my beloved Meija, Netta, Julia, Vilma and the goddess gang, and the Viikki girls, you made the moments outside lab full of love.

My dear friend Sanna, it's been a privilege to share such a long history with you, even as our lives have taken different paths. With you, I've always felt free to be my most unguarded self, screaming at the top of my lungs on the shores of Pielinen. I admire how you're tough and fierce, yet always authentic, joyful, and deeply loving. You inspire me to bring that same authenticity into academia, and you always give me fresh perspectives – truly one of the wisest people I know.

Lasse, my daily life companion, thank you for your relentless support, for always reminding me "Oot reipas – tietenkin!". I truly have appreciated the strategically isolated place to write this thesis, while listening to the animals of the forest creeping around. I admire how your mind works and I learn something from you every day. You keep on challenging the way I work and think, teaching me to fine-tune the balance between efficiency and precision, and to do things mindfully. I am excited to see where our shared path takes us.

Isi, thank you for always supporting my academic goals and emphasizing the importance of learning. Your calm, firm presence matters deeply in my life, and it is grounding to know I can rely on you. You are always a call away, and you make sure I don't get lost in the wilderness, like the big Totoro cushion that helped Mei land softly.

Mutteri, thank you for being the blazing, lively person you are: dancing through life and always reminding "Älä jää tuleen makaamaan." You have pushed me forward and encouraged me to make something of myself, while also reminding me that life is not only labor as it should include adventure and laughter.

Kiitos rakas Mumma, kaikista niistä päivistä kun sain paeta mummolaan ja purkaa huoleni helmoihisi. Syötit minut, juotit minut, ja annoit paikan mihin laskea pääni ja muistutit mikä on elämässä tärkeintä. Kiitos taatelikakuista, yhteisestä omenapuissa kiipeilystä, luonto-ohjelmien katselusta, ja keskusteluista elämän tärkeistä kysymyksistä.

Paula, my aunt, thank you for the lifelong support. Not only did you do the pagination and layout of this thesis and make it look amazing, you also took me under your wings whenever mine did not carry. I admire how you have built yourself despite life's hardships. You remind me how important family bonds are, and you are the force keeping us together. I also want to thank the rest of my close and extended family.

The greatest gratitude I owe to my older sister, Karita (tieto- ja tahtonainen). You told me not to follow but following you is all I have ever known. You guided me along a path full of branches that could hit, roots that could trip me, and turns that seemed to go on forever. I either ran after you (middle-Totoro), or you told me to slow down and came to find me when I got lost (Satsuki). Now it feels as if I'm standing with you in the clearing under the camphor tree, eyes open to the beauty of the world, full of different paths to follow.

This work – first as a research assistant and Bachelor's student, then as a Master's thesis student, and finally as a PhD researcher – took a decade. This journey was a deep dive into a fascinating herpesvirus and its complex strategies to persist and cause cancer, and how to prevent it. Stepping away from KSHV and moving to new topics will not be easy. It has been a long stretch up the mountain of knowledge, and I am proud to have climbed this ledge. The peak is still hidden in the clouds, and I am eager to see what is revealed beyond them. It is always better to try than never to start the hike at all. "To strive, to seek, to find, and not to yield," from Alfred Lord Tennyson's Ulysses, captures the spirit of perseverance that carried me through: the pursuit of knowledge and adventure, the willingness to push beyond what is known, and the determination to keep moving forward, despite doubt or fatigue. The journey demanded self-discipline, willpower, resilience, and humility in the face of the vast unknown still waiting to be discovered.

Sincerely,

Krista Tuohinto

9 REFERENCES

Adams, R. H., & Alitalo, K. (2007).
Molecular regulation of angiogenesis and lymphangiogenesis. Nat Rev Mol Cell Biol, 8(6), 464-478. https://doi.org/10.1038/nrm2183

Adang, L. A., Parsons, C. H., & Kedes, D. H. (2006).
Asynchronous progression through the lytic cascade and variations in intracellular viral loads revealed by high-throughput single-cell analysis of Kaposi's sarcoma-associated herpesvirus infection. J Virol, 80(20), 10073-10082.
https://doi.org/10.1128/JVI.01156-06

Aguilar, B., Choi, I., Choi, D., Chung, H. K., Lee, S., Yoo, J., Lee, Y. S., Maeng, Y. S., Lee, H. N., Park, E., Kim, K. E., Kim, N. Y., Baik, J. M., Jung, J. U., Koh, C. J., & Hong, Y. K. (2012).
Lymphatic reprogramming by Kaposi sarcoma herpes virus promotes the oncogenic activity of the virus-encoded G-protein-coupled receptor. Cancer Res, 72(22), 5833-5842.
https://doi.org/10.1158/0008-5472.CAN-12-1229

Alitalo, K., Tammela, T., & Petrova, T. V. (2005).
Lymphangiogenesis in development and human disease. Nature, 438(7070), 946-953.
https://doi.org/10.1038/nature04480

Alkharsah, K. R., Singh, V. V., Bosco, R., Santag, S., Grundhoff, A., Konrad, A., Sturzl, M., Wirth, D., Dittrich-Breiholz, O., Kracht, M., & Schulz, T. F. (2011).
Deletion of Kaposi's sarcoma-associated herpesvirus FLICE inhibitory protein, vFLIP, from the viral genome compromises the activation of STAT1-responsive cellular genes and spindle cell formation in endothelial cells. J Virol, 85(19), 10375-10388.
https://doi.org/10.1128/JVI.00226-11

Allis, C. D., & Jenuwein, T. (2016).
The molecular hallmarks of epigenetic control. Nat Rev Genet, 17(8), 487-500.
https://doi.org/10.1038/nrg.2016.59

Alve, S., Gramolelli, S., Jukonen, J., Juteau, S., Pink, A., Manninen, A. A., Hanninen, S., Monto, E., Lackman, M. H., Carpen, O., Saharinen, P., Karaman, S., Vaahtomeri, K., & Ojala, P. M. (2024).
DLL4/Notch3/WNT5B axis mediates bidirectional prometastatic crosstalk between melanoma and lymphatic endothelial cells. JCI Insight, 9(1).
https://doi.org/10.1172/jci.insight.171821

Ambinder, R. F., & Cesarman, E. (2007).
Clinical and pathological aspects of EBV and KSHV infection. In A. Arvin, G. Campadelli-Fiume, E. Mocarski, P. S. Moore, B. Roizman, R. Whitley, & K. Yamanishi (Eds.), Human Herpesviruses: Biology, Therapy, and Immunoprophylaxis.
https://www.ncbi.nlm.nih.gov/pubmed/21348099

Aneja, K. K., & Yuan, Y. (2017).
Reactivation and Lytic Replication of Kaposi's Sarcoma-Associated Herpesvirus: An Update. Front Microbiol, 8, 613. https://doi.org/10.3389/fmicb.2017.00613

Aranguren, X. L., Beerens, M., Coppiello, G., Wiese, C., Vandersmissen, I., Lo Nigro, A., Verfaillie, C. M., Gessler, M., & Luttun, A. (2013).
COUP-TFII orchestrates venous and lymphatic endothelial identity by homo- or hetero-dimerisation with PROX1. J Cell Sci, 126(Pt 5), 1164-1175. *https://doi.org/10.1242/jcs.116293*

Archer, C., Wiles, N., Kessler, D., Turner, K., & Caldwell, D. M. (2025).
Beta-blockers for the treatment of anxiety disorders: A systematic review and meta-analysis. J Affect Disord, 368, 90-99. *https://doi.org/10.1016/j.jad.2024.09.068*

Asahara, T., Murohara, T., Sullivan, A., Silver, M., van der Zee, R., Li, T., Witzenbichler, B., Schatteman, G., & Isner, J. M. (1997).
Isolation of putative progenitor endothelial cells for angiogenesis. Science, 275(5302), 964-967. *https://doi.org/10.1126/science.275.5302.964*

Bais, C., Santomasso, B., Coso, O., Arvanitakis, L., Raaka, E. G., Gutkind, J. S., Asch, A. S., Cesarman, E., Gershengorn, M. C., & Mesri, E. A. (1998).
G-protein-coupled receptor of Kaposi's sarcoma-associated herpesvirus is a viral oncogene and angiogenesis activator. Nature, 391(6662), 86-89. *https://doi.org/10.1038/34193*

Bais, C., Van Geelen, A., Eroles, P., Mutlu, A., Chiozzini, C., Dias, S., Silverstein, R. L., Rafii, S., & Mesri, E. A. (2003).
Kaposi's sarcoma associated herpesvirus G protein-coupled receptor immortalizes human endothelial cells by activation of the VEGF receptor-2/ KDR. Cancer Cell, 3(2), 131-143. *https://doi.org/10.1016/s1535-6108(03)00024-2*

Baker, K. M., Wei, G., Schaffner, A. E., & Ostrowski, M. C. (2003).
Ets-2 and components of mammalian SWI/SNF form a repressor complex that negatively regulates the BRCA1 promoter. J Biol Chem, 278(20), 17876-17884. *https://doi.org/10.1074/jbc.M209480200*

Ballestas, M. E., & Kaye, K. M. (2001).
Kaposi's sarcoma-associated herpesvirus latency-associated nuclear antigen 1 mediates episome persistence through cis-acting terminal repeat (TR) sequence and specifically binds TR DNA. J Virol, 75(7), 3250-3258. *https://doi.org/10.1128/JVI.75.7.3250-3258.2001*

Banerji, S., Ni, J., Wang, S. X., Clasper, S., Su, J., Tammi, R., Jones, M., & Jackson, D. G. (1999).
LYVE-1, a new homologue of the CD44 glycoprotein, is a lymph-specific receptor for hyaluronan. J Cell Biol, 144(4), 789-801. *https://doi.org/10.1083/jcb.144.4.789*

Bar, J., Bar-Ilan, E., Cleper, R., Sprecher, E., Samuelov, L., & Mashiah, J. (2022).
Monitoring oral propranolol for infantile hemangiomata. Dermatol Ther, 35(11), e15870. *https://doi.org/10.1111/dth.15870*

Barbera, A. J., Chodaparambil, J. V., Kelley-Clarke, B., Joukov, V., Walter, J. C., Luger, K., & Kaye, K. M. (2006).
The nucleosomal surface as a docking station for Kaposi's sarcoma herpesvirus LANA. Science, 311(5762), 856-861. *https://doi.org/10.1126/science.1120541*

Barozzi, P., Luppi, M., Facchetti, F., Mecucci, C., Alu, M., Sarid, R., Rasini, V., Ravazzini, L., Rossi, E., Festa, S., Crescenzi, B., Wolf, D. G., Schulz, T. F., & Torelli, G. (2003).
Post-transplant Kaposi sarcoma originates from the seeding of donor-derived progenitors. Nat Med, 9(5), 554-561. *https://doi.org/10.1038/nm862*

Bartkova, J., Moudry, P., Hodny, Z., Lukas, J., Rajpert-De Meyts, E., & Bartek, J. (2011).
Heterochromatin marks HP1gamma, HP1alpha and H3K9me3, and DNA damage response activation in human testis development and germ cell tumours. Int J Androl, 34(4 Pt 2), e103-113. https://doi.org/10.1111/j.1365-2605.2010.01096.x

Basilio, J., Hoeth, M., Holper-Schichl, Y. M., Resch, U., Mayer, H., Hofer-Warbinek, R., & de Martin, R. (2013).
TNFalpha-induced down-regulation of Sox18 in endothelial cells is dependent on NF-kappaB. Biochem Biophys Res Commun, 442(3-4), 221-226.
https://doi.org/10.1016/j.bbrc.2013.11.030

Battistello, E., Hixon, K. A., Comstock, D. E., Collings, C. K., Chen, X., Rodriguez Hernaez, J., Lee, S., Cervantes, K. S., Hinkley, M. M., Ntatsoulis, K., Cesarano, A., Hockemeyer, K., Haining, W. N., Witkowski, M. T., Qi, J., Tsirigos, A., Perna, F., Aifantis, I., & Kadoch, C. (2023).
Stepwise activities of mSWI/SNF family chromatin remodeling complexes direct T cell activation and exhaustion. Mol Cell, 83(8), 1216-1236 e1212.
https://doi.org/10.1016/j.molcel.2023.02.026

Bello, L. J., Davison, A. J., Glenn, M. A., Whitehouse, A., Rethmeier, N., Schulz, T. F., & Barklie Clements, J. (1999).
The human herpesvirus-8 ORF 57 gene and its properties. J Gen Virol, 80 (Pt 12), 3207-3215. https://doi.org/10.1099/0022-1317-80-12-3207

Benevenuto de Andrade, B. A., Ramirez-Amador, V., Anaya-Saavedra, G., Martinez-Mata, G., Fonseca, F. P., Graner, E., & Paes de Almeida, O. (2014).
Expression of PROX-1 in oral Kaposi's sarcoma spindle cells. J Oral Pathol Med, 43(2), 132-136. https://doi.org/10.1111/jop.12097

Beral, V. (1991).
Epidemiology of Kaposi's sarcoma. Cancer Surv, 10, 5-22.
https://www.ncbi.nlm.nih.gov/pubmed/1821323

Birkmann, A., Mahr, K., Ensser, A., Yaguboglu, S., Titgemeyer, F., Fleckenstein, B., & Neipel, F. (2001).
Cell surface heparan sulfate is a receptor for human herpesvirus 8 and interacts with envelope glycoprotein K8.1. J Virol, 75(23), 11583-11593.
https://doi.org/10.1128/JVI.75.23.11583-11593.2001

Blom, S., Paavolainen, L., Bychkov, D., Turkki, R., Maki-Teeri, P., Hemmes, A., Valimaki, K., Lundin, J., Kallioniemi, O., & Pellinen, T. (2017).
Systems pathology by multiplexed immunohistochemistry and whole-slide digital image analysis. Sci Rep, 7(1), 15580. https://doi.org/10.1038/s41598-017-15798-4

Boija, A., Klein, I. A., Sabari, B. R., Dall'Agnese, A., Coffey, E. L., Zamudio, A. V., Li, C. H., Shrinivas, K., Manteiga, J. C., Hannett, N. M., Abraham, B. J., Afeyan, L. K., Guo, Y. E., Rimel, J. K., Fant, C. B., Schuijers, J., Lee, T. I., Taatjes, D. J., & Young, R. A. (2018).
Transcription Factors Activate Genes through the Phase-Separation Capacity of Their Activation Domains. Cell, 175(7), 1842-1855 e1816.
https://doi.org/10.1016/j.cell.2018.10.042

Boshoff, C., & Weiss, R. (2002).
AIDS-related malignancies. Nat Rev Cancer, 2(5), 373-382.
https://doi.org/10.1038/nrc797

Bowles, J., Schepers, G., & Koopman, P. (2000).
Phylogeny of the SOX family of developmental transcription factors based on sequence and structural indicators. Dev Biol, 227(2), 239-255. https://doi.org/10.1006/dbio.2000.9883

Boyne, J. R., Jackson, B. R., & Whitehouse, A. (2010).
ORF57: Master regulator of KSHV mRNA biogenesis. Cell Cycle, 9(14), 2702-2703. https://doi.org/10.4161/cc.9.14.12627

Breiteneder-Geleff, S., Soleiman, A., Kowalski, H., Horvat, R., Amann, G., Kriehuber, E., Diem, K., Weninger, W., Tschachler, E., Alitalo, K., & Kerjaschki, D. (1999).
Angiosarcomas express mixed endothelial phenotypes of blood and lymphatic capillaries: podoplanin as a specific marker for lymphatic endothelium. Am J Pathol, 154(2), 385-394. https://doi.org/10.1016/S0002-9440(10)65285-6

Brown, H. J., Song, M. J., Deng, H., Wu, T. T., Cheng, G., & Sun, R. (2003).
NF-kappaB inhibits gammaherpesvirus lytic replication. J Virol, 77(15), 8532-8540. https://doi.org/10.1128/jvi.77.15.8532-8540.2003

Buenrostro, J. D., Wu, B., Chang, H. Y., & Greenleaf, W. J. (2015). A
TAC-seq: A Method for Assaying Chromatin Accessibility Genome-Wide. Curr Protoc Mol Biol, 109, 21 29 21-21 29 29. https://doi.org/10.1002/0471142727.mb2129s109

Bulyk, M. L., Drouin, J., Harrison, M. M., Taipale, J., & Zaret, K. S. (2023).
Pioneer factors - key regulators of chromatin and gene expression. Nat Rev Genet, 24(12), 809-815. https://doi.org/10.1038/s41576-023-00648-z

Burke, Z., & Oliver, G. (2002).
Prox1 is an early specific marker for the developing liver and pancreas in the mammalian foregut endoderm. Mech Dev, 118(1-2), 147-155. https://doi.org/10.1016/s0925-4773(02)00240-x

Cancian, L., Hansen, A., & Boshoff, C. (2013).
Cellular origin of Kaposi's sarcoma and Kaposi's sarcoma-associated herpesvirus-induced cell reprogramming. Trends Cell Biol, 23(9), 421-432. https://doi.org/10.1016/j.tcb.2013.04.001

Carmeliet, P., Lampugnani, M. G., Moons, L., Breviario, F., Compernolle, V., Bono, F., Balconi, G., Spagnuolo, R., Oosthuyse, B., Dewerchin, M., Zanetti, A., Angellilo, A., Mattot, V., Nuyens, D., Lutgens, E., Clotman, F., de Ruiter, M. C., Gittenberger-de Groot, A., Poelmann, R., . . . Dejana, E. (1999).
Targeted deficiency or cytosolic truncation of the VE-cadherin gene in mice impairs VEGF-mediated endothelial survival and angiogenesis. Cell, 98(2), 147-157. https://doi.org/10.1016/s0092-8674(00)81010-7

Carroll, P. A., Brazeau, E., & Lagunoff, M. (2004).
Kaposi's sarcoma-associated herpesvirus infection of blood endothelial cells induces lymphatic differentiation. Virology, 328(1), 7-18. https://doi.org/10.1016/j.virol.2004.07.008

Caruso, L. B., Guo, R., Keith, K., Madzo, J., Maestri, D., Boyle, S., Wasserman, J., Kossenkov, A., Gewurz, B. E., & Tempera, I. (2022).
The nuclear lamina binds the EBV genome during latency and regulates viral gene expression. PLoS Pathog, 18(4), e1010400. https://doi.org/10.1371/journal.ppat.1010400

Centore, R. C., Sandoval, G. J., Soares, L. M. M., Kadoch, C., & Chan, H. M. (2020).
Mammalian SWI/SNF Chromatin Remodeling Complexes: Emerging Mechanisms and Therapeutic Strategies. Trends Genet, 36(12), 936-950. https://doi.org/10.1016/j.tig.2020.07.011

Cesarman, E., Chang, Y., Moore, P. S., Said, J. W., & Knowles, D. M. (1995).
Kaposi's sarcoma-associated herpesvirus-like DNA sequences in AIDS-related body-cavity-based lymphomas. N Engl J Med, 332(18), 1186-1191. https://doi.org/10.1056/NEJM199505043321802

Cesarman, E., Damania, B., Krown, S. E., Martin, J., Bower, M., & Whitby, D. (2019).
Kaposi sarcoma. Nat Rev Dis Primers, 5(1), 9. https://doi.org/10.1038/s41572-019-0060-9

Chang, Y., Cesarman, E., Pessin, M. S., Lee, F., Culpepper, J., Knowles, D. M., & Moore, P. S. (1994).
Identification of herpesvirus-like DNA sequences in AIDS-associated Kaposi's sarcoma. Science, 266(5192), 1865-1869. https://doi.org/10.1126/science.7997879

Chen, J., Ye, F., Xie, J., Kuhne, K., & Gao, S. J. (2009).
Genome-wide identification of binding sites for Kaposi's sarcoma-associated herpesvirus lytic switch protein, RTA. Virology, 386(2), 290-302. https://doi.org/10.1016/j.virol.2009.01.031

Chen, J., Zhang, Z., Li, L., Chen, B. C., Revyakin, A., Hajj, B., Legant, W., Dahan, M., Lionnet, T., Betzig, E., Tjian, R., & Liu, Z. (2014).
Single-molecule dynamics of enhanceosome assembly in embryonic stem cells. Cell, 156(6), 1274-1285. https://doi.org/10.1016/j.cell.2014.01.062

Chen, Y., Liang, R., Li, Y., Jiang, L., Ma, D., Luo, Q., & Song, G. (2024).
Chromatin accessibility: biological functions, molecular mechanisms and therapeutic application. Signal Transduct Target Ther, 9(1), 340. https://doi.org/10.1038/s41392-024-02030-9

Cheng, F., Pekkonen, P., Laurinavicius, S., Sugiyama, N., Henderson, S., Gunther, T., Rantanen, V., Kaivanto, E., Aavikko, M., Sarek, G., Hautaniemi, S., Biberfeld, P., Aaltonen, L., Grundhoff, A., Boshoff, C., Alitalo, K., Lehti, K., & Ojala, P. M. (2011).
KSHV-initiated notch activation leads to membrane-type-1 matrix metalloproteinase-dependent lymphatic endothelial-to-mesenchymal transition. Cell Host Microbe, 10(6), 577-590. https://doi.org/10.1016/j.chom.2011.10.011

Cheng, F., Weidner-Glunde, M., Varjosalo, M., Rainio, E. M., Lehtonen, A., Schulz, T. F., Koskinen, P. J., Taipale, J., & Ojala, P. M. (2009).
KSHV reactivation from latency requires Pim-1 and Pim-3 kinases to inactivate the latency-associated nuclear antigen LANA. PLoS Pathog, 5(3), e1000324. https://doi.org/10.1371/journal.ppat.1000324

Choi, D., Park, E., Kim, K. E., Jung, E., Seong, Y. J., Zhao, L., Madhavan, S., Daghlian, G., Lee, H. H., Daghlian, P. T., Daghlian, S., Bui, K., Koh, C. J., Wong, A. K., Cho, I. T., & Hong, Y. K. (2020).
The Lymphatic Cell Environment Promotes Kaposi Sarcoma Development by Prox1-Enhanced Productive Lytic Replication of Kaposi Sarcoma Herpes Virus. Cancer Res, 80(15), 3130-3144. https://doi.org/10.1158/0008-5472.CAN-19-3105

Chokunonga, E., Levy, L. M., Bassett, M. T., Mauchaza, B. G., Thomas, D. B., & Parkin, D. M. (2000).
Cancer incidence in the African population of Harare, Zimbabwe: second results from the cancer registry 1993-1995. Int J Cancer, 85(1), 54-59. https://doi.org/10.1002/(sici)1097-0215(20000101)85:1<54::aid-ijc10>3.0.co;2-d

Clapier, C. R., & Cairns, B. R. (2009).
The biology of chromatin remodeling complexes. Annu Rev Biochem, 78, 273-304. https://doi.org/10.1146/annurev.biochem.77.062706.153223

Cohen, S. M., Chastain, P. D., 2nd, Rosson, G. B., Groh, B. S., Weissman, B. E., Kaufman, D. G., & Bultman, S. J. (2010).
BRG1 co-localizes with DNA replication factors and is required for efficient replication fork progression. Nucleic Acids Res, 38(20), 6906-6919. https://doi.org/10.1093/nar/gkq559

Corces, M. R., Trevino, A. E., Hamilton, E. G., Greenside, P. G., Sinnott-Armstrong, N. A., Vesuna, S., Satpathy, A. T., Rubin, A. J., Montine, K. S., Wu, B., Kathiria, A., Cho, S. W., Mumbach, M. R., Carter, A. C., Kasowski, M., Orloff, L. A., Risca, V. I., Kundaje, A., Khavari, P. A., . . . Chang, H. Y. (2017).
An improved ATAC-seq protocol reduces background and enables interrogation of frozen tissues. Nat Methods, 14(10), 959-962. https://doi.org/10.1038/nmeth.4396

Crameri, M., Bauer, M., Caduff, N., Walker, R., Steiner, F., Franzoso, F. D., Gujer, C., Boucke, K., Kucera, T., Zbinden, A., Munz, C., Fraefel, C., Greber, U. F., & Pavlovic, J. (2018).
MxB is an interferon-induced restriction factor of human herpesviruses. Nat Commun, 9(1), 1980. https://doi.org/10.1038/s41467-018-04379-2

Dailey, C., Oshodi, R. B., Boull, C., & Aggarwal, A. (2022).
Expanding the clinical spectrum of SOX18-related Hypotrichosis-lymphedema-telangiectasia-renal defect syndrome. Eur J Med Genet, 65(11), 104607. https://doi.org/10.1016/j.ejmg.2022.104607

Damania, B., & Dittmer, D. P. (2023).
Today's Kaposi sarcoma is not the same as it was 40 years ago, or is it? J Med Virol, 95(5), e28773. https://doi.org/10.1002/jmv.28773

de Martel, C., Georges, D., Bray, F., Ferlay, J., & Clifford, G. M. (2020).
Global burden of cancer attributable to infections in 2018: a worldwide incidence analysis. Lancet Glob Health, 8(2), e180-e190. https://doi.org/10.1016/S2214-109X(19)30488-7

Della Bella, S., Taddeo, A., Calabro, M. L., Brambilla, L., Bellinvia, M., Bergamo, E., Clerici, M., & Villa, M. L. (2008).
Peripheral blood endothelial progenitors as potential reservoirs of Kaposi's sarcoma-associated herpesvirus. PLoS One, 3(1), e1520. https://doi.org/10.1371/journal.pone.0001520

Digman, M. A., Dalal, R., Horwitz, A. F., & Gratton, E. (2008).
Mapping the number of molecules and brightness in the laser scanning microscope. Biophys J, 94(6), 2320-2332. https://doi.org/10.1529/biophysj.107.114645

Dillon, P. J., Gregory, S. M., Tamburro, K., Sanders, M. K., Johnson, G. L., Raab-Traub, N., Dittmer, D. P., & Damania, B. (2013).
Tousled-like kinases modulate reactivation of gammaherpesviruses from latency. Cell Host Microbe, 13(2), 204-214. https://doi.org/10.1016/j.chom.2012.12.005

DiMaio, T. A., Vogt, D. T., & Lagunoff, M. (2020).
KSHV requires vCyclin to overcome replicative senescence in primary human lymphatic endothelial cells. PLoS Pathog, 16(6), e1008634. https://doi.org/10.1371/journal.ppat.1008634

DiMaio, T. A., Wentz, B. L., & Lagunoff, M. (2016). I
solation and characterization of circulating lymphatic endothelial colony forming cells. Exp Cell Res, 340(1), 159-169. https://doi.org/10.1016/j.yexcr.2015.11.015

Dodonova, S. O., Zhu, F., Dienemann, C., Taipale, J., & Cramer, P. (2020).
Nucleosome-bound SOX2 and SOX11 structures elucidate pioneer factor function. Nature, 580(7805), 669-672. https://doi.org/10.1038/s41586-020-2195-y

Downes, M., & Koopman, P. (2001).
SOX18 and the transcriptional regulation of blood vessel development. Trends Cardiovasc Med, 11(8), 318-324. https://doi.org/10.1016/s1050-1738(01)00131-1

Dreier, M. R., Walia, J., & de la Serna, I. L. (2024).
Targeting SWI/SNF Complexes in Cancer: Pharmacological Approaches and Implications. Epigenomes, 8(1). https://doi.org/10.3390/epigenomes8010007

Ducoli, L., & Detmar, M. (2021).
Beyond PROX1: transcriptional, epigenetic, and noncoding RNA regulation of lymphatic identity and function. Dev Cell, 56(4), 406-426.
https://doi.org/10.1016/j.devcel.2021.01.018

Duong, T., Proulx, S. T., Luciani, P., Leroux, J. C., Detmar, M., Koopman, P., & Francois, M. (2012).
Genetic ablation of SOX18 function suppresses tumor lymphangiogenesis and metastasis of melanoma in mice. Cancer Res, 72(12), 3105-3114.
https://doi.org/10.1158/0008-5472.CAN-11-4026

Dupin, N., Fisher, C., Kellam, P., Ariad, S., Tulliez, M., Franck, N., van Marck, E., Salmon, D., Gorin, I., Escande, J. P., Weiss, R. A., Alitalo, K., & Boshoff, C. (1999).
Distribution of human herpesvirus-8 latently infected cells in Kaposi's sarcoma, multicentric Castleman's disease, and primary effusion lymphoma. Proc Natl Acad Sci U S A, 96(8), 4546-4551. https://doi.org/10.1073/pnas.96.8.4546

Duprez, R., Lacoste, V., Briere, J., Couppie, P., Frances, C., Sainte-Marie, D., Kassa-Kelembho, E., Lando, M. J., Essame Oyono, J. L., Nkegoum, B., Hbid, O., Mahe, A., Lebbe, C., Tortevoye, P., Huerre, M., & Gessain, A. (2007).
Evidence for a multiclonal origin of multicentric advanced lesions of Kaposi sarcoma. J Natl Cancer Inst, 99(14), 1086-1094. https://doi.org/10.1093/jnci/djm045

Elsir, T., Smits, A., Lindstrom, M. S., & Nister, M. (2012).
Transcription factor PROX1: its role in development and cancer. Cancer Metastasis Rev, 31(3-4), 793-805. https://doi.org/10.1007/s10555-012-9390-8

Eltom, M. A., Jemal, A., Mbulaiteye, S. M., Devesa, S. S., & Biggar, R. J. (2002).
Trends in Kaposi's sarcoma and non-Hodgkin's lymphoma incidence in the United States from 1973 through 1998. J Natl Cancer Inst, 94(16), 1204-1210.
https://doi.org/10.1093/jnci/94.16.1204

Erdos, G., & Dosztanyi, Z. (2024).
AIUPred: combining energy estimation with deep learning for the enhanced prediction of protein disorder. Nucleic Acids Res, 52(W1), W176-W181.
https://doi.org/10.1093/nar/gkae385

Farhy, C., Hariharan, S., Ylanko, J., Orozco, L., Zeng, F. Y., Pass, I., Ugarte, F., Forsberg, E. C., Huang, C. T., Andrews, D. W., & Terskikh, A. V. (2019).
Improving drug discovery using image-based multiparametric analysis of the epigenetic landscape. Elife, 8. https://doi.org/10.7554/eLife.49683

Farnaby, W., Koegl, M., Roy, M. J., Whitworth, C., Diers, E., Trainor, N., Zollman, D., Steurer, S., Karolyi-Oezguer, J., Riedmueller, C., Gmaschitz, T., Wachter, J., Dank, C., Galant, M., Sharps, B., Rumpel, K., Traxler, E., Gerstberger, T., Schnitzer, R., . . . Ciulli, A. (2019).
Publisher Correction: BAF complex vulnerabilities in cancer demonstrated via structure-based PROTAC design. Nat Chem Biol, 15(8), 846. *https://doi.org/10.1038/s41589-019-0329-z*

Fei, L., Zhang, K., Poddar, N., Hautaniemi, S., & Sahu, B. (2023).
Single-cell epigenome analysis identifies molecular events controlling direct conversion of human fibroblasts to pancreatic ductal-like cells. Dev Cell, 58(18), 1701-1715 e1708. *https://doi.org/10.1016/j.devcel.2023.08.023*

Ferrara, N., Gerber, H. P., & LeCouter, J. (2003).
The biology of VEGF and its receptors. Nat Med, 9(6), 669-676. *https://doi.org/10.1038/nm0603-669*

Fontaine, F., Overman, J., Moustaqil, M., Mamidyala, S., Salim, A., Narasimhan, K., Prokoph, N., Robertson, A. A. B., Lua, L., Alexandrov, K., Koopman, P., Capon, R. J., Sierecki, E., Gambin, Y., Jauch, R., Cooper, M. A., Zuegg, J., & Francois, M. (2017).
Small-Molecule Inhibitors of the SOX18 Transcription Factor. Cell Chem Biol, 24(3), 346-359. *https://doi.org/10.1016/j.chembiol.2017.01.003*

Fontijn, R. D., Favre, J., Naaijkens, B. A., Meinster, E., Paauw, N. J., Ragghoe, S. L., Nauta, T. D., van den Broek, M. A., Weijers, E. M., Niessen, H. W., Koolwijk, P., & Horrevoets, A. J. (2014).
Adipose tissue-derived stromal cells acquire endothelial-like features upon reprogramming with SOX18. Stem Cell Res, 13(3 Pt A), 367-378. *https://doi.org/10.1016/j.scr.2014.09.004*

Francois, M., Caprini, A., Hosking, B., Orsenigo, F., Wilhelm, D., Browne, C., Paavonen, K., Karnezis, T., Shayan, R., Downes, M., Davidson, T., Tutt, D., Cheah, K. S., Stacker, S. A., Muscat, G. E., Achen, M. G., Dejana, E., & Koopman, P. (2008).
Sox18 induces development of the lymphatic vasculature in mice. Nature, 456(7222), 643-647. *https://doi.org/10.1038/nature07391*

Friedman-Kien, A. E. (1981).
Disseminated Kaposi's sarcoma syndrome in young homosexual men. J Am Acad Dermatol, 5(4), 468-471. *https://doi.org/10.1016/s0190-9622(81)80010-2*

Ganem, D. (2010).
KSHV and the pathogenesis of Kaposi sarcoma: listening to human biology and medicine. J Clin Invest, 120(4), 939-949. *https://doi.org/10.1172/JCI40567*

Garber, A. C., Shu, M. A., Hu, J., & Renne, R. (2001).
DNA binding and modulation of gene expression by the latency-associated nuclear antigen of Kaposi's sarcoma-associated herpesvirus. J Virol, 75(17), 7882-7892. *https://doi.org/10.1128/jvi.75.17.7882-7892.2001*

Gasperini, P., Espigol-Frigole, G., McCormick, P. J., Salvucci, O., Maric, D., Uldrick, T. S., Polizzotto, M. N., Yarchoan, R., & Tosato, G. (2012).
Kaposi sarcoma herpesvirus promotes endothelial-to-mesenchymal transition through Notch-dependent signaling. Cancer Res, 72(5), 1157-1169. *https://doi.org/10.1158/0008-5472.CAN-11-3067*

Gessain, A., & Duprez, R. (2005). Spindle cells and their role in Kaposi's sarcoma. Int J Biochem Cell Biol, 37(12), 2457-2465. *https://doi.org/10.1016/j.biocel.2005.01.018*

Golas, G., Alonso, J. D., & Toth, Z. (2019).
Characterization of de novo lytic infection of dermal lymphatic microvascular endothelial cells by Kaposi's sarcoma-associated herpesvirus. Virology, 536, 27-31. *https://doi.org/10.1016/j.virol.2019.07.028*

Gramolelli, S., Cheng, J., Martinez-Corral, I., Vaha-Koskela, M., Elbasani, E., Kaivanto, E., Rantanen, V., Tuohinto, K., Hautaniemi, S., Bower, M., Haglund, C., Alitalo, K., Makinen, T., Petrova, T. V., Lehti, K., & Ojala, P. M. (2018).
PROX1 is a transcriptional regulator of MMP14. Sci Rep, 8(1), 9531. h *ttps://doi.org/10.1038/s41598-018-27739-w*

Gramolelli, S., Elbasani, E., Tuohinto, K., Nurminen, V., Gunther, T., Kallinen, R. E., Kaijalainen, S. P., Diaz, R., Grundhoff, A., Haglund, C., Ziegelbauer, J. M., Pellinen, T., Bower, M., Francois, M., & Ojala, P. M. (2020).
Oncogenic Herpesvirus Engages Endothelial Transcription Factors SOX18 and PROX1 to Increase Viral Genome Copies and Virus Production. Cancer Res, 80(15), 3116-3129. *https://doi.org/10.1158/0008-5472.CAN-19-3103*

Gramolelli, S., & Ojala, P. M. (2017).
Kaposi's sarcoma herpesvirus-induced endothelial cell reprogramming supports viral persistence and contributes to Kaposi's sarcoma tumorigenesis. Curr Opin Virol, 26, 156-162. *https://doi.org/10.1016/j.coviro.2017.09.002*

Gramolelli, S., & Schulz, T. F. (2015).
The role of Kaposi sarcoma-associated herpesvirus in the pathogenesis of Kaposi sarcoma. J Pathol, 235(2), 368-380. *https://doi.org/10.1002/path.4441*

Grossmann, C., & Ganem, D. (2008).
Effects of NFkappaB activation on KSHV latency and lytic reactivation are complex and context-dependent. Virology, 375(1), 94-102.
https://doi.org/10.1016/j.virol.2007.12.044

Grundhoff, A., & Ganem, D. (2004). I
nefficient establishment of KSHV latency suggests an additional role for continued lytic replication in Kaposi sarcoma pathogenesis. J Clin Invest, 113(1), 124-136.
https://doi.org/10.1172/JCI17803

Guito, J., & Lukac, D. M. (2012).
KSHV Rta Promoter Specification and Viral Reactivation. Front Microbiol, 3, 30.
https://doi.org/10.3389/fmicb.2012.00030

Gutierrez, K. D., Morris, V. A., Wu, D., Barcy, S., & Lagunoff, M. (2013).
Ets-1 is required for the activation of VEGFR3 during latent Kaposi's sarcoma-associated herpesvirus infection of endothelial cells. J Virol, 87(12), 6758-6768.
https://doi.org/10.1128/JVI.03241-12

Gwack, Y., Baek, H. J., Nakamura, H., Lee, S. H., Meisterernst, M., Roeder, R. G., & Jung, J. U. (2003).
Principal role of TRAP/mediator and SWI/SNF complexes in Kaposi's sarcoma-associated herpesvirus RTA-mediated lytic reactivation. Mol Cell Biol, 23(6), 2055-2067.
https://doi.org/10.1128/MCB.23.6.2055-2067.2003

Hagey, D. W., Bergsland, M., & Muhr, J. (2022).
SOX2 transcription factor binding and function. Development, 149(14).
https://doi.org/10.1242/dev.200547

Hahn, A. S., Kaufmann, J. K., Wies, E., Naschberger, E., Panteleev-Ivlev, J., Schmidt, K., Holzer, A., Schmidt, M., Chen, J., Konig, S., Ensser, A., Myoung, J., Brockmeyer, N. H., Sturzl, M., Fleckenstein, B., & Neipel, F. (2012).
The ephrin receptor tyrosine kinase A2 is a cellular receptor for Kaposi's sarcoma-associated herpesvirus. Nat Med, 18(6), 961-966. https://doi.org/10.1038/nm.2805

Haque, N., Parveen, S., Tang, T., Wei, J., & Huang, Z. (2022).
Marine Natural Products in Clinical Use. Mar Drugs, 20(8).
https://doi.org/10.3390/md20080528

He, M., Lv, X., Cao, X., Yuan, Z., Getachew, T., Li, Y., Wang, S., & Sun, W. (2023).
SOX18 Promotes the Proliferation of Dermal Papilla Cells via the Wnt/beta-Catenin Signaling Pathway. Int J Mol Sci, 24(23). https://doi.org/10.3390/ijms242316672

Hellert, J., Weidner-Glunde, M., Krausze, J., Richter, U., Adler, H., Fedorov, R., Pietrek, M., Ruckert, J., Ritter, C., Schulz, T. F., & Luhrs, T. (2013).
A structural basis for BRD2/4-mediated host chromatin interaction and oligomer assembly of Kaposi sarcoma-associated herpesvirus and murine gammaherpesvirus LANA proteins. PLoS Pathog, 9(10), e1003640. https://doi.org/10.1371/journal.ppat.1003640

Hoffman, G. R., Rahal, R., Buxton, F., Xiang, K., McAllister, G., Frias, E., Bagdasarian, L., Huber, J., Lindeman, A., Chen, D., Romero, R., Ramadan, N., Phadke, T., Haas, K., Jaskelioff, M., Wilson, B. G., Meyer, M. J., Saenz-Vash, V., Zhai, H., . . . Jagani, Z. (2014).
Functional epigenetics approach identifies BRM/SMARCA2 as a critical synthetic lethal target in BRG1-deficient cancers. Proc Natl Acad Sci U S A, 111(8), 3128-3133.
https://doi.org/10.1073/pnas.1316793111

Holm, A., Graus, M. S., Wylie-Sears, J., Tan, J. W. H., Alvarez-Harmon, M., Borgelt, L., Nasim, S., Chung, L., Jain, A., Sun, M., Sun, L., Brouillard, P., Lekwuttikarn, R., Qi, Y., Teng, J., Vikkula, M., Kozakewich, H., Mulliken, J. B., Francois, M., & Bischoff, J. (2025).
An endothelial SOX18-mevalonate pathway axis enables repurposing of statins for infantile hemangioma. J Clin Invest, 135(7). https://doi.org/10.1172/JCI179782

Holm, A., Mulliken, J. B., & Bischoff, J. (2024).
Infantile hemangioma: the common and enigmatic vascular tumor. J Clin Invest, 134(8).
https://doi.org/10.1172/JCI172836

Hong, Y. K., Foreman, K., Shin, J. W., Hirakawa, S., Curry, C. L., Sage, D. R., Libermann, T., Dezube, B. J., Fingeroth, J. D., & Detmar, M. (2004).
Lymphatic reprogramming of blood vascular endothelium by Kaposi sarcoma-associated herpesvirus. Nat Genet, 36(7), 683-685. https://doi.org/10.1038/ng1383

Hosking, B. M., Muscat, G. E., Koopman, P. A., Dowhan, D. H., & Dunn, T. L. (1995).
Trans-activation and DNA-binding properties of the transcription factor, Sox-18. Nucleic Acids Res, 23(14), 2626-2628. https://doi.org/10.1093/nar/23.14.2626

Hu, J., Garber, A. C., & Renne, R. (2002).
The latency-associated nuclear antigen of Kaposi's sarcoma-associated herpesvirus supports latent DNA replication in dividing cells. J Virol, 76(22), 11677-11687.
https://doi.org/10.1128/jvi.76.22.11677-11687.2002

Hu, J., Yang, Y., Turner, P. C., Jain, V., McIntyre, L. M., & Renne, R. (2014).
LANA binds to multiple active viral and cellular promoters and associates with the H3K4methyltransferase hSET1 complex. PLoS Pathog, 10(7), e1004240.
https://doi.org/10.1371/journal.ppat.1004240

Hu, Y., & Stillman, B. (2023).
Origins of DNA replication in eukaryotes. Mol Cell, 83(3), 352-372. https://doi.org/10.1016/j.molcel.2022.12.024

Ibrahim Khalil, A., Franceschi, S., de Martel, C., Bray, F., & Clifford, G. M. (2022).
Burden of Kaposi sarcoma according to HIV status: A systematic review and global analysis. Int J Cancer, 150(12), 1948-1957. https://doi.org/10.1002/ijc.33951

Irrthum, A., Devriendt, K., Chitayat, D., Matthijs, G., Glade, C., Steijlen, P. M., Fryns, J. P., Van Steensel, M. A., & Vikkula, M. (2003).
Mutations in the transcription factor gene SOX18 underlie recessive and dominant forms of hypotrichosis-lymphedema-telangiectasia. Am J Hum Genet, 72(6), 1470-1478. https://doi.org/10.1086/375614

Jung, H. S., Suknuntha, K., Kim, Y. H., Liu, P., Dettle, S. T., Sedzro, D. M., Smith, P. R., Thomson, J. A., Ong, I. M., & Slukvin, II. (2023).
SOX18-enforced expression diverts hemogenic endothelium-derived progenitors from T towards NK lymphoid pathways. iScience, 26(5), 106621. https://doi.org/10.1016/j.isci.2023.106621

Ka-Yue Chow, L., Lai-Shun Chung, D., Tao, L., Chan, K. F., Tung, S. Y., Cheong Ngan, R. K., Ng, W. T., Wing-Mui Lee, A., Yau, C. C., Lai-Wan Kwong, D., Ho-Fun Lee, V., Lam, K. O., Liu, J., Chen, H., Dai, W., & Lung, M. L. (2022).
Epigenomic landscape study reveals molecular subtypes and EBV-associated regulatory epigenome reprogramming in nasopharyngeal carcinoma. EBioMedicine, 86, 104357. https://doi.org/10.1016/j.ebiom.2022.104357

Kadoch, C., Hargreaves, D. C., Hodges, C., Elias, L., Ho, L., Ranish, J., & Crabtree, G. R. (2013).
Proteomic and bioinformatic analysis of mammalian SWI/SNF complexes identifies extensive roles in human malignancy. Nat Genet, 45(6), 592-601. https://doi.org/10.1038/ng.2628

Kamachi, Y., & Kondoh, H. (2013). Sox proteins: regulators of cell fate specification and differentiation. Development, 140(20), 4129-4144. https://doi.org/10.1242/dev.091793

Kedes, D. H., Lagunoff, M., Renne, R., & Ganem, D. (1997).
Identification of the gene encoding the major latency-associated nuclear antigen of the Kaposi's sarcoma-associated herpesvirus. J Clin Invest, 100(10), 2606-2610. https://doi.org/10.1172/JCI119804

Kgatle, M., Mbambara, S., Khoza, L., Fadebi, O., Mashamba-Thompson, T., & Sathekge, M. (2025).
The role of pioneering transcription factors, chromatin accessibility and epigenetic reprogramming in oncogenic viruses. Front Microbiol, 16, 1602497. https://doi.org/10.3389/fmicb.2025.1602497

Kirjavainen, A., Sulg, M., Heyd, F., Alitalo, K., Yla-Herttuala, S., Moroy, T., Petrova, T. V., & Pirvola, U. (2008).
Prox1 interacts with Atoh1 and Gfi1, and regulates cellular differentiation in the inner ear sensory epithelia. Dev Biol, 322(1), 33-45. https://doi.org/10.1016/j.ydbio.2008.07.004

Konrad, A., Wies, E., Thurau, M., Marquardt, G., Naschberger, E., Hentschel, S., Jochmann, R., Schulz, T. F., Erfle, H., Brors, B., Lausen, B., Neipel, F., & Sturzl, M. (2009).
A systems biology approach to identify the combination effects of human herpesvirus 8 genes on NF-kappaB activation. J Virol, 83(6), 2563-2574. https://doi.org/10.1128/JVI.01512-08

Kruger, W., Peterson, C. L., Sil, A., Coburn, C., Arents, G., Moudrianakis, E. N., & Herskowitz, I. (1995). *Amino acid substitutions in the structured domains of histones H3 and H4 partially relieve the requirement of the yeast SWI/SNF complex for transcription. Genes Dev, 9(22), 2770-2779.* https://doi.org/10.1101/gad.9.22.2770

Krump, N. A., & You, J. (2018). *Molecular mechanisms of viral oncogenesis in humans. Nat Rev Microbiol, 16(11), 684-698.* https://doi.org/10.1038/s41579-018-0064-6

Kumar, A., Lyu, Y., Yanagihashi, Y., Chantarasrivong, C., Majerciak, V., Salemi, M., Wang, K. H., Inagaki, T., Chuang, F., Davis, R. R., Tepper, C. G., Nakano, K., Izumiya, C., Shimoda, M., Nakajima, K. I., Merleev, A., Zheng, Z. M., Campbell, M., & Izumiya, Y. (2022). *KSHV episome tethering sites on host chromosomes and regulation of latency-lytic switch by CHD4. Cell Rep, 39(6), 110788.* https://doi.org/10.1016/j.celrep.2022.110788

Larson, A. G., Elnatan, D., Keenen, M. M., Trnka, M. J., Johnston, J. B., Burlingame, A. L., Agard, D. A., Redding, S., & Narlikar, G. J. (2017). *Liquid droplet formation by HP1alpha suggests a role for phase separation in heterochromatin. Nature, 547(7662), 236-240.* https://doi.org/10.1038/nature22822

Laux, G., Adam, B., Strobl, L. J., & Moreau-Gachelin, F. (1994). *The Spi-1/PU.1 and Spi-B ets family transcription factors and the recombination signal binding protein RBP-J kappa interact with an Epstein-Barr virus nuclear antigen 2 responsive cis-element. EMBO J, 13(23), 5624-5632.* https://doi.org/10.1002/j.1460-2075.1994.tb06900.x

Lavado, A., & Oliver, G. (2007). *Prox1 expression patterns in the developing and adult murine brain. Dev Dyn, 236(2), 518-524.* https://doi.org/10.1002/dvdy.21024

Le Ricousse-Roussanne, S., Barateau, V., Contreres, J. O., Boval, B., Kraus-Berthier, L., & Tobelem, G. (2004). *Ex vivo differentiated endothelial and smooth muscle cells from human cord blood progenitors home to the angiogenic tumor vasculature. Cardiovasc Res, 62(1), 176-184.* https://doi.org/10.1016/j.cardiores.2004.01.017

Leaute-Labreze, C., Boccara, O., Degrugillier-Chopinet, C., Mazereeuw-Hautier, J., Prey, S., Lebbe, G., Gautier, S., Ortis, V., Lafon, M., Montagne, A., Delarue, A., & Voisard, J. J. (2016). *Safety of Oral Propranolol for the Treatment of Infantile Hemangioma: A Systematic Review. Pediatrics, 138(4).* https://doi.org/10.1542/peds.2016-0353

Lebbe, C., Legendre, C., & Frances, C. (2008). *Kaposi sarcoma in transplantation. Transplant Rev (Orlando), 22(4), 252-261.* https://doi.org/10.1016/j.trre.2008.05.004

Lebedev, A., Kireev, D., Kirichenko, A., Mezhenskaya, E., Antonova, A., Bobkov, V., Lapovok, I., Shlykova, A., Lopatukhin, A., Shemshura, A., Kulagin, V., Kovelenov, A., Cherdantseva, A., Filoniuk, N., Turbina, G., Ermakov, A., Monakhov, N., Piterskiy, M., Semenov, A., . . . Bobkova, M. (2025). *The Molecular Epidemiology of HIV-1 in Russia, 1987-2023: Subtypes, Transmission Networks and Phylogenetic Story. Pathogens, 14(8).* https://doi.org/10.3390/pathogens14080738

Lee, D., Lee, D. Y., Hwang, Y. S., Seo, H. R., Lee, S. A., & Kwon, J. (2021). *The Bromodomain Inhibitor PFI-3 Sensitizes Cancer Cells to DNA Damage by Targeting SWI/SNF. Mol Cancer Res, 19(5), 900-912.* https://doi.org/10.1158/1541-7786.MCR-20-0289

Lee, M. J., Yeon, J. H., Lee, J., Kang, Y. H., Park, B. S., Park, J., Yun, S. H., Wirth, D., Yoo, S. M., Park, C., Gao, S. J., & Lee, M. S. (2024).
Senescence of endothelial cells increases susceptibility to Kaposi's sarcoma-associated herpesvirus infection via CD109-mediated viral entry. J Clin Invest, 135(4). https://doi.org/10.1172/JCI183561

Letang, E., Lewis, J. J., Bower, M., Mosam, A., Borok, M., Campbell, T. B., Naniche, D., Newsom-Davis, T., Shaik, F., Fiorillo, S., Miro, J. M., Schellenberg, D., & Easterbrook, P. J. (2013).
Immune reconstitution inflammatory syndrome associated with Kaposi sarcoma: higher incidence and mortality in Africa than in the UK. AIDS, 27(10), 1603-1613. https://doi.org/10.1097/QAD.0b013e328360a5a1

Leung, D. W., Cachianes, G., Kuang, W. J., Goeddel, D. V., & Ferrara, N. (1989).
Vascular endothelial growth factor is a secreted angiogenic mitogen. Science, 246(4935), 1306-1309. https://doi.org/10.1126/science.2479986

Lieberman, P. M. (2013).
Keeping it quiet: chromatin control of gammaherpesvirus latency. Nat Rev Microbiol, 11(12), 863-875. https://doi.org/10.1038/nrmicro3135

Liu, L., Eby, M. T., Rathore, N., Sinha, S. K., Kumar, A., & Chaudhary, P. M. (2002).
The human herpes virus 8-encoded viral FLICE inhibitory protein physically associates with and persistently activates the Ikappa B kinase complex. J Biol Chem, 277(16), 13745-13751. https://doi.org/10.1074/jbc.M110480200

Liu, X., Salokas, K., Tamene, F., Jiu, Y., Weldatsadik, R. G., Ohman, T., & Varjosalo, M. (2018).
An AP-MS- and BioID-compatible MAC-tag enables comprehensive mapping of protein interactions and subcellular localizations. Nat Commun, 9(1), 1188. https://doi.org/10.1038/s41467-018-03523-2

Liu, Y., Asakura, M., Inoue, H., Nakamura, T., Sano, M., Niu, Z., Chen, M., Schwartz, R. J., & Schneider, M. D. (2007).
Sox17 is essential for the specification of cardiac mesoderm in embryonic stem cells. Proc Natl Acad Sci U S A, 104(10), 3859-3864. https://doi.org/10.1073/pnas.0609100104

Losay, V. A., & Damania, B. (2025).
Unraveling the Kaposi Sarcoma-Associated Herpesvirus (KSHV) Lifecycle: An Overview of Latency, Lytic Replication, and KSHV-Associated Diseases. Viruses, 17(2). https://doi.org/10.3390/v17020177

Lotke, R., Schneeweiss, U., Pietrek, M., Gunther, T., Grundhoff, A., Weidner-Glunde, M., & Schulz, T. F. (2020).
Brd/BET Proteins Influence the Genome-Wide Localization of the Kaposi's Sarcoma-Associated Herpesvirus and Murine Gammaherpesvirus Major Latency Proteins. Front Microbiol, 11, 591778. https://doi.org/10.3389/fmicb.2020.591778

Lovell-Badge, R. (2010).
The early history of the Sox genes. Int J Biochem Cell Biol, 42(3), 378-380. https://doi.org/10.1016/j.biocel.2009.12.003

Lu, F., Tsai, K., Chen, H. S., Wikramasinghe, P., Davuluri, R. V., Showe, L., Domsic, J., Marmorstein, R., & Lieberman, P. M. (2012).
Identification of host-chromosome binding sites and candidate gene targets for Kaposi's sarcoma-associated herpesvirus LANA. J Virol, 86(10), 5752-5762. https://doi.org/10.1128/JVI.07216-11

Lu, F., Zhou, J., Wiedmer, A., Madden, K., Yuan, Y., & Lieberman, P. M. (2003).
Chromatin remodeling of the Kaposi's sarcoma-associated herpesvirus ORF50 promoter correlates with reactivation from latency. J Virol, 77(21), 11425-11435. https://doi.org/10.1128/jvi.77.21.11425-11435.2003

Lukac, D. M., Garibyan, L., Kirshner, J. R., Palmeri, D., & Ganem, D. (2001).
DNA binding by Kaposi's sarcoma-associated herpesvirus lytic switch protein is necessary for transcriptional activation of two viral delayed early promoters. J Virol, 75(15), 6786-6799. https://doi.org/10.1128/JVI.75.15.6786-6799.2001

Lunn, R. M., Jahnke, G. D., & Rabkin, C. S. (2017).
Tumour virus epidemiology. Philos Trans R Soc Lond B Biol Sci, 372(1732). https://doi.org/10.1098/rstb.2016.0266

Ma, T., Jham, B. C., Hu, J., Friedman, E. R., Basile, J. R., Molinolo, A., Sodhi, A., & Montaner, S. (2010).
Viral G protein-coupled receptor up-regulates Angiopoietin-like 4 promoting angiogenesis and vascular permeability in Kaposi's sarcoma. Proc Natl Acad Sci U S A, 107(32), 14363-14368. https://doi.org/10.1073/pnas.1001065107

Maestri, D., Caruso, L. B., Cable, J. M., Sklutuis, R., Preston-Alp, S., White, R. E., Luftig, M. A., & Tempera, I. (2025).
EBNA leader protein orchestrates chromatin architecture remodeling during Epstein-Barr virus-induced B cell transformation. Nucleic Acids Res, 53(12). https://doi.org/10.1093/nar/gkaf629

Makinen, T., Veikkola, T., Mustjoki, S., Karpanen, T., Catimel, B., Nice, E. C., Wise, L., Mercer, A., Kowalski, H., Kerjaschki, D., Stacker, S. A., Achen, M. G., & Alitalo, K. (2001).
Isolated lymphatic endothelial cells transduce growth, survival and migratory signals via the VEGF-C/D receptor VEGFR-3. EMBO J, 20(17), 4762-4773. https://doi.org/10.1093/emboj/20.17.4762

Malone, H. A., & Roberts, C. W. M. (2024).
Chromatin remodellers as therapeutic targets. Nat Rev Drug Discov, 23(9), 661-681. https://doi.org/10.1038/s41573-024-00978-5

Martin, J. N., Ganem, D. E., Osmond, D. H., Page-Shafer, K. A., Macrae, D., & Kedes, D. H. (1998).
Sexual transmission and the natural history of human herpesvirus 8 infection. N Engl J Med, 338(14), 948-954. https://doi.org/10.1056/NEJM199804023381403

Martinez, F. P., & Tang, Q. (2012).
Leucine zipper domain is required for Kaposi sarcoma-associated herpesvirus (KSHV) K-bZIP protein to interact with histone deacetylase and is important for KSHV replication. J Biol Chem, 287(19), 15622-15634. https://doi.org/10.1074/jbc.M111.315861

Mashtalir, N., D'Avino, A. R., Michel, B. C., Luo, J., Pan, J., Otto, J. E., Zullow, H. J., McKenzie, Z. M., Kubiak, R. L., St Pierre, R., Valencia, A. M., Poynter, S. J., Cassel, S. H., Ranish, J. A., & Kadoch, C. (2018).
Modular Organization and Assembly of SWI/SNF Family Chromatin Remodeling Complexes. Cell, 175(5), 1272-1288 e1220. https://doi.org/10.1016/j.cell.2018.09.032

McAllister, S. C., Hanson, R. S., & Manion, R. D. (2015).
Propranolol Decreases Proliferation of Endothelial Cells Transformed by Kaposi's Sarcoma-Associated Herpesvirus and Induces Lytic Viral Gene Expression. J Virol, 89(21), 11144-11149. https://doi.org/10.1128/JVI.01569-15

McElwee, P. D., Harrison, P. A., van Huysen, T. L., Alonso Roldán, V., Barrios, E., Dasgupta, P., DeClerck, F., Harmáčková, Z. V., Hayman, D. T. S., Herrero, M., Kumar, R., Ley, D., Mangalagiu, D., McFarlane, R. A., Paukert, C., Pengue, W. A., Prist, P. R., Ricketts, T. H., Rounsevell, M. D. A., Saito, O., Selomane, O., Seppelt, R., Singh, P. K., Sitas, N., Smith, P., Vause, J., Molua, E. L., Zambrana-Torrelio, C., and Obura, D. (eds.). IPBES secretariat, Bonn, Germany. (2024).
Summary for Policymakers of the Thematic Assessment Report on the Interlinkages among Biodiversity, Water, Food and Health of the Intergovernmental Science-Policy Platform on Biodiversity and Ecosystem Services. https://zenodo.org/records/13850290

McLaughlin-Drubin, M. E., & Munger, K. (2009).
Oncogenic activities of human papillomaviruses. Virus Res, 143(2), 195-208. https://doi.org/10.1016/j.virusres.2009.06.008

Medina, M. V., A, D. A., Ma, Q., Eroles, P., Cavallin, L., Chiozzini, C., Sapochnik, D., Cymeryng, C., Hyjek, E., Cesarman, E., Naipauer, J., Mesri, E. A., & Coso, O. A. (2020).
KSHV G-protein coupled receptor vGPCR oncogenic signaling upregulation of Cyclooxygenase-2 expression mediates angiogenesis and tumorigenesis in Kaposi's sarcoma. PLoS Pathog, 16(10), e1009006. https://doi.org/10.1371/journal.ppat.1009006

Mercier, A., Arias, C., Madrid, A. S., Holdorf, M. M., & Ganem, D. (2014).
Site-specific association with host and viral chromatin by Kaposi's sarcoma-associated herpesvirus LANA and its reversal during lytic reactivation. J Virol, 88(12), 6762-6777. https://doi.org/10.1128/JVI.00268-14

Miller, G., Heston, L., Grogan, E., Gradoville, L., Rigsby, M., Sun, R., Shedd, D., Kushnaryov, V. M., Grossberg, S., & Chang, Y. (1997).
Selective switch between latency and lytic replication of Kaposi's sarcoma herpesvirus and Epstein-Barr virus in dually infected body cavity lymphoma cells. J Virol, 71(1), 314-324. https://doi.org/10.1128/JVI.71.1.314-324.1997

Mody, A., Sohn, A. H., Iwuji, C., Tan, R. K. J., Venter, F., & Geng, E. H. (2024).
HIV epidemiology, prevention, treatment, and implementation strategies for public health. Lancet, 403(10425), 471-492. https://doi.org/10.1016/S0140-6736(23)01381-8

Montaner, S., Sodhi, A., Molinolo, A., Bugge, T. H., Sawai, E. T., He, Y., Li, Y., Ray, P. E., & Gutkind, J. S. (2003).
Endothelial infection with KSHV genes in vivo reveals that vGPCR initiates Kaposi's sarcomagenesis and can promote the tumorigenic potential of viral latent genes. Cancer Cell, 3(1), 23-36. https://doi.org/10.1016/s1535-6108(02)00237-4

Moustaqil, M., Fontaine, F., Overman, J., McCann, A., Bailey, T. L., Rudolffi Soto, P., Bhumkar, A., Giles, N., Hunter, D. J. B., Gambin, Y., Francois, M., & Sierecki, E. (2018).
Homodimerization regulates an endothelial specific signature of the SOX18 transcription factor. Nucleic Acids Res, 46(21), 11381-11395. https://doi.org/10.1093/nar/gky897

Muchardt, C., & Yaniv, M. (1999). ATP-dependent chromatin remodelling: SWI/SNF and Co. are on the job. J Mol Biol, 293(2), 187-198. https://doi.org/10.1006/jmbi.1999.2999

Myoung, J., & Ganem, D. (2011).
Generation of a doxycycline-inducible KSHV producer cell line of endothelial origin: maintenance of tight latency with efficient reactivation upon induction. J Virol Methods, 174(1-2), 12-21. https://doi.org/10.1016/j.jviromet.2011.03.012

Nakagawa, M., Koyanagi, M., Tanabe, K., Takahashi, K., Ichisaka, T., Aoi, T., Okita, K., Mochiduki, Y., Takizawa, N., & Yamanaka, S. (2008).
Generation of induced pluripotent stem cells without Myc from mouse and human fibroblasts. Nat Biotechnol, 26(1), 101-106. https://doi.org/10.1038/nbt1374

Navarro, P., Ruco, L., & Dejana, E. (1998).
Differential localization of VE- and N-cadherins in human endothelial cells: VE-cadherin competes with N-cadherin for junctional localization. J Cell Biol, 140(6), 1475-1484. https://doi.org/10.1083/jcb.140.6.1475

Neugebauer, E., Bastidas-Quintero, A. M., Weidl, D., & Full, F. (2023).
Pioneer factors in viral infection. Front Immunol, 14, 1286617. https://doi.org/10.3389/fimmu.2023.1286617

Newman, D. J., & Cragg, G. M. (2020).
Natural Products as Sources of New Drugs over the Nearly Four Decades from 01/1981 to 09/2019. J Nat Prod, 83(3), 770-803. https://doi.org/10.1021/acs.jnatprod.9b01285

Newman, P. J. (1997).
The biology of PECAM-1. J Clin Invest, 99(1), 3-8. https://doi.org/10.1172/JCI119129

Nobuhisa, I., Melig, G., & Taga, T. (2024).
Sox17 and Other SoxF-Family Proteins Play Key Roles in the Hematopoiesis of Mouse Embryos. Cells, 13(22). https://doi.org/10.3390/cells13221840

Ogarkova, D., Antonova, A., Kuznetsova, A., Adgamov, R., Pochtovyi, A., Kleimenov, D., Tsyganova, E., Gushchin, V., Gintsburg, A., & Mazus, A. (2023).
Current Trends of HIV Infection in the Russian Federation. Viruses, 15(11). https://doi.org/10.3390/v15112156

Ojala, P. M., & Schulz, T. F. (2014).
Manipulation of endothelial cells by KSHV: implications for angiogenesis and aberrant vascular differentiation. Semin Cancer Biol, 26, 69-77. https://doi.org/10.1016/j.semcancer.2014.01.008

Olofsson, B., Pajusola, K., Kaipainen, A., von Euler, G., Joukov, V., Saksela, O., Orpana, A., Pettersson, R. F., Alitalo, K., & Eriksson, U. (1996).
Vascular endothelial growth factor B, a novel growth factor for endothelial cells. Proc Natl Acad Sci U S A, 93(6), 2576-2581. https://doi.org/10.1073/pnas.93.6.2576

Overman, J., Fontaine, F., Moustaqil, M., Mittal, D., Sierecki, E., Sacilotto, N., Zuegg, J., Robertson, A. A. B., Holmes, K., Salim, A. A., Mamidyala, S., Butler, M. S., Robinson, A. S., Lesieur, E., Johnston, W., Alexandrov, K., Black, B. L., Hogan, B. M., De Val, S., . . . Francois, M. (2017).
Pharmacological targeting of the transcription factor SOX18 delays breast cancer in mice. Elife, 6. https://doi.org/10.7554/eLife.21221

Overman, J., Fontaine, F., Wylie-Sears, J., Moustaqil, M., Huang, L., Meurer, M., Chiang, I. K., Lesieur, E., Patel, J., Zuegg, J., Pasquier, E., Sierecki, E., Gambin, Y., Hamdan, M., Khosrotehrani, K., Andelfinger, G., Bischoff, J., & Francois, M. (2019).
R-propranolol is a small molecule inhibitor of the SOX18 transcription factor in a rare vascular syndrome and hemangioma. Elife, 8. https://doi.org/10.7554/eLife.43026

Pauk, J., Huang, M. L., Brodie, S. J., Wald, A., Koelle, D. M., Schacker, T., Celum, C., Selke, S., & Corey, L. (2000).
Mucosal shedding of human herpesvirus 8 in men. N Engl J Med, 343(19), 1369-1377. https://doi.org/10.1056/NEJM200011093431904

Pei, Y., Wong, J. H., & Robertson, E. S. (2020).
Herpesvirus Epigenetic Reprogramming and Oncogenesis. Annu Rev Virol, 7(1), 309-331. https://doi.org/10.1146/annurev-virology-020420-014025

Pekkonen, P., Alve, S., Balistreri, G., Gramolelli, S., Tatti-Bugaeva, O., Paatero, I., Niiranen, O., Tuohinto, K., Perala, N., Taiwo, A., Zinovkina, N., Repo, P., Icay, K., Ivaska, J., Saharinen, P., Hautaniemi, S., Lehti, K., & Ojala, P. M. (2018).
Lymphatic endothelium stimulates melanoma metastasis and invasion via MMP14-dependent Notch3 and beta1-integrin activation. Elife, 7.
https://doi.org/10.7554/eLife.32490

Petrova, T. V., Makinen, T., Makela, T. P., Saarela, J., Virtanen, I., Ferrell, R. E., Finegold, D. N., Kerjaschki, D., Yla-Herttuala, S., & Alitalo, K. (2002).
Lymphatic endothelial reprogramming of vascular endothelial cells by the Prox-1 homeobox transcription factor. EMBO J, 21(17), 4593-4599.
https://doi.org/10.1093/emboj/cdf470

Purushothaman, P., Dabral, P., Gupta, N., Sarkar, R., & Verma, S. C. (2016).
KSHV Genome Replication and Maintenance. Front Microbiol, 7, 54.
https://doi.org/10.3389/fmicb.2016.00054

Pusztaszeri, M. P., Seelentag, W., & Bosman, F. T. (2006).
Immunohistochemical expression of endothelial markers CD31, CD34, von Willebrand factor, and Fli-1 in normal human tissues. J Histochem Cytochem, 54(4), 385-395.
https://doi.org/10.1369/jhc.4A6514.2005

Renne, R., Lagunoff, M., Zhong, W., & Ganem, D. (1996).
The size and conformation of Kaposi's sarcoma-associated herpesvirus (human herpesvirus 8) DNA in infected cells and virions. J Virol, 70(11), 8151-8154.
https://doi.org/10.1128/JVI.70.11.8151-8154.1996

Ringelhan, M., McKeating, J. A., & Protzer, U. (2017).
Viral hepatitis and liver cancer. Philos Trans R Soc Lond B Biol Sci, 372(1732).
https://doi.org/10.1098/rstb.2016.0274

Risebro, C. A., Searles, R. G., Melville, A. A., Ehler, E., Jina, N., Shah, S., Pallas, J., Hubank, M., Dillard, M., Harvey, N. L., Schwartz, R. J., Chien, K. R., Oliver, G., & Riley, P. R. (2009).
Prox1 maintains muscle structure and growth in the developing heart. Development, 136(3), 495-505. https://doi.org/10.1242/dev.030007

Rous, P. (1911).
A Sarcoma of the Fowl Transmissible by an Agent Separable from the Tumor Cells. J Exp Med, 13(4), 397-411. https://doi.org/10.1084/jem.13.4.397

Roux, K. J., Kim, D. I., Burke, B., & May, D. G. (2018).
BioID: A Screen for Protein-Protein Interactions. Curr Protoc Protein Sci, 91, 19 23 11-19 23 15. https://doi.org/10.1002/cpps.51

Sabari, B. R., Dall'Agnese, A., Boija, A., Klein, I. A., Coffey, E. L., Shrinivas, K., Abraham, B. J., Hannett, N. M., Zamudio, A. V., Manteiga, J. C., Li, C. H., Guo, Y. E., Day, D. S., Schuijers, J., Vasile, E., Malik, S., Hnisz, D., Lee, T. I., Cisse, II, . . . Young, R. A. (2018).
Coactivator condensation at super-enhancers links phase separation and gene control. Science, 361(6400). https://doi.org/10.1126/science.aar3958

Sadek, J., Wuo, M. G., Rooklin, D., Hauenstein, A., Hong, S. H., Gautam, A., Wu, H., Zhang, Y., Cesarman, E., & Arora, P. S. (2020).
Modulation of virus-induced NF-kappaB signaling by NEMO coiled coil mimics. Nat Commun, 11(1), 1786. https://doi.org/10.1038/s41467-020-15576-3

Salido-Vallejo, R., Gonzalez-Menchen, A., Alcantara-Reifs, C., & Espana, A. (2022).
Treatment With Oral Propranolol for Refractory Classic Cutaneous Kaposi Sarcoma. JAMA Dermatol, 158(7), 832-834. https://doi.org/10.1001/jamadermatol.2022.1278

Schiller, J. T., & Lowy, D. R. (2021).
An Introduction to Virus Infections and Human Cancer. Recent Results Cancer Res, 217, 1-11. https://doi.org/10.1007/978-3-030-57362-1_1

Schmitz, M. L., & Baeuerle, P. A. (1991).
The p65 subunit is responsible for the strong transcription activating potential of NF-kappa B. EMBO J, 10(12), 3805-3817. https://doi.org/10.1002/j.1460-2075.1991.tb04950.x

Schneider, J. W., & Dittmer, D. P. (2017).
Diagnosis and Treatment of Kaposi Sarcoma. Am J Clin Dermatol, 18(4), 529-539. https://doi.org/10.1007/s40257-017-0270-4

Schock, E. N., & LaBonne, C. (2020).
Sorting Sox: Diverse Roles for Sox Transcription Factors During Neural Crest and Craniofacial Development. Front Physiol, 11, 606889. https://doi.org/10.3389/fphys.2020.606889

Schoelz, J. M., & Riddle, N. C. (2022).
Functions of HP1 proteins in transcriptional regulation. Epigenetics Chromatin, 15(1), 14. https://doi.org/10.1186/s13072-022-00453-8

Seebauer, C. T., Graus, M. S., Huang, L., McCann, A., Wylie-Sears, J., Fontaine, F., Karnezis, T., Zurakowski, D., Staffa, S. J., Meunier, F., Mulliken, J. B., Bischoff, J., & Francois, M. (2022).
Non-beta blocker enantiomers of propranolol and atenolol inhibit vasculogenesis in infantile hemangioma. J Clin Invest, 132(3). https://doi.org/10.1172/JCI151109

Shaban, H. A., Friman, E. T., Deluz, C., Tollenaere, A., Katanayeva, N., & Suter, D. M. (2024).
Individual transcription factors modulate both the micromovement of chromatin and its long-range structure. Proc Natl Acad Sci U S A, 121(18), e2311374121. https://doi.org/10.1073/pnas.2311374121

Sherwood, R. I., Hashimoto, T., O'Donnell, C. W., Lewis, S., Barkal, A. A., van Hoff, J. P., Karun, V., Jaakkola, T., & Gifford, D. K. (2014).
Discovery of directional and nondirectional pioneer transcription factors by modeling DNase profile magnitude and shape. Nat Biotechnol, 32(2), 171-178. https://doi.org/10.1038/nbt.2798

Si, H., Verma, S. C., & Robertson, E. S. (2006).
Proteomic analysis of the Kaposi's sarcoma-associated herpesvirus terminal repeat element binding proteins. J Virol, 80(18), 9017-9030. https://doi.org/10.1128/JVI.00297-06

Sin, S. H., Eason, A. B., Kim, Y., Schneider, J. W., Damania, B., & Dittmer, D. P. (2024).
The complete Kaposi sarcoma-associated herpesvirus genome induces early-onset, metastatic angiosarcoma in transgenic mice. Cell Host Microbe, 32(5), 755-767 e754. https://doi.org/10.1016/j.chom.2024.03.012

Sinclair, A. H., Berta, P., Palmer, M. S., Hawkins, J. R., Griffiths, B. L., Smith, M. J., Foster, J. W., Frischauf, A. M., Lovell-Badge, R., & Goodfellow, P. N. (1990).
A gene from the human sex-determining region encodes a protein with homology to a conserved DNA-binding motif. Nature, 346(6281), 240-244. https://doi.org/10.1038/346240a0

Singh, A., Modak, S. B., Chaturvedi, M. M., & Purohit, J. S. (2023).
SWI/SNF Chromatin Remodelers: Structural, Functional and Mechanistic Implications. Cell Biochem Biophys, 81(2), 167-187. https://doi.org/10.1007/s12013-023-01140-5

Sosa-Pineda, B., Wigle, J. T., & Oliver, G. (2000).
Hepatocyte migration during liver development requires Prox1. Nat Genet, 25(3), 254-255. https://doi.org/10.1038/76996

Soulier, J., Grollet, L., Oksenhendler, E., Cacoub, P., Cazals-Hatem, D., Babinet, P., d'Agay, M. F., Clauvel, J. P., Raphael, M., Degos, L., & et al. (1995).
Kaposi's sarcoma-associated herpesvirus-like DNA sequences in multicentric Castleman's disease. Blood, 86(4), 1276-1280. https://www.ncbi.nlm.nih.gov/pubmed/7632932

Srinivasan, R. S., Geng, X., Yang, Y., Wang, Y., Mukatira, S., Studer, M., Porto, M. P., Lagutin, O., & Oliver, G. (2010).
The nuclear hormone receptor Coup-TFII is required for the initiation and early maintenance of Prox1 expression in lymphatic endothelial cells. Genes Dev, 24(7), 696-707. https://doi.org/10.1101/gad.1859310

Stapleton, M. P. (1997).
Sir James Black and propranolol. The role of the basic sciences in the history of cardiovascular pharmacology. Tex Heart Inst J, 24(4), 336-342. https://www.ncbi.nlm.nih.gov/pubmed/9456487

Stehelin, D., Varmus, H. E., Bishop, J. M., & Vogt, P. K. (1976).
DNA related to the transforming gene(s) of avian sarcoma viruses is present in normal avian DNA. Nature, 260(5547), 170-173. https://doi.org/10.1038/260170a0

Sternbach, G., & Varon, J. (1995).
Moritz Kaposi: idiopathic pigmented sarcoma of the skin. J Emerg Med, 13(5), 671-674. https://doi.org/10.1016/0736-4679(95)00077-n

Strom, A. R., Emelyanov, A. V., Mir, M., Fyodorov, D. V., Darzacq, X., & Karpen, G. H. (2017).
Phase separation drives heterochromatin domain formation. Nature, 547(7662), 241-245. https://doi.org/10.1038/nature22989

Sun, R., Lin, S. F., Gradoville, L., Yuan, Y., Zhu, F., & Miller, G. (1998).
A viral gene that activates lytic cycle expression of Kaposi's sarcoma-associated herpesvirus. Proc Natl Acad Sci U S A, 95(18), 10866-10871. https://doi.org/10.1073/pnas.95.18.10866

Tammela, T., & Alitalo, K. (2010).
Lymphangiogenesis: Molecular mechanisms and future promise. Cell, 140(4), 460-476. https://doi.org/10.1016/j.cell.2010.01.045

Tian, S. Z., Yang, Y., Ning, D., Yu, T., Gao, T., Deng, Y., Fang, K., Xu, Y., Jing, K., Huang, G., Chen, G., Yin, P., Li, Y., Zeng, F., Tian, R., & Zheng, M. (2025).
Landscape of the Epstein-Barr virus-host chromatin interactome and gene regulation. EMBO J, 44(13), 3872-3915. https://doi.org/10.1038/s44318-025-00466-5

Torne, A. S., & Robertson, E. S. (2024).
Epigenetic Mechanisms in Latent Epstein-Barr Virus Infection and Associated Cancers. Cancers (Basel), 16(5). https://doi.org/10.3390/cancers16050991

Toth, Z., Brulois, K., & Jung, J. U. (2013).
The chromatin landscape of Kaposi's sarcoma-associated herpesvirus. Viruses, 5(5), 1346-1373. https://doi.org/10.3390/v5051346

Tuohinto, K., DiMaio, T. A., Kiss, E. A., Laakkonen, P., Saharinen, P., Karnezis, T., Lagunoff, M., & Ojala, P. M. (2023).
KSHV infection of endothelial precursor cells with lymphatic characteristics as a novel model for translational Kaposi's sarcoma studies. PLoS Pathog, 19(1), e1010753. https://doi.org/10.1371/journal.ppat.1010753

Uldrick, T. S., Wang, V., O'Mahony, D., Aleman, K., Wyvill, K. M., Marshall, V., Steinberg, S. M., Pittaluga, S., Maric, I., Whitby, D., Tosato, G., Little, R. F., & Yarchoan, R. (2010).
An interleukin-6-related systemic inflammatory syndrome in patients co-infected with Kaposi sarcoma-associated herpesvirus and HIV but without Multicentric Castleman disease. Clin Infect Dis, 51(3), 350-358. https://doi.org/10.1086/654798

Uppal, T., Banerjee, S., Sun, Z., Verma, S. C., & Robertson, E. S. (2014).
KSHV LANA--the master regulator of KSHV latency. Viruses, 6(12), 4961-4998. https://doi.org/10.3390/v6124961

Uppal, T., Jha, H. C., Verma, S. C., & Robertson, E. S. (2015).
Chromatinization of the KSHV Genome During the KSHV Life Cycle. Cancers (Basel), 7(1), 112-142. https://doi.org/10.3390/cancers7010112

van der Meulen, E., Anderton, M., Blumenthal, M. J., & Schafer, G. (2021).
Cellular Receptors Involved in KSHV Infection. Viruses, 13(1). https://doi.org/10.3390/v13010118

Varjosalo, M., Bjorklund, M., Cheng, F., Syvanen, H., Kivioja, T., Kilpinen, S., Sun, Z., Kallioniemi, O., Stunnenberg, H. G., He, W. W., Ojala, P., & Taipale, J. (2008).
Application of active and kinase-deficient kinome collection for identification of kinases regulating hedgehog signaling. Cell, 133(3), 537-548. https://doi.org/10.1016/j.cell.2008.02.047

Verma, R. P., & Hansch, C. (2007).
Matrix metalloproteinases (MMPs): chemical-biological functions and (Q)SARs. Bioorg Med Chem, 15(6), 2223-2268. https://doi.org/10.1016/j.bmc.2007.01.011

Verma, S. C., Cai, Q., Kreider, E., Lu, J., & Robertson, E. S. (2013).
Comprehensive analysis of LANA interacting proteins essential for viral genome tethering and persistence. PLoS One, 8(9), e74662. https://doi.org/10.1371/journal.pone.0074662

Verma, S. C., Lan, K., Choudhuri, T., Cotter, M. A., & Robertson, E. S. (2007).
An autonomous replicating element within the KSHV genome. Cell Host Microbe, 2(2), 106-118. https://doi.org/10.1016/j.chom.2007.07.002

Verma, S. C., Lu, J., Cai, Q., Kosiyatrakul, S., McDowell, M. E., Schildkraut, C. L., & Robertson, E. S. (2011).
Single molecule analysis of replicated DNA reveals the usage of multiple KSHV genome regions for latent replication. PLoS Pathog, 7(11), e1002365. https://doi.org/10.1371/journal.ppat.1002365

Vieira, J., Huang, M. L., Koelle, D. M., & Corey, L. (1997).
Transmissible Kaposi's sarcoma-associated herpesvirus (human herpesvirus 8) in saliva of men with a history of Kaposi's sarcoma. J Virol, 71(9), 7083-7087. https://doi.org/10.1128/JVI.71.9.7083-7087.1997

Vieira, J., & O'Hearn, P. M. (2004).
Use of the red fluorescent protein as a marker of Kaposi's sarcoma-associated herpesvirus lytic gene expression. Virology, 325(2), 225-240. https://doi.org/10.1016/j.virol.2004.03.049

Wabinga, H. R., Parkin, D. M., Wabwire-Mangen, F., & Mugerwa, J. W. (1993).
Cancer in Kampala, Uganda, in 1989-91: changes in incidence in the era of AIDS. Int J Cancer, 54(1), 26-36. https://doi.org/10.1002/ijc.2910540106

Wang, C., Liu, X., Liang, J., Narita, Y., Ding, W., Li, D., Zhang, L., Wang, H., Leong, M. M. L., Hou, I., Gerdt, C., Jiang, C., Zhong, Q., Tang, Z., Forney, C., Kottyan, L., Weirauch, M. T., Gewurz, B. E., Zeng, M. S., . . . Zhao, B. (2023).
A DNA tumor virus globally reprograms host 3D genome architecture to achieve immortal growth. Nat Commun, 14(1), 1598. https://doi.org/10.1038/s41467-023-37347-6

Wang, H. W., Trotter, M. W., Lagos, D., Bourboulia, D., Henderson, S., Makinen, T., Elliman, S., Flanagan, A. M., Alitalo, K., & Boshoff, C. (2004).
Kaposi sarcoma herpesvirus-induced cellular reprogramming contributes to the lymphatic endothelial gene expression in Kaposi sarcoma. Nat Genet, 36(7), 687-693. https://doi.org/10.1038/ng1384

Wang, L., & Damania, B. (2008).
Kaposi's sarcoma-associated herpesvirus confers a survival advantage to endothelial cells. Cancer Res, 68(12), 4640-4648. https://doi.org/10.1158/0008-5472.CAN-07-5988

Wang, W., Xue, Y., Zhou, S., Kuo, A., Cairns, B. R., & Crabtree, G. R. (1996).
Diversity and specialization of mammalian SWI/SNF complexes. Genes Dev, 10(17), 2117-2130. https://doi.org/10.1101/gad.10.17.2117

Wang, Y., Sathish, N., Hollow, C., & Yuan, Y. (2011).
Functional characterization of Kaposi's sarcoma-associated herpesvirus open reading frame K8 by bacterial artificial chromosome-based mutagenesis. J Virol, 85(5), 1943-1957. https://doi.org/10.1128/JVI.02060-10

Wanior, M., Kramer, A., Knapp, S., & Joerger, A. C. (2021).
Exploiting vulnerabilities of SWI/SNF chromatin remodelling complexes for cancer therapy. Oncogene, 40(21), 3637-3654. https://doi.org/10.1038/s41388-021-01781-x

Weissmann, S., Robitaille, A., Günther, T., Ziegler, M., & A., G. (2025).
Polycomb group proteins protect latent Kaposi sarcoma-associated herpesvirus from episome clearance and HUSH-dependent chromatin silencing [preprint]. https://www.biorxiv.org/content/10.1101/2025.02.10.637455v1

Whitby, D., Howard, M. R., Tenant-Flowers, M., Brink, N. S., Copas, A., Boshoff, C., Hatzioannou, T., Suggett, F. E., Aldam, D. M., Denton, A. S., & et al. (1995).
Detection of Kaposi sarcoma associated herpesvirus in peripheral blood of HIV-infected individuals and progression to Kaposi's sarcoma. Lancet, 346(8978), 799-802. https://doi.org/10.1016/s0140-6736(95)91619-9

Wigle, J. T., Chowdhury, K., Gruss, P., & Oliver, G. (1999).
Prox1 function is crucial for mouse lens-fibre elongation. Nat Genet, 21(3), 318-322. https://doi.org/10.1038/6844

Wigle, J. T., & Oliver, G. (1999).
Prox1 function is required for the development of the murine lymphatic system. Cell, 98(6), 769-778. https://doi.org/10.1016/s0092-8674(00)81511-1

Wilson, M., & Koopman, P. (2002).
Matching SOX: partner proteins and co-factors of the SOX family of transcriptional regulators. Curr Opin Genet Dev, 12(4), 441-446.
https://doi.org/10.1016/s0959-437x(02)00323-4

Witte, M. H., Bernas, M. J., Martin, C. P., & Witte, C. L. (2001).
Lymphangiogenesis and lymphangiodysplasia: from molecular to clinical lymphology. Microsc Res Tech, 55(2), 122-145. https://doi.org/10.1002/jemt.1163

Wu, L., Lo, P., Yu, X., Stoops, J. K., Forghani, B., & Zhou, Z. H. (2000).
Three-dimensional structure of the human herpesvirus 8 capsid. J Virol, 74(20), 9646-9654. https://doi.org/10.1128/jvi.74.20.9646-9654.2000

Yang, Y., & Oliver, G. (2014).
Development of the mammalian lymphatic vasculature. J Clin Invest, 124(3), 888-897.
https://doi.org/10.1172/JCI71609

Ye, X., Guerin, L. N., Chen, Z., Rajendren, S., Dunker, W., Zhao, Y., Zhang, R., Hodges, E., & Karijolich, J. (2024).
Enhancer-promoter activation by the Kaposi sarcoma-associated herpesvirus episome maintenance protein LANA. Cell Rep, 43(3), 113888.
https://doi.org/10.1016/j.celrep.2024.113888

Yoo, S., Kim, S., Yoo, S., Hwang, I. T., Cho, H., & Lee, M. S. (2011).
Kaposi's sarcoma-associated herpesvirus infection of endothelial progenitor cells impairs angiogenic activity in vitro. J Microbiol, 49(2), 299-304.
https://doi.org/10.1007/s12275-011-0408-7

Yoshimatsu, Y., Yamazaki, T., Mihira, H., Itoh, T., Suehiro, J., Yuki, K., Harada, K., Morikawa, M., Iwata, C., Minami, T., Morishita, Y., Kodama, T., Miyazono, K., & Watabe, T. (2011).
Ets family members induce lymphangiogenesis through physical and functional interaction with Prox1. J Cell Sci, 124(Pt 16), 2753-2762.
https://doi.org/10.1242/jcs.083998

Yu, F., Harada, J. N., Brown, H. J., Deng, H., Song, M. J., Wu, T. T., Kato-Stankiewicz, J., Nelson, C. G., Vieira, J., Tamanoi, F., Chanda, S. K., & Sun, R. (2007).
Systematic identification of cellular signals reactivating Kaposi sarcoma-associated herpesvirus. PLoS Pathog, 3(3), e44. https://doi.org/10.1371/journal.ppat.0030044

Zaneveld, J. R., McMinds, R., & Vega Thurber, R. (2017).
Stress and stability: applying the Anna Karenina principle to animal microbiomes. Nat Microbiol, 2, 17121. https://doi.org/10.1038/nmicrobiol.2017.121

Zaret, K. S., & Carroll, J. S. (2011).
Pioneer transcription factors: establishing competence for gene expression. Genes Dev, 25(21), 2227-2241. https://doi.org/10.1101/gad.176826.111

Zesiewicz, T. A., Elble, R. J., Louis, E. D., Gronseth, G. S., Ondo, W. G., Dewey, R. B., Jr., Okun, M. S.*, Sullivan, K. L., & Weiner, W. J. (2011*).
Evidence-based guideline update: treatment of essential tremor: report of the Quality Standards subcommittee of the American Academy of Neurology. Neurology, 77(19), 1752-1755. https://doi.org/10.1212/WNL.0b013e318236f0fd

Zhang, G., Chan, B., Samarina, N., Abere, B., Weidner-Glunde, M., Buch, A., Pich, A., Brinkmann, M. M., & Schulz, T. F. *(2016).*
Cytoplasmic isoforms of Kaposi sarcoma herpesvirus LANA recruit and antagonize the innate immune DNA sensor cGAS. Proc Natl Acad Sci U S A, 113(8), E1034-1043. https://doi.org/10.1073/pnas.1516812113

Zhao, B., Zou, J., Wang, H., Johannsen, E., Peng, C. W., Quackenbush, J., Mar, J. C., Morton, C. C., Freedman, M. L., Blacklow, S. C., Aster, J. C., Bernstein, B. E., & Kieff, E. (*2011).*
Epstein-Barr virus exploits intrinsic B-İymphocyte transcription programs to achieve immortal cell growth. Proc Natl Acad Sci U S A, 108(36), 14902-14907. https://doi.org/10.1073/pnas.1108892108

Zhu, F. X., Chong, J. M., Wu, L., & Yuan, Y. (2005).
Virion proteins of Kaposi's sarcoma-associated herpesvirus. J Virol, 79(2), 800-811. https://doi.org/10.1128/JVI.79.2.800-811.2005

Zhu, F. X., Cusano, T., & Yuan, Y. (1999).
Identification of the immediate-early transcripts of Kaposi's sarcoma-associated herpesvirus. J Virol, 73(7), 5556-5567. https://doi.org/10.1128/JVI.73.7.5556-5567.1999